



TECHNISCHE UNIVERSITÄT MÜNCHEN
Lehrstuhl für Ernährung und Immunologie

Impact of dietary iron on chronic intestinal inflammation: role of iron storage protein ferritin H and replacement therapy

Annemarie Schmidt

Vollständiger Abdruck der von der Fakultät Wissenschaftszentrum Weihenstephan für Ernährung und Landnutzung und Umwelt der Technischen Universität München zur Erlangung des akademischen Grades eines

Doktors der Naturwissenschaften

genehmigten Dissertation.

Vorsitzender: Prof. Dr. Martin Klingenspor
Prüfer der Dissertation: 1. Prof. Dr. Dirk Haller
2. Prof. Dr. Hannelore Daniel

Die Dissertation wurde am 16.08.2019 bei der Technischen Universität München eingereicht und durch die Fakultät Wissenschaftszentrum Weihenstephan für Ernährung, Landnutzung und Umwelt am 27.02.2020 angenommen.

Content

ABSTRACT	6
ZUSAMMENFASSUNG	8
1. INTRODUCTION	10
1.1 Inflammatory bowel diseases	10
1.1.1. Epidemiology of IBD	11
1.1.2 Genetic alteration of IBD.....	13
1.1.3 Treatment.....	15
1.2 The human intestinal microbiota	15
1.2.1 Composition of the human intestinal microbiota	16
1.2.2 Gastrointestinal microbiota and IBD.....	17
1.3 Iron appearance, bioavailability and intake recommendations	19
1.3.1 Iron in the human body.....	20
1.3.2 Iron deficiency in inflammatory bowel diseases.....	23
1.3.3. Iron and gastrointestinal bacteria	24
1.3.4 Clinical efficacy of oral <i>versus</i> intravenous iron treatment	24
1.4 The iron storage protein ferritin	25
1.4.1 Regulation of ferritin	28
1.4.2 Ferritin and inflammation	28
1.4.3 Altered ferritin expression	28
1.4.4 Ferritin H deletion in intestinal epithelial cells	30
1.5 Model of inflammation: DSS-induced colitis.....	30
2. AIM	32
3. MATERIALS AND METHODS	33
3.1 Human trial.....	33
3.1.1 Study design	33
3.1.2 Stool sampling.....	35
3.1.3 Microbiota analysis	36
3.1.3 Iron measurement.....	37
3.2 Mouse model experiments	38
3.2.1 Ferritin H deletion in intestinal epithelial cells of C57BL/6 mice	39
3.2.2 Genotyping.....	40
3.2.3 Characterization of mice	41
3.2.4 Induction of colitis.....	41

3.2.5 Macroscopical scoring	42
3.2.6 H & E staining and histological scoring	43
3.2.7 Hematocrit determination	44
3.2.8 Hemoglobin determination.....	44
3.2.9 Non-heme iron determination.....	45
3.2.10 Iron staining.....	45
3.2.11 SAA – ELISA.....	45
3.3 Statistical analysis.....	45
4. RESULTS.....	46
4.1 Open-labelled clinical trial to compare oral vs. intravenous iron replacement therapy in IBD patients	46
4.1.1 Characteristics of participants.....	46
4.1.2 IRT restores iron storage independently of the administration route.....	47
4.1.3 Impact of iron treatment on disease activity and quality of life.....	48
4.1.4 IBD is linked to specific fecal microbiota fingerprints.....	50
4.1.5 Bacterial communities are prone to instability after iron intervention in anemic IBD patients compared to NI patients	54
4.1.6 The gut ecosystem is affected by oral iron treatment.....	58
4.2 Fth ^{Δ/Δ} Mouse model did not show any spontaneous effects but is susceptible for DSS-induced colitis	60
4.2.1 Ferritin H deletion in intestinal epithelial cells	60
4.2.2 Body weight development did not show any abnormalities	60
4.2.3 Regular organ weight parameters in both genotypes	61
4.2.3 Iron status tend to be higher in Fth ^{Δ/Δ} mice.....	61
4.2.4 Histological tissue staining revealed no abnormalities in gut tissue structure.....	63
4.2.5 High susceptibility of Fth ^{Δ/Δ} mice to DSS-induced colitis	64
5. DISCUSSION.....	72
5.1 Oral versus intravenous iron replacement therapy alters gut microbiota in patients with IBD	72
5.2 Ferritin H deletion in intestinal epithelial cells alters susceptibility to DSS-induced colitis in mice.....	77
CONCLUSION.....	81
APPENDIX	82
Supplemental data	82
List of figures	83
List of tables	87
List of abbreviations.....	88

References.....	92
Lebenslauf	102
List of publications	105

Lieber Dirk, für die fachliche Betreuung und die Unterstützung darüber hinaus möchte ich mich sehr herzlich bei dir bedanken.

Annemarie

ABSTRACT

Iron deficiency is a common complication in patients with inflammatory bowel diseases (IBD) and oral iron therapy is suggested to exacerbate IBD symptoms. We performed an open-labelled clinical trial to compare the effects of per oral (PO) versus intravenous (IV) iron replacement therapy (IRT). The study population included patients with Crohn's disease (CD, n = 31), patients with ulcerative colitis (UC, n = 22) and non-inflamed control subjects with iron deficiency (NI = 19). After randomization, participants received iron sulfate (PO) or iron sucrose (IV) over 3 months. Clinical parameters, fecal bacterial communities and metabolomes were assessed before and after the intervention. Both PO treatment and IV treatment ameliorated iron deficiency but higher ferritin level were observed with the IV treatment. Changes in disease activity were independent of iron treatment types. Fecal samples in IBD were characterized by marked inter-individual differences, lower phylotype richness and proportions of *Clostridiales*. Metabolite analysis also showed separation of both UC and CD from control anemic participants. Major shifts in bacterial diversity occurred in approximately half of all participants after IRT but patients with CD were most susceptible. Despite individual-specific changes in phylotypes due to IRT, PO treatment was associated with decreased abundance of operational taxonomic units (OTU) assigned to the species *Faecalibacterium prausnitzii*, *Ruminococcus bromii*, *Dorea sp.* and *Collinsella aerofaciens*. Clear IV-specific and PO-specific fingerprints were evident at the level of metabolomes with changes affecting cholesterol-derived host substrates. Shifts in gut bacterial diversity and composition associated with iron treatment are pronounced in IBD patients. Despite similar clinical outcomes, oral administration differentially affects bacterial phylotypes and fecal metabolites compared with IV therapy suggesting that IV iron therapy might be specifically benefit anemic patients with CD with an instable microbiota. This hypothesis is underlined by data from animal experiments suggesting that systemic iron repletion should be preferred for the treatment of anemic patients with CD as an oral iron deprivation prevents chronic ileal inflammation in $TNF^{\Delta ARE^{WT}}$ mice. Coherent, luminal iron sulfate deprivation downregulates ferritin expression in primary ileal intestinal epithelial cells (IECs). Here we addressed a possible protective role of the epithelial cellular iron storage protein ferritin in context of intestinal inflammation. Thus, we

challenged intestinal ferritin-deleted mice ($Fth^{\Delta/\Delta}$ mice) with intestinal inflammation-inducing dextran sodium sulfate (DSS). $Fth^{\Delta/\Delta}$ mice were significantly more prone to DSS-induced colitis compared to control mice with a strong gender-specific difference towards more severe inflammation in male mice.

ZUSAMMENFASSUNG

Eisenmangel ist eine häufig auftretende Komplikation bei Patienten mit chronisch-entzündlicher Darmerkrankung (CED) und es wird vermutet, dass eine orale Eisentherapie die Krankheitssymptome verstärkt. In einer offenen klinischen Studie haben wir eine orale Eisentherapie mit einer intravenösen Eisentherapie verglichen. Die Studienpopulation bestand aus Patienten mit Morbus Crohn (MC, n = 31), Patienten mit Colitis Ulcerosa (UC, n = 22) und Kontrollpersonen mit Eisenmangel (n = 19). Nach der Randomisierung erhielten die Studienteilnehmer über drei Monate entweder Eisensulfat (oral) oder Eisensaccharose (intravenös). Klinische Parameter, die fäkale bakterielle Zusammensetzung sowie Metabolite wurden vor und nach der Intervention bestimmt. Sowohl die orale als auch die intravenöse Eisentherapie führten zu einer Verbesserung des Eisenmangels, wobei nach einer intravenösen Eisengabe höhere Ferritinwerte gemessen wurden. Änderungen in der Krankheitsaktivität waren unabhängig von der Art der Therapie. Die Fäkalproben der CED-Patienten waren durch interindividuelle Unterschiede, eine geringere Vielfalt im Phylotyp sowie kleinere Anteile an *Clostridiales* charakterisiert. Die Analyse der Metabolite zeigte ebenfalls eine Trennung sowohl der MC-Patienten als auch der UC-Patienten von den Teilnehmern mit Eisenmangel der Kontrollgruppe. In etwa der Hälfte aller Teilnehmer fand sich eine starke Veränderung der bakteriellen Diversität nach der Eisentherapie, wobei die Mikrobiota von MC-Patienten am anfälligsten war. Neben der durch die Eisentherapie hervorgerufenen individuellen Änderungen im Phylotyp war die orale Eisentherapie charakterisiert durch eine verringerte Häufigkeit der OTUs assoziiert, welche den Spezies *Faecalibacterium prausnitzii*, *Ruminococcus bromii*, *Dorea sp.* and *Collinsella aerofaciens* zuzuordnen sind. Auf Ebene der Metabolite waren spezifische Muster nach der intravenösen Eisentherapie und sowie nach der oralen Eisentherapie erkennbar. Die Auswirkungen betrafen den Cholesterollowerstoffwechsel des Wirtes. Änderungen in der bakteriellen Diversität und der bakteriellen Zusammensetzung in CED-Patienten unter Eisentherapie sind ausgeprägt. Trotz ähnlicher Ergebnisse in den klinischen Parametern beeinflusst eine orale Eisengabe die bakteriellen Phylotypen und die fäkale Zusammensetzung der Metaboliten in einer anderen Weise als die intravenöse Eisengabe.

Eisenarme Fütterung schützt $TNF^{\Delta ARE/WT}$ Mäuse vor der Entwicklung einer Ileitis. Damit einhergehend führt eine Eisensulfat-freie Fütterung zu einer herabgesenkten Ferritin-Expression in intestinalen Epithelzellen. Wir haben Mäuse mit Ferritin-Deletion in den intestinalen Epithelzellen ($Fth^{\Delta/\Delta}$ Mäuse) mit DSS stimuliert. $Fth^{\Delta/\Delta}$ Mäuse zeigten eine deutlich erhöhte Anfälligkeit gegenüber DSS verglichen zu den Kontrollmäusen ohne intestinalen Ferritin-Deletion. Ein starker geschlechtsspezifischer Unterschied in der Anfälligkeit gegenüber DSS wurde beobachtet, wobei sich männliche Tiere anfälliger für eine intestinale Entzündung zeigten.

1. INTRODUCTION

1.1 Inflammatory bowel diseases

Inflammatory bowel disease (IBD) is a broader term for different chronically inflammatory conditions. The two main subtypes are Crohn's disease (CD), first described in 1932 by Burrill Bernhard Crohn (Crohn *et al.* 1932) and ulcerative colitis (UC), first described by Samuel Wilks in 1859 (Wilks *et al.* 1859). Both are characterized by chronically active or relapsing intestinal inflammation. CD and UC share many common characteristics, especially regarding the symptoms, but they are both characterized by unique features. CD is characterized by transmural, segmental inflammatory sites affecting any part of the gastrointestinal tract (GIT) from the mouth to the anus. The most frequently affected intestinal regions in CD are the terminal ileum and the colon with more than 80 % of all CD patients showing a terminal ileitis. CD lesions are characterized by a segmental, discontinuous distribution of typically aphthous or confluent deep linear ulcers. UC mainly affects the colon and the rectum with the exception of 10 % – 20 % of the patients suffering from an additional ileal manifestation, a so called backwash-ileitis. Intestinal manifestations of UC are characterized by chronically persisting ulcers within the large bowel that are morphologically superficial (Podolsky 2002). UC typically affects only the inner lining of the mucosa. It is characterized by continuous patches of inflammation and ulceration. Damage to the tight junctions and mucus film covering epithelial barrier, which act as the first line of defence, increase permeability, leading to an increased uptake of luminal antigens. Innate immune cells, macrophages and dendritic cells recognize the commensal microbiota via Toll-like receptors (TLR) and become activated (Ordás *et al.* 2012).

Clinical signs of IBD include diarrhea, bloody stools, weight loss, and abdominal pain. Extra-intestinal manifestations mainly affect the skin, joints and eyes. Although the mechanisms underlying these extra-intestinal manifestations are largely unknown it is suggested that they are provoked by the pro-inflammatory milieu due to the gastrointestinal inflammation (Levine *et al.* 2011).

The pathogenesis of IBD is not yet fully understood but there is consensus that genetic alterations predispose individuals and environmental factors including microbial factors might provoke IBD in predisposed individuals (Silva *et al.* 2016,

Venema *et al.* 2017). Genome-wide association studies (GWAS) as well as data from animal experiments point to an interplay between the intestinal microbiota, the epithelial interface and the immune system driving the pathogenesis of IBD (Khor *et al.* 2011, see figure 1.1.)

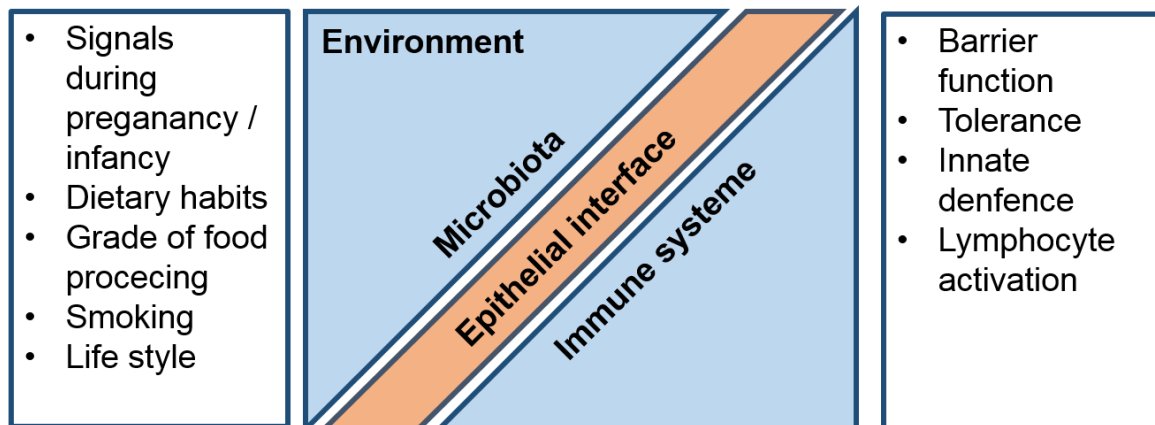


Figure 1.1: Interacting players for disease initiation, progression and persistence.

The integrity of the epithelial interface between environmental factors and the immune system is crucial to keep a healthy gut ecosystem. The interface consists of a mucous layer formed by an inner layer (small intestine) and an inner and outer layer (colon) which is produced by the polymerization of gel-forming mucins secreted by goblet cells and of the intestinal epithelium comprised by enterocytes and specialized cells such as goblet cells, Paneth cells and intestinal epithelial cells (Silva *et al.* 2016).

Today, IBD is assumed to be an incurable disease. Severity, clinical manifestations and characteristics vary largely among patients.

1.1.1. Epidemiology of IBD

IBD appears frequently in the population of the Northern hemisphere with the highest prevalence in Northern Europe, Western Europe and North America (Molodecky *et al.* 2012, Podolsky 2002). Both prevalence and incidence rate of CD are rising since decades not only in western countries but worldwide. Nevertheless, the reasons for rising CD cases are poorly understood. In contrast, the prevalence

of UC has reached a stable phase in the last decade (Kaplan 2015). The in-homogenous distribution of CD and UC implicates difficulties to estimate an overall prevalence of IBD. It also needs to be considered that data from developing countries are rare (Molodecky *et al.* 2012) complicating a worldwide estimation. The peak incidence rate for both CD and UC is between the second and fourth decade of life with the highest incidence rate between the age of 20 years and 29 years. The incidence rates are lower for CD compared to UC and differ around the world with a west-east gradient. The annual incidence rates per 100.000 person-years for UC in Europe are 0.6 – 24.3, in North America 0 – 19.2 and in Asia and Middle East 0.1 – 6.3. The incidence rates for CD in Europe are 0.3 – 12.7, in North America 0 – 20.2 and in Asia and Middle East 0.04 – 5. The data cover the years 1930 – 2008 for European studies, 1950 – 2008 for Asian and Middle Eastern studies and 1960 – 2004 for North American studies. The prevalence per 100,000 persons for UC in Europe ranges from 4.9 – 505, in North America 37.5 – 248.6 and in Asia and Middle East: 4.9 – 168.9. The prevalence for CD in Europe is between 0.6 – 322, in North America, 16.7 – 318.5 and in Asia and Middle East 0.88 – 67.9, see table 1.1. 10 % - 15 % of the patients suffering from IBD are children (Molodecky *et al.* 2012). Men are more frequent affected by UC compared to women. In countries with high socio-economic standards women are more often affected by CD while men outnumber women in low-incidence countries (Kelsen *et al.* 2008, see table 1.1).

*Table 1.1: Annual incidence rates and prevalence values for ulcerative colitis (UC) and Crohn's disease (CD). Incidence rates are given as 100,000 per person-years. Prevalence values are given per 100,000 persons. Incidence rates and prevalence values range from 1930 to 208 for European studies, 1950 to 2008 for Asian and Middle Eastern studies and 1920 to 2004 for North American studies (Molodecky *et al.* 2012).*

	Europe	North America	Asia / Middle East	
UC	0.6 - 24.3	0 - 19.2	0.1 - 6.3	Incidence rates
MC	0.3 - 12.7	0 - 20.2	0.04 – 5	
UC	4.9 – 505	37.5 - 248.6	4.9 - 168.9	Prevalence values
MC	0.6 – 322	16.7 - 318.5	0.88 - 67.9	

It is hypothesized that the increased risk of developing IBD in Western life-style populations is related to changes in dietary habits over the last decades, such as an increased consumption of industrialized food or a diet high in fat, salt and/or

sugar. This hypothesis is supported by the observation of increasing IBD rates in developing countries such as China or India that slowly adapt to Western life-style habits (Kaplan 2015).

Furthermore, epidemiological studies showed higher IBD prevalence values in industrialized countries and adoption of higher incidence rates in the second generation of immigrants. That points to the fact that adoption of lifestyle factors, such as dietary habits might be a risk factor for later IBD development (Schaubeck *et al.* 2015).

Diet can influence inflammatory processes either directly or indirectly, e.g. by changing the intestinal microbial composition or function. Despite the fact that several experimental studies, clinical trials and cohort studies address the role of diet in the development of IBD until today no strong risk association between a single nutrient and the pathogenesis of IBD could be identified. Associations between a high intake rates of omega 6 fatty acids with increased IBD incidence rates were observed in cohort studies. A possible hypothesis to explain this association might be that omega 6 fatty acids, such as linoleic acid, can be metabolized to arachidonic acid which is a precursor molecule of proinflammatory eicosanoids. Low intake of fiber was also observed to be associated with a higher risk for CD but not for UC. This observation might be related to the fact that the colonic microbiota metabolize fiber to short chain fatty acids such as butyrate which is suggested to support the epithelial barrier integrity and bacterial translocation. This theory is supported by the observation that the abundance of *Faecalibacterium prausnitzii*, a butyrate producer of the colonic microbiota, is reduced in the microbiome of IBD patients (Schaubeck *et al.* 2015).

1.1.2 Genetic alteration of IBD

Genome wide association studies (GWAS) scan the entire genome for statistical associations between common variants and disease status (Momozawa *et al.* 2018). The application of GWAS and next-generation sequencing technologies (NGS) enables the association between genetic traits with IBD. The benefits of GWAS besides the understanding of IBD pathology are to identify new drug targets and to develop effective predictive and diagnostic tools. Studies that analyzed the familiar occurrence of IBD cases indicate that familiar cases of IBD have a higher

risk for developing IBD (Orholm *et al.* 1991) and the clinical presentation of intra-familial cases of IBD is rather consistent while it is rather inconsistent in inter-familial cases (Satsangi *et al.* 1996; Colombel *et al.* 1996). Further, studies in twins revealed a higher concordance rate in monozygotic twins compared to dizygotic twins pointing to the importance of genetic alterations in the development of IBD. This observation was more prominent in CD than in UC leading to the conclusion that a genetic predisposition is from greater influence in the pathogenesis of CD compared to the pathogenesis of UC (Tysk *et al.* 1988). Still, it needs to be considered that concordance between twins could be due to a shared genetic pool but also due to similar environmental signals during pregnancy, birth and infancy. In numbers, it is calculated that 5 % – 20 % of patients suffering from IBD have a family history of the disease (Lepage *et al.* 2011).

To the presence, GWAS revealed more than 250 genetic risk loci which are associated with IBD. These studies aim to link abnormal chromosomal regions that are enriched in IBD patients compared to healthy individuals. However, for the majority of the risk-associated genes the causal genomic variants remain unclear. Only for a handful of candidate genes causal genetic variants are sufficiently understood (Jostins *et al.* 2012) and a minority of causative variants are coding (Momozawa *et al.* 2018).

The most prominent gene variant assumed to play a role in the pathogenesis of IBD is found within the IBD1 locus and encodes the *nucleotide-binding oligomerization domain containing protein 2* (NOD2 / CARD15). NOD2 belongs to the family of pattern recognition receptors (PRR) and plays a role in human innate immunity. It is expressed in both immune cells and epithelial cells. Variations of the *nod2* gene are specifically linked to CD. Carriage of one risk-conferring allele leads to a 2 - 3-fold increased risk of CD. Homozygosity as well as the heterozygous presence of two risk alleles enhances the risk up to 20 - 40 fold (Lesage *et al.* 2002). NOD2 binds to *muramyl dipeptide* (MDP), a cell wall component of most bacteria, leading to nuclear factor 'kappa-light chain enhancer' of activated B-cells (NF-κB) activation. The three most abundant single nucleotide polymorphisms (SNPs) of NOD2 result in a constrained NOD2 activation and in consequence to a diminished activation of NF-κB. One possible hypothesis for the pathogenesis of CD in patients carrying NOD2 associated risk factors is an impaired microbe-host interaction, increased microbe translocation in case of epithelial barrier disruption and limited

elimination of those bacteria, probably leading to an inadequate immune response. NOD2 alleles that confer an increased risk of CD are found in > 5 % of the human population (Hugot *et al.* 2001).

Further candidate genes code for proteins with impact on the innate and the adaptive immune response, the epithelial barrier function, integrity and repair as well as for the autophagy response. The majority of the identified risk loci is not specifically associated with CD or UC and a single allelic variant hardly affects the individuals risk to develop IBD. It is estimated that the current known risk loci account for only about 13 % of the CD cases and 8 % of the UC cases (Jostins *et al.* 2012).

1.1.3 Treatment

The goal of treating IBD patients is to reach “steroid-free deep remission”. This term refers to remission status without clinical symptoms, complete mucosal healing and disappearance of histological signs of inflammation. In the last decade, application of biological therapies based on monoclonal antibodies and fusion proteins has increased beside well established drugs used to treat IBD. The range of therapies covers conventional therapies including 5-aminosalicylates and corticosteroids, immunomodulatory drugs and other immunosuppressants such as thiopurine, methotrexate and cyclosporine, tacrolimus, biologic therapies (antibodies), small molecular therapies (Janus kinase inhibitor, SMAD 7 inhibitor) and other novel therapies such as mesenchymal stem cell transplantation or fecal microbiota transplantation. Despite such a broad spectrum of therapeutically approaches, almost one third of patients remain unresponsive to existing therapies (Su *et al.* 2018).

1.2 The human intestinal microbiota

Microbes occupy habitats of the human body such as the gastrointestinal tract (GI), the skin and the vagina (Huttenhower *et al.* 2012). With a microbial load of 10^{11} bacteria/mL content the colon of the human GI is the most densely colonized organ of the body (Sartor *et al.* 2008). The human stomach, the duodenum and the jejunum harbor lower numbers of commensal bacteria due to the low pH,

pancreatic enzymes and motility patterns that hinder colonization (Ohland *et al.* 2010). The ileum and colon are colonized by a higher number and diversity compared to the upper parts of the GI (Tlaskalova-Hogenova *et al.* 2010) characterizing an increasing density of colonization in the GI from proximal regions to distal regions.

1.2.1 Composition of the human intestinal microbiota

The number of different species of the complex community of microorganisms estimated by culturing and 16S rRNA sequencing is estimated to be more than 1000. However, the number of different bacterial species in a single individual is limited to approximately 100 - 200 species (Qin *et al.* 2010, Li *et al.* 2014). The human intestinal microbiota is dominated by the four phyla *Actinobacteria*, *Bacteroidetes* (e.g. *Bacteroides* spp.), *Firmicutes* (e.g. *Clostridium*, *Roseburia*, *Ruminococcus* or *Lactobacillus* spp.) and *Proteobacteria* (e.g. *Enterobacteria*) with more than 90 % of the bacteria belonging to the phyla *Firmicutes* and *Bacteroidetes*. Most of the *Firmicutes* belong to the Clostridia class (Eckburg *et al.* 2005, see figure 1.2). Only around 5 % belong to other phyla such as *Proteobacteria* and *Actinobacteria* (e.g. *Bifidobacteria*), *Fusobacteria*, *Verrucomicrobia* or *Tenericutes* (Hörmansperger *et al.* 2016). Bacteria dominate the microbial ecosystem of the GI but archaea, viruses, yeasts and protozoa contribute to the diversity of the intestinal microbiota (Eckburg *et al.* 2005, Human Microbiome project 2012). Diversity rises with descending taxonomic rank.

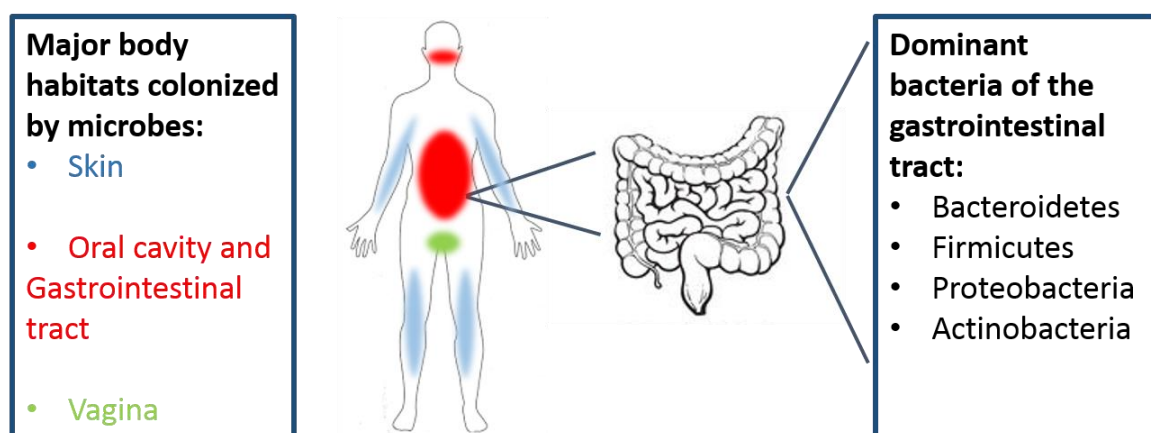


Figure 1.2: Microbial habitats on the human body and dominant phyla of bacteria in the gastrointestinal tract.

The human intestinal microbiota contributes to an intact gut homeostasis. Commensal bacteria supply energy to the host by fermentation of non-digestible molecules, including cellulose, inulin and resistant starch (Minemura *et al.* 2015). End products of fermentation are short chain fatty acids (SCFA), such as acetate, butyrate and propionate, which impose modulatory effects on the host (Topping *et al.* 2001, Smith *et al.* 2013). By occupying mucosal attachment sites the established microbiota protects the host from pathogens. This is supported by the secretion of bacteriocides and the competition for micronutrients (Levy 2000). The host's immune system is influenced by the microbial community.

The microbiota is capable of adapting to external and intrinsic factors such as dietary habits or genetic dispositions. Although both extrinsic and intrinsic factors are able to shape the microbial composition diet seem to overwrite the influence of the genetic imprint. Short-term interventions demonstrate the plasticity of the human microbiota to rapidly adapt to external factors and the microbiota can change quickly upon perturbation without pathologic consequences (Schaubeck *et al.* 2015). The composition of the intestinal microbiota also varies with environmental factors such as antibiotic intake and lifestyle, and on host characteristics, such as age and health status.

Besides that, there is evidence that many chronic disorders, such as for example allergies, autoimmune diseases and metabolic diseases are associated with compositional shifts of the gut microbiota (Geuking *et al.* 2014). Further features of the human intestinal microbiota are to modulate the intestinal permeability and the mucus layer (Hollister *et al.* 2014).

1.2.2 Gastrointestinal microbiota and IBD

In recent times, the role of the microbiota is discussed as a key player in the pathogenesis of IBD (Colman *et al.* 2014). First clinical evidence for a role of bacteria in the pathogenesis of chronic inflammatory disorders came in 1991 from Rutgeerts and colleagues (Rutgeerts *et al.* 1991). Later, GWAS identified a variety of target genes that point towards a disrupted microbe-host interaction (Fritz *et al.* 2011) and high-throughput sequencing analysis of microbial communities was used to identify risk patterns associated with distinct phenotypes of IBD (Frank *et*

al. 2007). An increasing number of studies have used non-cultivated 16S rRNA sequencing technology to reveal intestinal microbial profiles in IBD patients and in healthy control humans (Gong *et al.* 2016).

Microbial dysbiosis, reduced microbiome richness and reduced biodiversity have been observed in patients with IBD (Colman *et al.* 2014). Still, a causal relationship between the reduced microbial diversity and intestinal inflammatory processes remains unclear. Studies on the microbial profile of CD patients and their healthy siblings revealed that healthy siblings of CD patients had a lower abundance compared to unrelated healthy individuals. The abundance was still higher compared to the siblings suffering from CD. This suggest that a loss in intestinal microbial diversity might be one of several steps in the pathogenesis of IBD (Hedin *et al.* 2016). Biodiversity is important to maintain a stable ecosystem and is related to ecological functionality. A loss of biodiversity means higher susceptibility to external influences and decreased functionality (Gong *et al.* 2016).

Microbial changes in IBD can be characterized for example by an alteration of the abundance of *Firmicutes*. In particular bacteria belonging to *Lachnospiraceae*, e.g. *Roseburia*, and bacteria belonging to the former Clostridium Cluster XIVa and IX, e.g. *Faecalibacterium prausnitzii*, are often reduced in IBD patients. Other bacteria such as *Bacteroidetes*, e.g. *Bacteroides fragilis* gain in abundance. Still, disease-specific taxa or IBD-relevant phylotypes could not be identified yet (Buttó *et al.* 2016).

Subtype-specific for UC, higher abundance of *Bacteroides*, *Enterococcus*, *Blautia* or *Escherichia-Shigella* genera were observed while the abundance of *Coprocuccos* was decreased in UC patients compared to healthy controls. In CD patients higher abundance of *Streptococcus* and *Enterococcus* and lower abundance of *Caprocuccous*, *Roseburia*, *Faecalibacterium* and *Ruminococcus* was observed (Gong *et al.* 2016).

Despite the studies characterizing the microbial composition of IBD patients there are only few studies focusing on the influence of single nutrients, microbial changes and intestinal inflammation. An important tool to characterize the pathophysiological role of diet-induced intestinal microbial changes are animal models. IBD-relevant mouse models might confirm the role of dietary modulation and the microbial ecosystem in intestinal inflammation. For example, the

observation that enhanced fat intake increases the risk to develop IBD in humans was underlined in TNF^{ΔARE} mice on a high fat diet showing aggravated development of IBD (Gruber *et al.* 2013).

1.3 Iron appearance, bioavailability and intake recommendations

The chemical element iron (Fe; from Latin *ferrum*), atomic number 26, group 8 element, first transition series, amphoteric, is a solid metal essential for almost all living organisms ranging from archaea to humans. It is the fourth most common element in the earth's crust (6 %) and by mass the most common element on earth. Although the oxidation statuses 2+ (Fe(II)), traditionally called ferrous iron, and 3+ (Fe(III)), traditionally called ferric iron, are the most common oxidative statuses, iron exist in the oxidation statuses ranging from 2- to 6+. In living organisms iron is present in form of iron-proteins such as heme enzymes or non-heme enzymes and is particularly important for an adequate production of red blood cells. Iron is often bound as a co-factor and involved in many cellular redox reactions, oxygen transport, electron transfer, DNA synthesis and energy metabolism (Girelli *et al.* 2017).

Almost all forms of food contain iron, either in form of inorganic, non-heme iron including ferritin or in form of organic heme iron from animal tissue with non-heme being the predominant form. The iron absorption is regulated by dietary and systemic factors. One determinant for the bioavailability of iron is its biochemical form. Although heme iron is the smaller quantity of dietary iron it is highly bioavailable. Non-heme iron is less absorbed compared to heme iron with a higher rate of variability (Beck *et al.* 2014). Ascorbic acid and foods containing animal protein such as meat, fish and poultry can enhance the bioavailability of non-heme iron whereas polyphenols contained in vegetables, coffee, tea and wine as well as soy protein, calcium and phytic acid contained in grains and cereals can inhibit the bioavailability of non-heme iron (Hunt *et al.* 2007). Polyphenols and phytic acids inhibit the iron absorption due to their chelating properties. Calcium is suggested to inhibit the transport of heme iron into the enterocytes. Still, effects of different

foods on the iron absorption are not necessarily associated with the iron status or the body's iron stores (Beck *et al.* 2014).

Especially rich sources for dietary iron include red meat, lentils and leaf vegetables. Food that contain relative high level of iron include fish, cereals, nuts and potatoes. Iron absorption depends on the body status and requirement. Especially the absorption rate of non-heme iron is variable and depends on the body's iron stores (Dainty *et al.* 2014).

The recommendations for the daily intake of iron according to the D-A-CH dietary reference values of the German Nutrition Society (Deutsche Gesellschaft für Ernährung, DGE) are 10 milligram (mg) per day for men and 15 mg per day for women aged 19 to 51 years with the exception of pregnant and lactating women. Higher values are hold for pregnant women (30 mg/d) and breastfeeding mothers (20 mg/d), as they have special needs (DGE 2017).

Similar recommendations are given by the European food safety authority (EFSA) with 11 mg per day for men and postmenopausal women and 16 mg per day for women of reproductive age based on the amount of ingested iron necessary for the absorption of the estimated average amount of iron lost each day (EFSA 2015).

1.3.1 Iron in the human body

The entire iron in a well-nourished adult human body amounts to 2 – 5 g. The most important storage organs for iron are the liver, the spleen, the gastrointestinal mucosa and the bone marrow. About 60 % of the body's iron is an active constituent of hemoglobin (Hb) and about 10 % is incorporated in muscle myoglobin. The daily absorption rate counts 0.5 – 2 mg. There is no known controlled mechanism of iron excretion. Iron loss via feces, urine, blood loss, sweat, hair loss, desquamation and sloughing of intestinal epithelial cells is a passive, uncontrolled process and amounts to 1 – 2 mg per day. As the excretion of iron is not controlled, the body status of iron is tightly regulated by the amount of iron absorption in the gastrointestinal (GI) tract. The maintenance of a robust and steady extra- and intracellular iron concentration is required to keep vital processes and to avoid unwanted adverse effects of iron in the human body. Hemoglobin synthesis alone

requires 20 – 25 mg iron per day. To cover the requirements iron is also recycled within the human body (Chifman *et al.* 2014, Rochette *et al.* 2015, see figure 1.3).

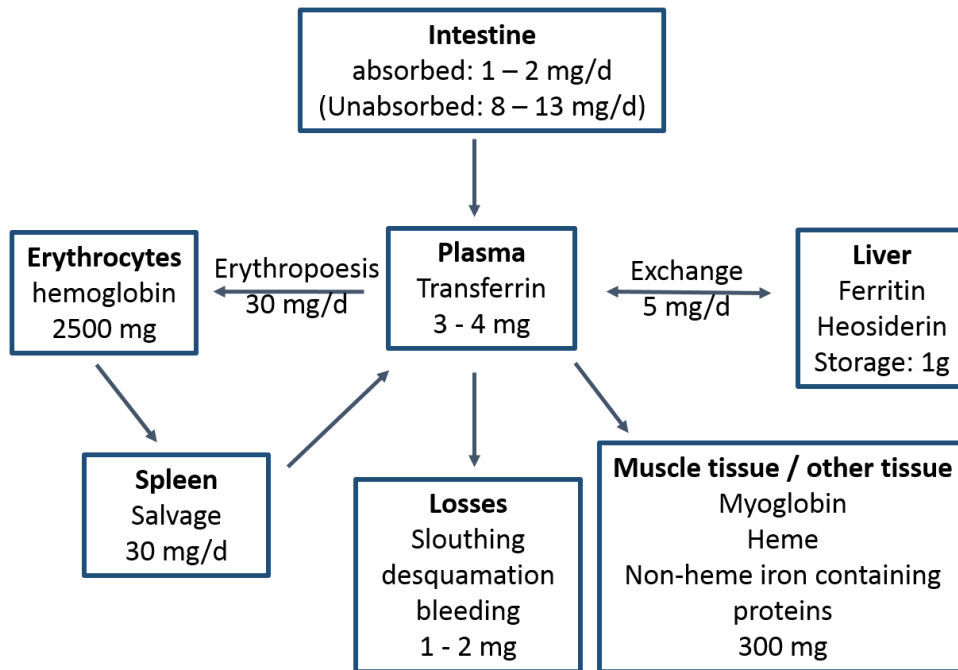


Figure 1.3: Iron absorption, distribution and recycling in the human body (adapted from Pantopoulos *et al.* 2012).

Iron is absorbed by mature enterocytes located at the tips of intestinal villi. Iron absorption mainly occurs in the proximal small intestine. Heme iron is suggested to be absorbed by the heme carrier protein 1 (HCP-1). Human HCP-1 is a hydrophobic protein composed of 446 amino acids (aa), located on 17q11.1 with nine transmembrane domains. After its absorption heme iron is modified by heme oxygenases (HO). HO-1 is expressed by cellular and/or oxidative stress and HO-2 constantly expressed, respectively) leading to the release of Fe(II). Non-heme iron is absorbed via the divalent metal transporter 1 (DMT-1). The absorption of trivalent non-heme iron requires its reduction to divalent iron catalyzed by the ferrireductase duodenal cytochrome b (DCytb). Fe(II) is then transported into the duodenal enterocytes via DMT-1. Another suggested route of iron absorption is via the direct binding of Fe(II) or Fe(III) to mucins (glycoproteins) followed by its incorporation into enterocytes (Prybyszewska *et al.* 2014). Depending on the systemic iron status ionic Fe(II) is either transported to the basal membrane, released and carried to its place of destination or stored bound to ferritin inside the enterocytes

(Prybylska *et al.* 2014). The release of cytosolic iron into the plasma is done by the basolateral iron transporter ferroportin (Fp-1, SLC40A1). Ferroportin is a multidomain transmembrane protein and the only known protein exporting iron out of cells. Ferroportin is expressed in cells involved in iron homeostasis such as duodenal enterocytes, macrophages and hepatocytes (Girelli *et al.* 2017).

The ferroxidase Hephhaestin (HEPH) oxidases divalent iron to trivalent iron which is then transported through the plasma bound to transferrin (Tf) (Chifman *et al.* 2014).

It is further considered that dietary iron is also absorbed in form of ferritin molecules that are resistant to proteolytic digestion. Ferritin molecules are probably absorbed into enterocytes via endocytosis (Beck *et al.* 2014, Girelli *et al.* 2017).

Hepcidin is a small cysteine-rich hormone peptide only made by 25 amino acids. It plays a key role in controlling the iron homeostasis on a systematic level and thereby tuning the balance between iron absorption and iron need for e.g. the erythropoiesis. Hepcidin is mainly produced by hepatocytes and its circulating levels adapt to inflammatory signals, iron overload, iron deficiency, hypoxia and hepatic iron stores. By binding to the iron exporter protein ferroportin hepcidin inhibits iron release from enterocytes. The hepcidin-ferroportin complex is internalized and lysosomal degraded, facilitated by Janus kinase 2 (Jak2) (Chifman *et al.* 2014, Girelli *et al.* 2017). Hepcidin levels are mainly determined by body iron stores, erythropoietic activities and inflammation. It is suppressed by iron deficiency to enable a maximum of iron absorption from the gut. When the iron stores are replete hepcidin expression is stimulated mainly through Bone morphogenetic protein 6 (BMP6), which responds to increased transferrin saturation. In order to increase the production of red blood cells hepcidin expression is also suppressed. Under inflammation, hepcidin synthesis is stimulated mainly by interleukin 1 β (IL-1 β) and IL-6.

The body's iron status can be categorized in iron deficiency with anemia (IDA), iron deficiency (ID), normal iron status and iron overload. Generally, ID is defined as a status with empty iron storages meaning a compromised iron supply to the tissues. When the iron deficiency limits the erythropoiesis, IDA is present. According to the World Health Organization (WHO) IDA is measured as a hemoglobin value (Hb) below a 2-fold standard deviation (SD) of a comparable population, e.g. of a similar

age group or a similar gender group (WHO, 2001). Causes for both ID and IDA can be blood loss or a low dietary iron bioavailability. Functional consequences of ID can include adverse effects to cognitive performance and to the immune status, physical growth retardation in children and impairment of energy supply to by muscles. IDA increases the infant mortality and the perinatal risks for both neonates and mothers. ID is the most frequent nutritional disorder worldwide. It affects more than 2 billion of people worldwide (Girelli *et al.* 2017). Affected are not only non-industrialized countries and here mostly preschool children and pregnant women but also most of the industrialized countries with 30 – 40 % of preschool children and pregnant women being iron deficient. According to the WHO, prevention strategies should involve governmental strategies and strategies from non-governmental organizations such as reduction of poverty, improve access to diversified diets and improved health service systems (WHO 2001).

The most common method to screen for ID is to determine the prevalence of anemia by measuring the blood hemoglobin (Hb) levels and hematocrit (Hkt) levels. Anemia is defined as a Hb level below 120 g/L in women and 130 g/L in men and a Hkt level below 7.45 mmol/L in women and 8.07 mmol/L in men. Still, anemia is not a specific indicator for ID. ID occurs about 2 – 5 times more often than IDA in individuals (WHO, 2001). Even though each method has its own limitations, measurements of serum ferritin, serum Fe and transferrin saturation in combination with the Hb level and the Hkt levels enable to characterize the body's iron status in detail (WHO 2001).

1.3.2 Iron deficiency in inflammatory bowel diseases

The prevalence of anemia in IBD patients was denoted as 27 % for CD patients, as 21 % for UC patients and as 24 % for IBD patients in European countries. In total 57 % of the anemic patients were iron deficient (Filmann *et al.* 2014). Anemia and iron deficiency are considered to be the most common systemic complications in IBD (Avni *et al.* 2013).

1.3.3. Iron and gastrointestinal bacteria

Iron is an essential nutrient for almost all gut bacteria including enteric pathogens such as *Salmonella*, *Shigella* or pathogenic *Escherichia coli*. An exception are *Lactobacilli* which are able to grow without iron if they are kept in a nucleotide-rich medium (Dostal *et al.* 2013, Zimmermann *et al.* 2010, Imbert *et al.* 1998).

Members of the genus *Lactobacillus* are thought to be beneficial for the host i.e. by preventing the colonization of pathogens. Although their number (< 1 %) of the total bacterial population in the gut is small. *Lactobacilli* are also used as probiotics in fermented food or in supplements. Still, their role in different diseases remains unclear. It is observed that in CD patients the abundance of *Lactobacilli* is often enriched. So far it is not explained whether *Lactobacilli* participate in the disease or just adapt to the inflammatory milieu (Heeney *et al.* 2017).

Other exceptions of iron-dependency for bacteria, although not in context of the gut microbiota, are *Borrelia burgdorferi*, the lyme disease pathogen, which doesn't possess iron-protein-encoding genes and *Treponema pallidum*, the syphilis pathogen. Nevertheless, it needs to be added that *B. burgdorferi* and *T. pallidum* both are obligate intracellular parasites and thereby probably indirectly dependent on the iron metabolism of the host (Andrews *et al.* 2003). A large number of bacteria have iron transport systems or other systems to scavenge iron, including siderophores (*Enterobacteriaceae*), to compete for iron with other bacteria and with the host (Dostal *et al.* 2012). The availability of iron and the competition for iron influences the virulence and the colonization of bacteria in the gut (Zimmermann *et al.* 2010). The majority of the body's iron pool is tightly bound to several proteins and thereby its availableness to pathogens is limited. But there is no comparable system for dietary iron sequestration in the gut. It is therefore obvious that the availability of iron in the gut impacts the microbial composition. Iron might be a growth-limiting factor for many bacteria and several iron-dependent bacteria might compete for the unabsorbed iron in the colon (Zimmermann *et al.* 2010, Andrews *et al.* 2003).

1.3.4 Clinical efficacy of oral versus intravenous iron treatment

In human IBD patients, the high prevalence of iron deficiency anemia requires therapeutic intervention. Depending on the cohort the prevalence of ID/anemia in

IBD patients ranges from 6 % up to 74 %. Anemia can be an additional burden due to an impaired cognitive function and might negatively affect the quality of life (Avni *et al.* 2013).

Iron can be applied on an oral basis or an intravenous basis. Although the oral iron treatment is the standard therapy, gastrointestinal side effects and the potency to exacerbate intestinal inflammation support clinical implementation of an intravenous iron treatment. It is also known that a high concentration of luminal iron might affect the gut microbiota composition and disease activity in patients suffering from IBD.

The pharmacokinetic of an oral iron treatment differs from that of an intravenous iron treatment. Oral iron is absorbed as described above and incorporated into plasma transferrin after its basolateral release from duodenal cells. It is easy applied, cheap and effective in mild to moderate iron deficiency. The most common oral iron replacement compound is ferrous sulfate containing iron in its divalent form of iron salt. Intravenous given iron is first taken up by macrophages and then released into the blood. The efficacy of intravenous iron is superior to an oral iron treatment and rapid-acting. Intravenous iron preparations contain ferric iron in its core surrounded by a carbohydrate shell that acts as a stabilizer and prevents uncontrolled iron release (Girelli *et al.* 2017).

1.4 The iron storage protein ferritin

Ferritin has been purified from horse spleen tissue and described for the first time in 1937 by Vilem Laufenberger and named “iron rich protein” (Arosio *et al.* 2008). Laufenberger speculated correctly that ferritin serves as an iron depot in the body. Ferritin is probably the most important iron storage protein. It is found in all cell types including plants and bacteria with the exception of yeast and it is expressed in most tissues. The most common function of ferritin is the storage of iron via binding and sequestering intracellular iron (Arosio *et al.* 2008).

The typical ferritin structure is composed of 24 subunits. Vertebrates have two, sometimes three different subunits. The different subunits are named after their relative molecular mass as light, “L”, 20 kDa with 173 amino acids (aa), middle “M”, 21,1 kDa and heavy, “H”, 22,8 kDa with 183 aa. The subunits H and L self-assemble to a 450 kDa protein and build a large cavity which is able to harbor up

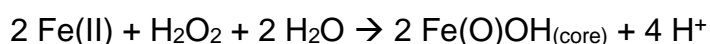
to 4500 iron atoms. Although the amino acid sequence identity is only around 15 % to 55 % the ferritin structure in eukaryotes and prokaryotes is highly conserved (Arosio *et al.* 2008, Ebrahimi *et al.* 2015, Kell *et al.* 2014, Alkhateeb *et al.* 2010). Bacteria and plants have only one type of subunit. They form homopolymers only of 12 subunits (Ferreira *et al.* 2000).

Ferritin H and ferritin L are encoded by different genes. Ferritin H is located on chromosome 19, 19q13.1, and ferritin L is located on chromosome 11, 11q13, in humans (Kato *et al.* 2001, Di Sanzo *et al.* 2016). Ferritin H and ferritin L have different properties and compose the ferritin molecule as a heteropolymere. Ferritin H has ferroxidase activity, whereas ferritin L facilitates the storage of Fe inside the protein shell (Kell *et al.* 2014). The ratio of ferritin H to ferritin L differs between species and tissues. Ferritins rich in L subunits are found in spleen and liver, both in organs which are characterized by a high iron turnover (spleen) or iron storage (liver). Ferritins rich in H subunits are found in heart and brain, both important organs with highly need of defense for oxidative damage. Heteropolymers rich in the L subunit are more stable and capable to harbor a higher numbers of iron atoms, whereas heteropolymers rich in the H subunit have a greater anti-oxidative potential due to the ferroxidase activity of this subunit. However, the H:L ration is not fixed but rather variable and can be modulated, e.g. by inflammatory conditions (Torti *et al.* 2002).

The subunits fold into a 4 helix bundle and assemble into a nanocage of around 12 nm in diameter (Kell *et al.* 2014) with hydrophilic channels for transporting iron atoms into the ferritin cavity. The incorporation of iron into ferritin molecules is facilitated by the iron chaperone poly (rC)-binding protein 1 (PCBP1). During the transportation of iron into the inner side of ferritin oxidation of ferrous iron (Fe(II)) is catalyzed by the ferroxidase activity of ferritin H inducing ferric iron Fe(III) deposition in the ferritin cavity as oxohydroxide core. This “ferroxidation center” catalyzes Fenton-like reactions to sequester iron (Arosio *et al.* 2008).



or



The Fenton-reaction was first published by and named after Henry Fenton in 1894. Ferritin L doesn't have ferroxidase activity but is indispensable to facilitate iron hydrolysis and mineralization (Keogh, 2013). The oxidation of iron not only enables the tight packing of iron atoms inside the cavity but at the same time the risk of spontaneous oxidation of the Fe(II) is avoided. Spontaneous oxidation would lead to the formation of reactive oxygen species (ROS), e.g. H₂O₂. ROS in consequence might cause cell damage. Besides its function as iron storage, ferritin protein acts as an important inhibitor of such free radical production. Iron release from ferritin is not yet fully understood. Channel-gated pathway release and lysosomal proteolytic pathways have both been suggested (Keogh, 2013).

Besides the cytosolically expressed ferritin which is assembled from ferritin H and ferritin L, there is a mitochondrial ferritin, encoded by the mitochondrial ferritin chain gene FTMT. It is located on chromosome 5 (Keogh *et al.* 2013). The precursoral protein contains a mitochondrial leader sequence which is cleaved upon entry to the mitochondria. The mature protein assembles to ferritin shells and has intact ferroxidase activity (Alkhateeb *et al.* 2010). Mitochondrial ferritin has structural and functional similarities to cytosolic ferritin H. It is mainly expressed in testis and brain and participates in the regulation of iron distribution between cytosol and mitochondria (Gao *et al.* 2014). Since a while it is known that ferritin can also appear in the cell nucleus. It is the same ferritin found in the cytoplasm and not coded on a separate gene. However, the function of nuclear ferritin and the transportation mechanism still needs to be clarified (Alkhateeb *et al.* 2010). Ferritin is also found in serum and is measured as a marker of body iron status. Thus, serum ferritin alone is not informative as it not only affected by iron load but also by inflammatory status (Kell *et al.* 2014).

Until now, there is only one gene known coding for ferritin H consisting three introns. Beside the coding gene there are more than 20 intron-less copies spread around different chromosomes. The function of these so called "pseudogenes" needs yet to be clarified but there is evidence that they play a role in regulation ferritin expression (Di Sanzo *et al.* 2016).

1.4.1 Regulation of ferritin

The expression of both ferritin subunits H and L is under transcriptional and translational control of iron, cytokines, hormones and oxidative stress. Ferritin as part of the iron homeostasis is controlled by a group of iron regulatory proteins including transferrin and transferrin receptor. On a translational level, the synthesis of the ferritin H subunit and the ferritin L subunits is controlled by iron regulatory proteins (IRP 1 and IRP 2) binding to iron responsive elements (IRE) in both ferritin H and ferritin L mRNAs. IREs bound to IRPs block the translation in the absence of available iron. IRP degradation is induced by iron or heme. Ferritin is also controlled by proteins that coordinate the cellular immune defense against stress and inflammation. Tumor necrosis factor (TNF) and interleukin-1 α (IL-1 α) alone or together are able to induce ferritin H expression. Oxidative stress influences the ferritin H expression either directly or via influencing the activity of IRPs (Zandman-Goddard *et al.* 2007). The H:L ratio is regulated on a transcriptional level: the H subunit is redox sensitive via antioxidant responsive elements (ARE) (Kato *et al.* 2001).

1.4.2 Ferritin and inflammation

Perturbation in ferritin homeostasis are detrimental for the iron homeostasis but might also play a role in inflammatory conditions. Altered ferritin levels are reported for numerous diseases, infections and malignancies. Whether this is a cause or consequence remains to be explored in most of the inflammatory conditions (Zandman-Goddard *et al.* 2007).

1.4.3 Altered ferritin expression

In one Japanese family a single point mutation in the IRE motif of the ferritin H subunit is reported to cause an inherited iron overload, in particular increased serum iron, increased transferrin saturation, maximal iron deposition in hepatocytes and high serum ferritin level. The heterozygous A49T mutation probably leads to a higher binding affinity of IRP to the ferritin H subunit mRNA suppressing the translation of the H subunit mRNA (Kato *et al.* 2001).

Neuroferritinopathy is an adult-onset neurodegenerative disease affecting the basal ganglia and clinically leading to movement disorders. It is also known as hereditary ferritinopathy and neurodegeneration with brain iron accumulation type 2 (NBIA2) and cataloged as MIM 606159 (Koegh, 2013). It is associated with iron accumulation in the brain, predominantly in the basal ganglia and was first described and named by Curtis *et al.* in 2001. They identified an adenine insertion at position 460-461 in the gene coding for the ferritin L chain which might cause the disease. Aggregates of ferritin and iron in the brain are accompanied by low serum ferritin level in patients suffering from neuroferritinopathy (Curtis *et al.* 2001). By now, there are around 70 reported cases all carrying a mutation in the ferritin L gene (Koegh *et al.* 2013). Hyperferritinemia with or without cataract (MIM 600886) is another genetic disease caused by various mutations touching the ferritin L gene. One of these mutations was reported by Beaumont and colleagues in 1995. A single point mutation in the IRE region of ferritin L, an adenine (A) to guanine (G) substitution, leading to a disturbed binding affinity of IRPs to the IRE region (Beaumont *et al.* 1995).

Several studies suggest that ferritin H might be involved in the pathogenesis of malignancies. Elevated serum ferritin level are found in colon cancer, breast cancer and esophageal adenocarcinoma. Overexpression of ferritin H in transgenic mice was associated with a fast development of thymic lymphoma/leukemia (Hasegawa *et al.* 2012).

IRP2-knockout leads to an overexpression of ferritin H and ferritin L in IRP2^{-/-} mice. These mice have accumulated iron in the brain and accumulated ferric iron in the cytosol of neurons. They develop a neurodegenerative disease characterized by ataxia, bradykinesia and tremor (Rouault 2001 and LaVaute *et al.* 2001).

The opposite, a downregulation of ferritin H, is observed in heart failure. In this context, Omiya and colleagues describe an elevated load of oxidative stress and cardiomyocyte cell death in rats with downregulated ferritin H (Omiya *et al.* 2008). For the L subunit of ferritin several genetic variations are known leading to different disorders ranging from hereditary ferritinopathy to chronic anemia (Arosio *et al.* 2008).

1.4.4 Ferritin H deletion in intestinal epithelial cells

It is already known that a complete knockout of ferritin H in mice leads to embryonic lethality between day 3.5 and day 9.5 of development indicating not only the importance of ferritin already in early stage but also the different functional roles of the H and L subunit. As the ferroxidase activity of ferritin H is the only known cytoplasmatic activity which is able to convert toxic Fe^{2+} to less toxic Fe^{3+} , embryonic lethality might be based on toxic damages or the loss of bioavailability of iron. In the absence of ferritin H, homopolymers are not able to compensate the missing function of ferritin H.

In contrast, heterozygous $\text{H}^{+/-}$ mice develop without any phenotypical abnormalities despite a lower level of ferritin (Ferreira *et al.* 2000).

Mice with a conditional ferritin H deletion lost their cellular iron stores and showed increased serum Fe level. Still, they did not show any further abnormalities and survived for two years if kept on a normal diet. Severe liver damage was observed when the mice were fed a diet high in iron (Darshan *et al.* 2009).

Kistler *et al.* investigated if and to what extent ferritin-H deletion influences body's iron distribution. Splenic and hepatic iron content was decreased.

A disturbed iron metabolism of $\text{Fth}^{\Delta/\Delta}$ mice was extensively described by Vanoaica *et al.*. A loss of the mucosal iron storage was observed concomitant with increasing iron load in serum, liver and spleen which was enhanced with increasing age. Increased iron absorption rates lead to the assumption that ferritin h is involved in limiting iron absorption.

No morphological changes were observed along the intestinal tract (Vanoaica *et al.* 2010).

1.5 Model of inflammation: DSS-induced colitis

Animal models of inflammation are widely used to study the pathogenesis of IBD. DSS-induced colitis mimics the clinical and histological characteristics of UC. DSS is a heparin-like polysaccharide with a variable molecular weight (MW) from 5 to 1400 Kilodalton (kDa). To induce colitis it is given via the drinking water. The polymere is degraded in the stomach and reaches the cecum with a MW of 750 to 5000 Da. Typical signs of inflammation appear on day 3 and are maximal

expressed on day 7 of DSS application. The severity of inflammation depends on the mouse strain, the dosage of DSS, length of treatment and the sex of mice. By varying the dose and the administration days it is possible to induce acute, chronic or relapsing colitis (Laroui *et al* 2012; De Fazio *et al.* 2014).

DSS-induced colonic inflammation is characterized by rectal bleeding, loss of body weight, diarrhea, ulcerations and infiltration of granulocytes. Experiments with T- and B-cell deficient mice (C.B.-17scid, Rag1^{-/-}) could show that the adaptive immune system doesn't seem to play an important role in DSS-mediated inflammation. DSS impairs the integrity of the mucosal barrier via a direct toxic effect on epithelial cells (Wirtz *et al.* 2007). Further, pro-inflammatory cytokines such as IL-1, IL-6, TNF and IFN γ are upregulated. Laroui describes a DSS-MCFA (medium chain length fatty acids) vesicles which can fuse with the colonic cell membrane allowing the DSS to enter the colonocytes. The presence of such DSS-MCFA vesicles may influence the cellular pathways and reduce the intestinal barrier functions (Laroui *et al.* 2012).

It is known that DSS administration induces changes in the gut microbiota. De Fazio describes a reduction of *Bacteroides/Prevotella* whilst *Bacillaceae* were increased. This was reversed after 4 days on water without DSS.

2. AIM

This thesis aims for a better understanding of the involvement of iron in the pathogenesis of IBD focusing on the composition of the intestinal microbiota in dependency to iron in an inflamed environment. We hypothesized that oral iron replacement in IBD patients with iron deficiency would exacerbate gut microbial dysbiosis in contrast to intravenous iron replacement. Therefore, an open-labelled clinical trial with iron deficient patients with or without IBD was conducted with pre- and post-iron therapy measurements. The individuals served as their own controls. This open labelled randomized control study was performed at the University of Alberta, Edmonton, Canada. We measured fecal bacterial communities by high-throughput sequencing.

The iron status and the metabolite profile were assessed at baseline and after three month of iron treatment.

Based on the observation that ferritin is higher expressed in inflamed $TNF^{\Delta ARE/WT}$ mice compared to non-inflamed $TNF^{\Delta ARE/WT}$ mice (Werner *et al.* 2011) the aim of this thesis was to elucidate the role of the epithelial cell-specific iron storage protein ferritin H in the context of chronic intestinal inflammation. Therefore, mice carrying a ferritin H deletion in the intestinal epithelium were challenge with DSS to investigate the susceptibility to a triggered inflammation (see figure 2.1).

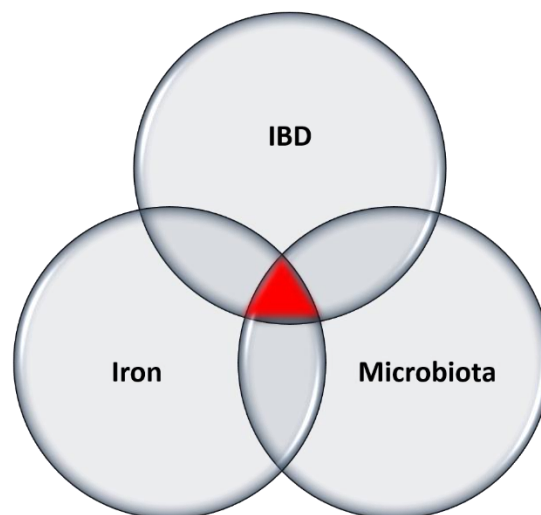


Figure 2.1: Schematic diagram of the interdependent topics of this thesis.

3. MATERIALS AND METHODS

3.1 Human trial

3.1.1 Study design

The study subjects were recruited during 2010 from two tertiary centers in Edmonton, University of Alberta Hospital, UAH, and Royal Alexandra Hospital, RAH. The participants were identified by their treating gastroenterologists. Written consent was obtained prior to web-based randomization, with an allocation of 1:1 to either IV or oral iron therapy. The including criteria and the excluding criteria are given in in table 3.1.

Table 3.1: Inclusion and exclusion criteria for subjects participating in the clinical iron trial. CRP: C-reactive protein, IBD: inflammatory bowel diseases, IRT: iron replacement therapy, IV: intravenous.

Inclusion criteria	Exclusion criteria
Iron deficient as defined by ferritin < 30 µg/L (if CRP normal) and/or iron saturation < 16 % measured within 2 weeks of enrolment (Ferritin < 100 µg/L if CRP was elevated)	Coeliac disease, known malignancy other than skin cancer, primary hematological disorder
No oral iron therapy within 2 weeks of enrolment	Known hypersensitivity to iron sucrose
No IV iron therapy within 3 months of enrolment	History of intolerance to IRT
18 years of age and older and able to give written consent	Severe or multiple medical co-morbidities
	Active IBD that require surgery within 12 weeks of enrolment
	Ferritin > 200 µg/L
	pregnant
Confirmed diagnosis of IBD by standard radiology, endoscopy and histopathology findings	Blood transfusion
	Antibiotics within the last 3 months of enrolment
	Iron supplementation
	Untreated folate and/or vitamin B ₁₂ deficiency

The control group consisted of participants with a recent upper GI bleeding such as peptic ulcer disease, with a deliberate low iron diet (vegetarians), or women with non-specific GI symptoms and menorrhagia.

All subjects were iron deficient, as defined as iron saturation < 16 % with or without ferritin < 30 µg/L if the CRP level was normal or ferritin < 100 µg/L if the CRP level was elevated.

The study population included 31 patients with Crohn’s disease (CD N = 31), and 22 patients with ulcerative colitis (UC N = 22) as well as 19 subjects with iron deficiency without IBD as control group (NI N = 19). The diagnosis of IBD was made by standard radiology, endoscopy and histopathology findings. A written informed consent was obtained prior to web-based randomization.

For patients in the PO cohort, 300 mg iron sulfate PO twice a day was prescribed for 3 months. For those in the IV cohort, 4 or 3 separate 300 mg iron sucrose infusions were given to subjects with iron deficient anemia or iron deficiency without anemia, respectively. The study was approved by the local ethics committee and registered with clinicaltrial.gov (NCT01067547).

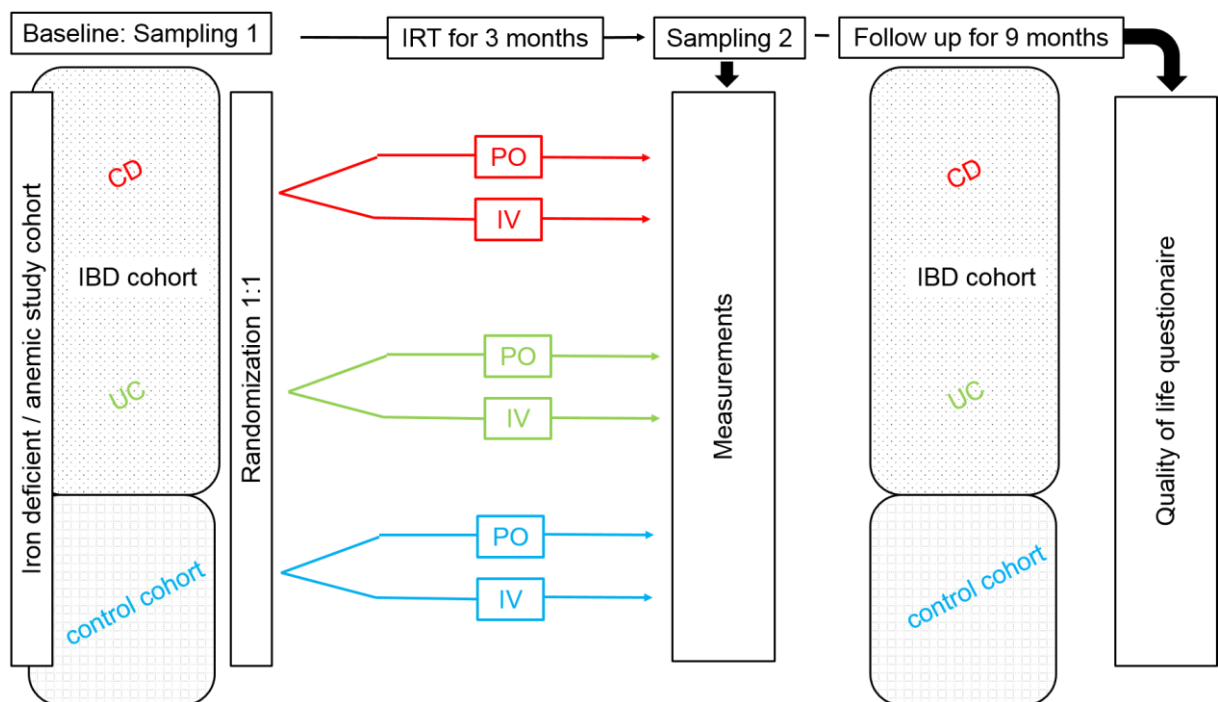


Figure 3.1: Study design. CD: Crohn’s disease, IV: intravenous iron therapy, PO: oral iron therapy, UC: ulcerative colitis.

All participants were reviewed at the baseline time point and three months after initiating the iron treatment. After randomization, all subjects underwent two unprepared flexible sigmoidoscopies, one at baseline and the other one 3 months later. At these time points stool specimens as well as Shorten Inflammatory Bowel Diseases Questionnaires (SIBDQ) and Euro Quality 5 dimensions questionnaire

combined with an Visual analogue scale Questionnaire (EQ5D) were also collected. At 3 months, all subjects were reviewed for medication adherence and possible adverse event. IBD activity was assessed with the Modified Harvey Bradshaw Index (HBI) for CD and with the Partial Mayo (pMayo) for UC. In addition, CRP was determined. Adherence to the PO treatment was assessed by pill count at week 12 and adherence to the IV treatment was determined by attendance at the infusion clinic (see figure 3.1).

The disease activity and clinical course of IBD cohort were also reviewed at 12 months after the initiation of the treatment. Any replacement therapy related event was recorded in a descriptive fashion.

This was an open label study where the patients and investigators were not blinded. However, the final results were coded prior to analysis, therefore the final analysis was performed in a blinded fashion.

3.1.2 Stool sampling

For the collection of stool samples, all participants received a stool collection kit with a pictorial instruction on how to collect stool samples and to minimize contaminations. Stool samples were frozen within 30 min and kept at – 80°C until further processing for sequencing.

One aliquot (100 mg) of each fecal sample was mixed with 500 µl phenol:chloroform:isoamyl, 900 µl of ASL buffer (Qiagen, QIAamp® stool mini kit) and 200 mg zirconia beads. Cells were lyzed using a bead beater (FastPrep-24; MP Biomedicals LLC) at 6.5 M/s, 0.5 min (4 cycles interrupted by 3 minutes on ice) and incubated at 95 °C (5 min, 800 rpm). After centrifugation (1 min, 13,000 g) the aqueous phase was collected into a fresh Eppendorf tube and filled up to 1.2 ml with ASL buffer. DNA was purified using the QIAamp® stool mini kit following the manufacturer's instructions, with addition of RNase treatment (37 °C, 30 min). The DNA concentrations and the purity (A260/A280 ratio) was determined by spectrophotometric analysis (ND-1000 spectrophotometer, NanoDrop Technologies, Willigton, USA). The V4 region (253 bp) of 16S rRNA genes was amplified (30 cycles) as described previously (Caporaso *et al.* 2011; Caporaso *et al.* 2012). Amplicons were purified using the AMPure XP system (Beckmann), pooled in equimolar amount and sequenced in paired-end modus (PE200) using

the MiSeq system (Illumina Inc) following the manufacturer's instructions and a final DNA concentration of 16 pM and 5 % (v/v) PhiX standard library.

3.1.3 Microbiota analysis

Raw read files were demultiplexed (allowing a maximum of 2 errors in barcodes) and each sample was processed using usearch (Edgar *et al.* 2010) following the UPARSE approach (Edgar *et al.* 2013). First, all reads were trimmed to the position of the first base with quality score < 3 and then paired. The resulted sequences were size filtered excluding those with assembled size < 380 and > 440 nucleotides. Paired reads with expected error > 3 were further filtered out and the remaining sequences were trimmed by 10 nucleotides on each side to avoid GC bias and non-random base composition. For each sample, sequences were de-replicated and checked for chimeras with UCHIME (Edgar *et al.* 2011). Sequences from all samples were merged, sorted by abundance, and operational taxonomic units (OTUs) were picked at a threshold of 97 % similarity. Finally, all sequences were mapped back to the representative sequences resulting in one OTU table for all samples. Only those OTUs with a relative abundance above 0.5 % total sequences in at least one sample were kept. RDP classifier (Wang *et al.* 2007) was used to assign taxonomic classification to the OTUs representative sequences (80 % confidence). A phylogenetic tree was constructed using fasttree (Price *et al.* 2010). OTU counts were expressed as proportions of total sequences per sample and normalized to the minimum count of total sequences observed across samples. For estimation of diversity within samples (alpha-diversity), the Shannon index was calculated and transformed to the corresponding effective number of species as described by Jost (Jost *et al.* 2007). Sequences of candidate OTUs were assigned to taxa with valid names in nomenclature using the EzTaxon database (Chun *et al.* 2007).

All datasets, including OTU counts and abundances of taxonomic groups are provided in the supplemental data. Statistical analyses were performed in the R programming environment or using SIMCA-P+12 (Umetrics, Umeå, Sweden). For all tests, p-values below 0.05 were considered of significant effects. The Benjamini-Hochberg method was used for adjustment after multiple testing. Because the

present study is explorative and our intention was to generate hypotheses on possible associations between fecal bacterial populations and metabolites production rather than to make statements on the clinical relevance of some bacterial taxa, and because p-values adjustment is still a matter of debate in clinical science (Feise *et al.* 2002), interpretations were based on p-values prior to adjustment. Nevertheless, for the sake of clarity and transparency, adjusted p-values are provided in the supplemental data.

Variations of OTU and taxonomic counts were tested using one-way ANOVA followed by heteroscedastic t-test for pairwise comparisons. Prior to testing for variations in OTU or taxonomic counts the individual counts < 0.5 % were zeroed and only prevalent and dominant taxonomic groups or molecular species (i.e. detected in at least 30 % of the participants, with a median sequence abundance of > 1 % in at least one group) were considered. For beta-diversity analysis, generalized Unifrac distances were calculated using the package GUniFrac (Chen *et al.* 2012). For visualization of the relationships between bacterial profiles, non-parametric multiple dimensional scaling (NMDS) plots were computed using the packages vegan and ade4.

3.1.3 Iron measurement

Fecal samples were freeze-dried (Christ-Heraeus), weighed and introduced into quartz vessels. Subsequently, 1 mL of suprapure HNO₃ (Merck) subjected to sub-boiling distillation (Berghoff distillation apparatus) was added. Vessels were introduced into a pressure digestion system for 10 h at 170 °C. Resulting solutions were filled up to 10 mL with Milli-Q H₂O and iron content was determined using an ICP-AES Spectro Ciros Vision system (SPECTRO Analytical Instruments). Samples were introduced at a flow rate of 0.6 mL/min using a peristaltic pump connected to a Meinhard nebulizer with a cyclone spray chamber. The measured spectral line corresponding to iron was 259.941 nm. Radiofrequency power was set to 1400 W. The flow of plasma and nebulizer gas was set to 13 L Ar/min and to approximately 0.6 L Ar/min, respectively. Three blank samples followed by one control sample of a certified standard were acquired each ten measurements. Iron levels were calculated on a computerized lab-data management system integrating

sample measurements with calibration curves, output from blank and control samples, and digested sample weight.

3.2 Mouse model experiments

The mouse model used for all experiments is a cross breeding between a mouse model with a ferritin H allele carrying loxP sites ($Fth^{lox/lox}$ mice, Darshan *et al.* 2009) and a transgenic villin-Cre mouse.

The cre/lox recombination system provides the ability to excise DNA flanked by loxP sites in a tissue-specific manner. The Cre-recombinase is an integrase from bacteriophage P1, catalyzes DNA recombination between two loxP sites. A loxP site consists of 34 bp: two 13 bp inverted repeats separated by an 8 bp spacer. The Cre-recombinase recognizes loxP and excises the intervening DNA sequence between two loxP sites (Chambers, 1994; el Marjou *et al.* 2005).

Targeting intestinal epithelial cells via exogenous transgenes is limited regarding the renewal of the epithelium every 2 – 5 days. For this project we used a constitutively recombination system combining a powerful recombinase with a tissue-specific promoter.

Villin is a cytoskeletal protein. Its expression pattern is strictly tissue-specific in proliferative stem cells and differentiated cells. Villin is mainly produced in epithelial cells which develop a brush boarder (epithelial cells of the small and large intestine) and in kidney proximal tubulus (Pinto *et al.* 1999).

The specific expression of the Cre-recombinase (El Marjou *et al.* 2004) in intestinal cells leads to a cut out of the “floxed” ferritin H allele only in intestinal cells ($Fth^{\Delta/\Delta}$ mice, Vanoaica *et al.* 2010). Hereby, the cre-recombinase is expressed under the control of a regulatory region of the villin gene, in combination named vil-cre. The chosen 9 kb regulatory region which was shown to target stable and homogenous expression of transgenes in small and large intestine along the crypt-villus axis and in differentiated enterocytes as well as in the immature cells of the crypts (El Marjou *et al.* 2004, see figure 3.2).

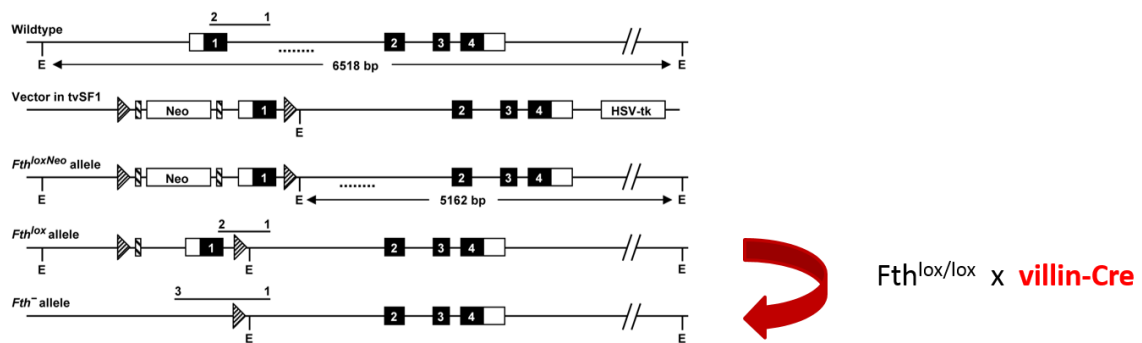


Figure 3.2: Genetic background of the mouse model $Fth^{\Delta\Delta}$ (Darshan et al. 2009).

3.2.1 Ferritin H deletion in intestinal epithelial cells of C57BL/6 mice

$Fth^{lox/lox}$ mice on a C57BL/6 background were kindly donated by Lukas Kühn (ISREC Swiss Institute for experimental Cancer Research, Ecole Polytechnique Fédérale de Lausanne (EPFL), 1015 Lausanne, Switzerland) and transferred to the specific pathogen-free facilities (SPF) at the Chair of Nutrition and Immunology, Technical University of Munich (TUM), Campus Weihenstephan, via *in-vitro* fertilization (IVF). After breeding homozygous mice from $Fth^{wt/lox}$ mice, $Fth^{lox/lox}$ mice were backcrossed with heterozygous Villin-Cre mice on a C57BL/6 background to generate $Fth^{\Delta\Delta}$ mice (El Marjou et al. 2004). Mice were raised under SPF conditions and kept on a standard chow diet (Ssniff) or on a control diet (Altromin, C1000) *ad libitum* (*ad lib.*) for experiments. Mice were kept in plastic cages with wood shavings placed on the bottom and under a 12 h light and 12 h dark photoperiodic cycle. Drinking water was provided *ad lib.*.

Under experimental conditions, mice were observed, weighted and monitored for mortality daily. The severity of colitis was assessed using disease activity index (DAI) as described below. Mice were killed by using CO₂.

All mice experiments were performed in accordance with the local standing committee for ethical experimentation on animals approved by the Animal protection authority of the District government (Regierung von Oberbayern, München, Germany, 55.2-1-54-2532-17-2013).

3.2.2 Genotyping

Mouse tails were digested in 190 microliter (μ l) tail buffer (see table 3.2) with 10 μ l Proteinase K at 65 °C, 1000 revolutions per minute (rpm) for 8 hours (h). Proteinase K (Roth) was inactivated by heating up to 95 °C for 10 min. After short centrifugation 1 μ l supernatant was used for the polymerase chain reaction (PCR; Biometra T personal). Genotyping was performed using Crimson Taq DNA polymerase (BioLabs, #M03525, 5000 U/ml, see table 3.3, Peglab, peqstar). PCR products were run through a 1 percentage (%) agarose gel containing gel red (Biotium, 41003) at 100 volt (V). Bands were visualised under ultraviolet (UV) light.

Table 3.2. Tail buffer. Tail buffer was mixed in ddH₂O. pH was set to 8.3 using 6 M HCl.

Chemical compound	concentration
TRIS	10 mM
KCl	50 mM
Nonidet	0.45 %
Tween	0.45 %
Gelatine	1mg/mL

Table 3.3: Primer sequences for genotyping. Bp: base pair, PCR: polymerase chain reaction, WT: wildtype.

Gene	Forward primer	Reverse primer	Annealing temperature	Length of PCR product
Ferritin H	5'-cca-tca-acc-gcc-aga-tca-ac-3'	5'-cgc-cat-atc-cca-gga-gga-c-3'	58	WT: 419 bp Fth ^{lox} : 337 bp
Vilin-Cre	5'-caa-gcc-tgg-ctc-gac-ggc-c-3'	5'-cgc-gaa-cat-ctt-cag-gtt-ct-3'N	55	WT: 585 bp Vilin-Cre: 200 bp

Table 3.4: PCR mix for genotyping.

Reagent	Volume [μ l] per sample	Final concentration
5 x Crimson tag buffer	5	1x
dNTPs, 10 mM each	0.5	200 μ M
MgCl ₂ 25 mM	1.5	1.5 mM
Forward primer, 10pmol/ μ l	0.5	200 nM
Reverse primer, 10pmol/ μ l	0.5	200 nM
Crimson tag, 5 U/ μ l	0.125	0.625 U
ddH ₂ O	14.9	
DNA	2	
Σ	25 μ l	

Table 3.5: PCR program for genotyping with Crimson tag polymerase.

Step	Temperature [$^{\circ}$ C]	duration	No. of cycles/step
I	95	60 sec	1
II	95	30 sec	35
	58	20 sec	
	68	45 sec	
III	68	5 min	1
IV	4	endless	1

3.2.3 Characterization of mice

Mice were kept as described above. Body weight development was assessed daily. Mice were killed after 12 and 20 weeks for phenotypical characterization. Tissue weight of spleen, liver, caecum and kidneys was determined after 12 and 20 weeks. Histological sections of different gut sections were examined by H & E staining to evaluate morphological and cellular structures. Iron status was characterized by measuring hematocrit level and hemoglobin level.

3.2.4 Induction of colitis

Colitis was induced using DSS. All mice were single caged during the phase of experiments and daily monitored for weight, general behavior, drinking rate, stool consistency and rectal bleeding.

DSS was applied by the drinking water, control animals received plain water. Mice were challenged at the age of 12 weeks. In a first experiment 1 % DSS was given

for a time period of 14 days (d) followed by a recovery phase of 14 d to female $Fth^{lox/lox}$ and $Fth^{\Delta/\Delta}$ mice and male $Fth^{lox/lox}$ and $Fth^{\Delta/\Delta}$ mice. Mice were kept on plain water during the recovery phase (see figure 3.3). The drinking volumes were recorded for 7 days and the DSS load was calculated as:

total drinking water [ml] x (DSS [g] / 100 ml).

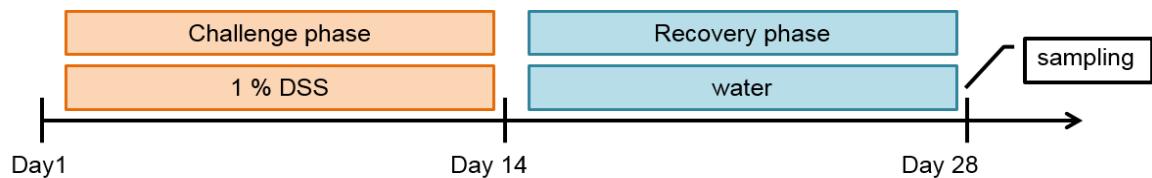


Figure 3.3: DSS challenge with recovery phase.

In a second experiment, 1 % DSS was given only to female $Fth^{lox/lox}$ and $Fth^{\Delta/\Delta}$ mice for a time period of 12 d without a following recovery phase, control animals received plain water. The point of time of 12 days was chosen in dependence of the maximal differences in changes of DAI in the recovery experiment (see figure 3.4).

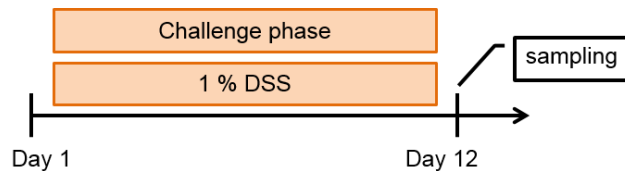


Figure 3.4: DSS challenge with optimized sampling time point.

3.2.5 Macroscopical scoring

Mice in an experimental setting were monitored daily for body weight changes, stool consistency and rectal bleeding and evaluated according to table 3.6. A disease activity index (DAI) was determined for each animal as the sum of the scores divided by 3, giving a DAI ranging from a minimum of 0 to a maximum of 4 points.

Table 3.6: Evaluation of mice. Composition of disease of activity index.

Score	Loss of body weight [%]	Stool consistency	Rectal bleeding
0	0	normal	negative
1	1 – 5		
2	5 – 10	pasty	first appearance
3	10 – 15		> 1 d
4	> 15	diarrhea	> 2 d

3.2.6 H & E staining and histological scoring

Tissue samples were fixed in 4 % neutral buffered formalin for 48 h. After dehydration (Leica, TP 1020, see table 3.8) tissue samples were embedded in paraffin (Leica, EG 1150H) in embedding cassettes (Roth RotiLab®, E479.1) and cut into sections of 5 micrometer (μm , Leica, RM 2225). Sections were stained with hematoxylin and eosin (H & E) (Sigma-Aldrich, Steinheim, Germany, Leica ST 5020, see table 3.7). The sections were examined by microscopy (Precipoint, digital microscope M8). Histological scoring of cross-sectioned cuts was performed by blindly assessing the degree of lamina propria mononuclear cell infiltration, crypt hyperplasia, goblet cell depletion and architectural distortion in the different gut sections, resulting in a score from 0 (not inflamed) to 12 (massively inflamed).

Table 3.7: Staining program for H & E staining.

Step	Compound	Duration	Step	Compound	Duration
1	Xylene	3	9	Eosin yellow	2
2	Xylene	3	10	70 % EtOH	1
3	100% EtOH	2	11	96 % EtOH	1
4	96 % EtOH	2	12	100 % EtOH	1
5	70 % EtOH	1	13	100 % EtOH	1.5
6	dest. H ₂ O	1	14	xylene/EtOH	1.5
7	Hemalaun	4	15	Xylene	2
8	Water	2	16	Xylene	2

Table 3.8: Dehydration program.

Station	Vacuum	Compound	Duration [h]
1	no	70 % EtOH	1
2	yes	70 % EtOH	1
3	yes	80 % EtOH	1
4	yes	96 % EtOH	1
5	yes	96 % EtOH	1
6	yes	100 % EtOH	1
7	yes	100 % EtOH	1
8	yes	100 % EtOH	1
9	yes	Xylene	1
10	yes	Xylene	1
11	yes	Paraffin	1
12	yes	Paraffin	1

3.2.7 Hematocrit determination

Hematocrit (Hkt) concentrations were measured using the microhematocrit method (No. 749311, Brand, Wertheim, Germany; Hematocrit-centrifuge 2104, Hettlich, Tuttlingen, Germany). Briefly, blood from the *vena cava caudalis* was taken with ethylenediaminetetraacetic acid (EDTA) –flushed syringes (60 % EDTA). Heparanized capillaries (microhematocrit tubes, brand, 749311) were filled to $\frac{2}{3}$ with EDTA-blood, closed and centrifuged for 5 min at 8000 rpm (Hearaeus instruments Biofuge haemo). The hematocrit value was assed using a stencil provided by the manufactor of the named kit.

3.2.8 Hemoglobin determination

Hemoglobin (Hb) concentrations were measured using the methemoglobin method (reagent: Bioanalytic 4001-1010, Umrich, Freiburg, Germany; photometer: UV-DK-20, Beckmann, Munich, Germany). Briefly, 10 µl EDTA-blood taken from the *vena cava caudalis* were incubated with 2, 5 ml Drabkin solution (Hb-solution, analyticon, 6942) for 5 min. Cyanomethemoglobin concentration was photometrically assed at 600 nm.

3.2.9 Non-heme iron determination

The concentration of non-heme iron in liver, spleen and serum was determined from Fth^{flox/flox} and Fth^{Δ/Δ} mice. Tissue samples were cut in pieces (approximately 1 cubic millimeter, mm³) and 30 mg of tissue samples were dissolved in acid-mix (6 M hydrochloric acid (HCl) and 20 % trichloroacetic acid (TCA, Sigma-Aldrich T 9159) (v/v)). After incubation (65 °C, 20 h) the non-heme iron content was measured photometrically by using a commercial kit (Feren-B 6501-6001, Bioanalytic, Umrich/Freiburg, Germany).

3.2.10 Iron staining

Staining of iron in formalin-fixed tissue sections (4 μm) was performed using a commercial kit (Sigma-Aldrich Accustain Iron Stain®), HT20).

3.2.11 SAA – ELISA

The concentration of serum amyloid A (SAA) in plasma was measured using the Mouse SAA ELISA kit (Immunology Consultants Laboratory, E-90SA).

Blood was taken from the *vena cava* immediately after sacrificing and opening the mouse and centrifuged for 10 min at 3000 rpm (Eppendorf Centrifuge 5415 R). The plasma was stored at – 80°C until used for the analysis. All further steps were done according to the manufacture's protocol.

3.3 Statistical analysis

Statistical analysis was performed using GraphPad Prism version 6.0 (GraphPad Software, San Diego, California). Data comparing two groups were analyzed using the unpaired t test. Data comparing more than two groups were analyzed using One-Way or Two-Way ANOVA followed by an appropriate multiple comparison procedure. Differences between groups were considered significant if p values were < 0.05, < 0.01 or < 0.001.

4. RESULTS

4.1 Open-labelled clinical trial to compare oral vs. intravenous iron replacement therapy in IBD patients

An open-labelled clinical trial was performed to compare the effects of per oral versus intravenous iron replacement therapy (IRT). Eligible subjects were identified through the University of Alberta Hospital and Royal Alexandra Hospital gastroenterology and inflammatory bowel disease outpatient clinics and inpatients services.

The baseline characteristics between the oral group and the intravenous group were similar in terms of age, sex, hemoglobin, CRP in patients with IBD, disease activity index and quality of life scores, shorten form inflammatory bowel disease questionnaire and EuroQuality 5 Dimension Visual analogue scale.

In terms of concurrent medication, the most striking differences between the oral group and the intravenous group were that more subjects in the IV group took prebiotics, probiotics or antibiotics compared to the subjects in the PO group and more subjects in the IV group took either a combination of an immunosuppressant and a biological drug (infliximab, adalimumab or vedolizumab) compared to the subjects in the PO group.

4.1.1 Characteristics of participants

Anemic subjects diagnosed with IBD and control anemic participants without gastrointestinal disorders were enrolled in the study and randomized into the oral and intravenous iron replacement therapy. Fecal samples were collected at baseline and after the end of intervention, 3 months later, from each participant of the study. The stool samples were analyzed by high-throughput 16S rRNA gene sequencing for analysis of bacterial communities.

A total of 72 participants completed the study, 36 persons in each of the PO and IV group, 19 non-inflamed controls, 31 patients with CD and 22 patients with UC. Medication adherence was validated after 3 months by iron pill count. The mean percentage of pills taken was 80 %, the range was 70 % to 100 %. All subjects in the IV group completed their prescribed course of iron infusion indication 100 %

adherence. The PO route was therefore associated with a higher risk of medication non adherence compared with the IV route in all subgroups.

4.1.2 IRT restores iron storage independently of the administration route

After the iron intervention the mean iron saturation level in the control group was not different between the PO route and the IV route (23.3 % +/- 6.3 % vs. 23.9 % +/- 9.9 %). Comparable mean iron saturation was archived after 3 months in the IBD group with 24.7 % +/- 15.8 % for the PO route and 24.2 +/- 13.4 % for the IV route. Numerically more patients in the IV treatment group normalized their iron saturation than in the PO treatment group (82 % vs. 76 %). This difference was not statistical significant. In the CD subgroup, the mean iron saturation at 3 months was 25.3 % +/- 13 in the IV group and 17.7 % +/- 10.5 in the PO group, which was not statistically different. Numerically more patients in the IV treatment group normalized their iron saturation level than in the PO group (77% vs. 50 %). This difference was not statistically significant ($p = 0.3$). In the UC subgroup the mean iron saturation at 3 months was 21.8 % +/- 14.7 in the IV group and 32.3 % +/- 17.4 in the PO group, which was not statistically significant different. Numerically, more subjects in the PO group normalized their iron saturation level than in the IV group (64 % vs. 50 %). However, this did not reach statistical significance ($p = 0.4$).

A statistically significant higher serum ferritin level at 3 months was noted in the IV group compared to the PO group in both control and IBD cohort (Figure 4.1) with 113.2 $\mu\text{g/L}$ vs. 57.3 $\mu\text{g/L}$ for the CD group and 146 $\mu\text{g/L}$ vs. 40.2 $\mu\text{g/L}$ for the UC group. The mean serum ferritin level after 3 months in the non-inflamed group was 24.7 $\mu\text{g/L}$ +/- 15.8 in the PO group and 100 $\mu\text{g/L}$ +/-74.4 in the IV group, which was statistically higher ($p = 0.0007$). The mean serum ferritin after 3 months in the CD subgroup was significantly higher in the IV group than in the PO group (57.3 $\mu\text{g/L}$ +/- 34.3 vs. 113.2 $\mu\text{g/L}$ +/- 106, $p = 0.01$).The mean serum ferritin after 3 months in the UC subgroups was significantly higher in the IV group than in the PO group (146 $\mu\text{g/L}$ +/- 143.8 vs. 40.2 $\mu\text{g/L}$ +/- 21.4, $p = 0.003$).

The route of IRT did not affect the hemoglobin levels at 3 months (data not shown). This does not seem to be surprisingly as more than 75 % of the participants were not anemic. The mean hemoglobin level of IBD patients after 3 months was 135.8 g/L +/-12.7 in the PO group and 134.3 g/L +/-12.8 in the IV group with no statistical

difference. The mean hemoglobin in the non-inflamed group was 139.1 g/L +/-19.4 in the PO group and 131.4 g/L +/- 8.1 in the IV group with no statistical difference.

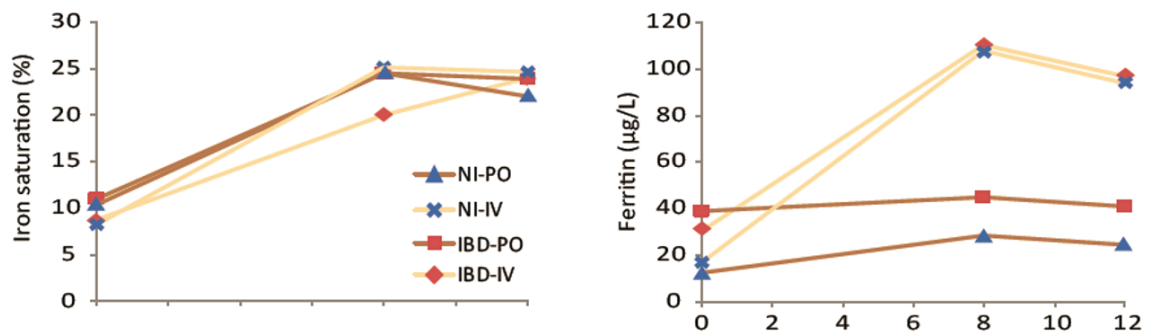


Figure 4.1: Iron replacement therapy restores iron storage independently of the route of administration. Left: Iron saturation in % after two months of iron replacement therapy and after three months iron replacement therapy. Right: Serum ferritin level in µg/L after two months of iron replacement therapy and after three months iron replacement therapy. IBD: inflammatory bowel disease, IV: intravenous, NI: non-inflamed, PO: per oral.

4.1.3 Impact of iron treatment on disease activity and quality of life

Quality of life was assessed via Euro Quality 5 Dimension in combination with a Visual analogue scale (EQ5D). EQ5D is a self-administered questionnaire used to describe health related quality of life. It consists of five dimensions: mobility, self-care, usual activities, pain/discomfort and anxiety/depression and a visual analogue scale for general well-being scored from 0 (worse possible imagined health state) to 100 (best possible imagined health state). Each dimension has three level of severity: no problem (1), some problem (2) and extreme problem (3). EQD% has been validated against Shorten Form 36, a representative questionnaire for general quality of life and against IBD Questionnaire 32 for validity, reliability and responsiveness. EQ5D was selected for this study because it is a generic questionnaire of life assessment and user friendly as it is short and easy to complete.

A shorten form of the Inflammatory bowel disease questionnaire, SIBDQ, containing 10 items in 4 dimensions was also used for this study. The 4 dimensions are bowel symptoms (3 items), systemic symptoms (2 items), emotional functions (3 items) and social functions (2 items).

Overall, there was a trend towards higher magnitude of improved SIBDQ scores in the IBD-IV group but the results did not reach significance. The EQ5D indicated an improvement in CD patients on the IV treatment also suggesting that IV might be associated with a better quality of life in CD (see figure 4.2).

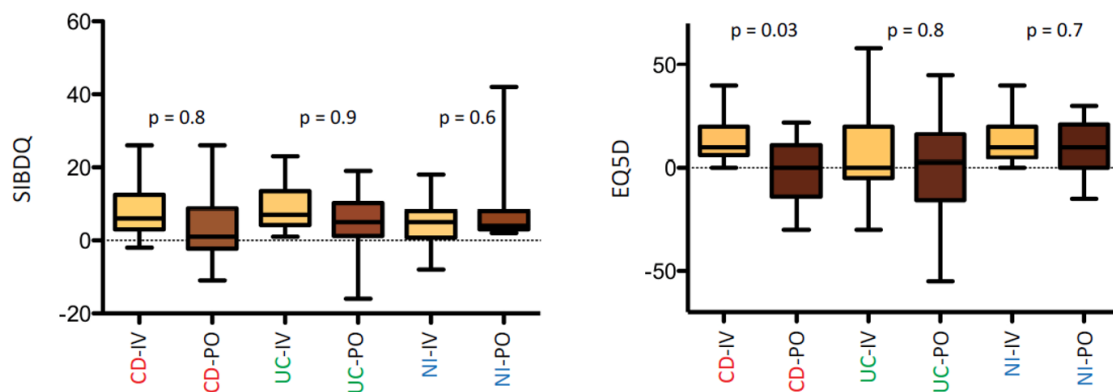


Figure 4.2: % of changes in quality of life was scored according to Shorten IBD questionnaire (SIBDQ) and Euro Quality 5 Dimension Visual Analogue Scale (EQ5D). CD: Crohn's disease, IV: intravenous, NI: non-IBD control anemic subjects, PO: per oral, UC: ulcerative colitis.

To assess the disease activity index in CD patients a modified Harvey Bradshaw Index (MHBI) was used. The MHBI is simplified version of the Crohn's disease activity index with only 5 items. By convention, an increase of HBI by 3 points or more indicates worsening of disease and a HBI of 5 or less points indicates remission.

To assess the disease activity index in UC patients the partial mayo score (p-mayo) was used. It is based on the mayo score but excludes the endoscopic sub-score. The components assessed in this score are bowel frequency, per rectal bleeding, and physician global assessment. By convention, 2 points reduction in p-mayo indicates clinical improvement and a score of 2 or less points indicates clinical remission. This score was chosen because it is widely accepted and a non-invasive tool in monitoring UC activity. It is also user friendly.

The route of IRT did not affect disease activity based on changes in the clinical disease activity indices MHBI and pMayo and serum concentration of CRP (see figure 4.3).

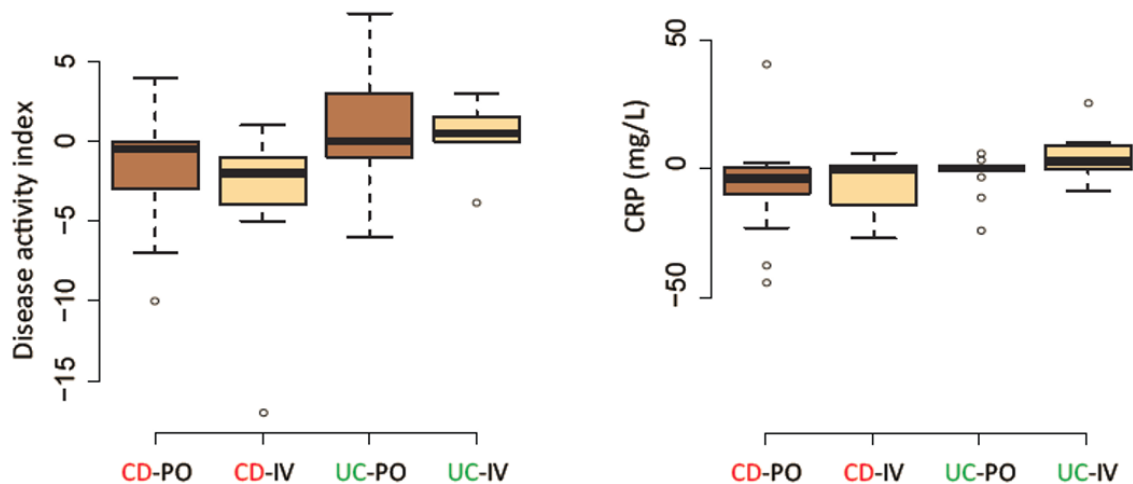


Figure 4.3: IBD activity was assessed with modified Harvey Bradshaw index (MHBI) for CD and partial Mayo score (pMayo) for UC. Values are % changes. CD: Crohn's disease, CRP: C-reactive protein, IV: intravenous, PO: per oral, UC: ulcerative colitis.

With respect to adverse events, one CD participant in the IV group developed arterial thrombosis of the left leg requiring below knee amputation. Other adverse events included generalized arthralgia and headache. In the PO group one participant had self-limiting nausea. No adverse event was reported in the control group.

4.1.4 IBD is linked to specific fecal microbiota fingerprints

Stool samples were collected and fecal bacterial communities of the participants were assessed before and after the iron replacement therapy. A total of 6 726 192 chimera-checked 16S rRNA gene sequences (53 382 +/- 13 153 per sample) were obtained after sequence processing and filtering including a total of 372 OTUs – 121 +/- 37 per sample. Looking at IBD-specific differences in the bacterial diversity and composition, we analyzed all samples independently of the time point of measure. A significant clustering of the samples according to the appearance of IBD was revealed, using multidimensional scaling. Both IBD groups were characterized by marked interindividual differences in the 16S rRNA profiles when compared with samples from non-inflamed participants. The samples from the non-inflamed participants were more homogenous than the samples from inflamed participants.

Regarding to the subtypes of IBD, the CD group were most distinguishable from the non-inflamed control group whilst the UC group was less distinguishable from the non-inflamed group. No specific subclustering according to the disease state was detected. Likewise, patients in an active phase of inflammation or in remission were scattered across the clusters in both subtypes of IBD, UC and CD respectively (see figure 4.4).

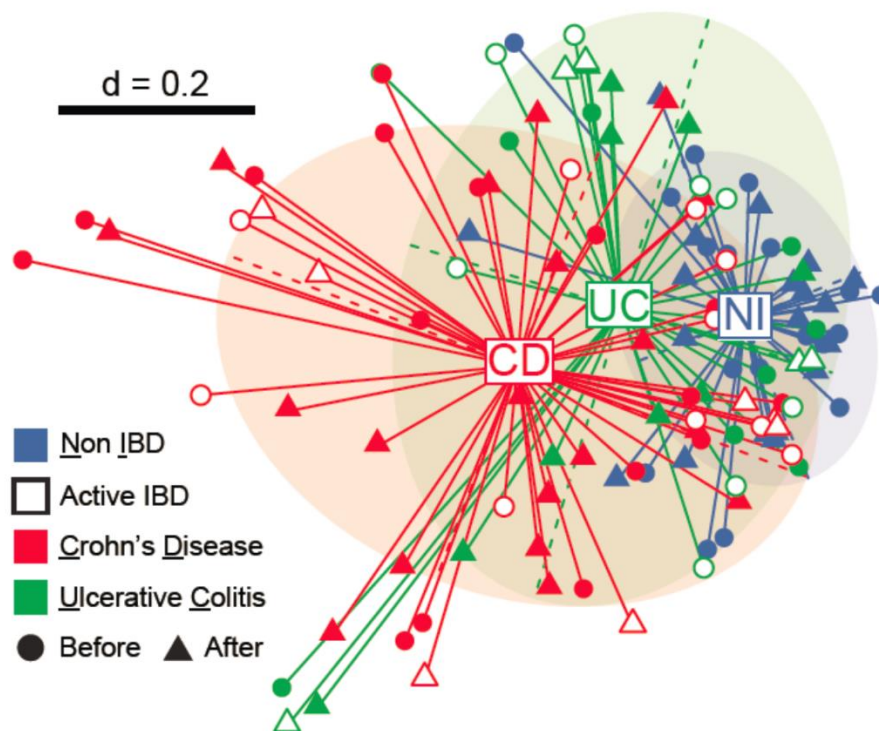


Figure 4.4: NMDS plot based on generalized UniFrac distances, including all patients before and after the iron replacement therapy. Patients with CD are most heterogeneous and in distance to UC and control subjects. CD: Crohn's disease, NMDS: Non-parametric multidimensional scaling, UC: ulcerative colitis.

The Shannon effective diversity analysis was assessed to quantitative measure the count of different species. It was assessed on the species level.

IBD subjects were characterized by a drop of richness in taxa based on the Shannon effective diversity analysis. The drop of taxa richness was seen in both IBD subgroups, CD and UC. It was strongest in CD patients with a median effective count < 15 species (see figure 4.5).

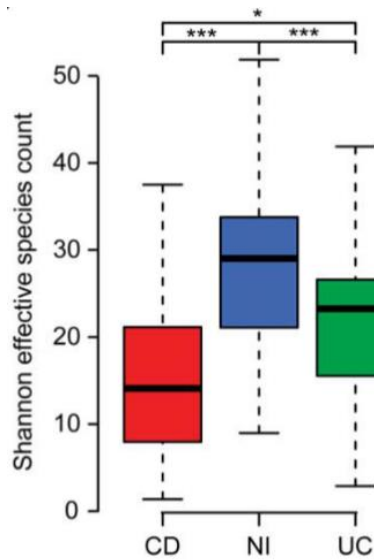


Figure 4.5: Shannon effective diversity box plot shows decreased number of species in both IBD groups, CD and UC. CD: Crohn's disease, NI: non-IBD control anemic subjects; UC: ulcerative colitis.

To see whether differences observed at the level of diversity were associated with changes in the relative abundance of specific bacteria, we looked for significant differences in sequence proportions of taxonomic groups from phyla down to families (see figure 4.6). UC patients and CD patients were sub-divided in subjects with active disease status and subjects in remission.

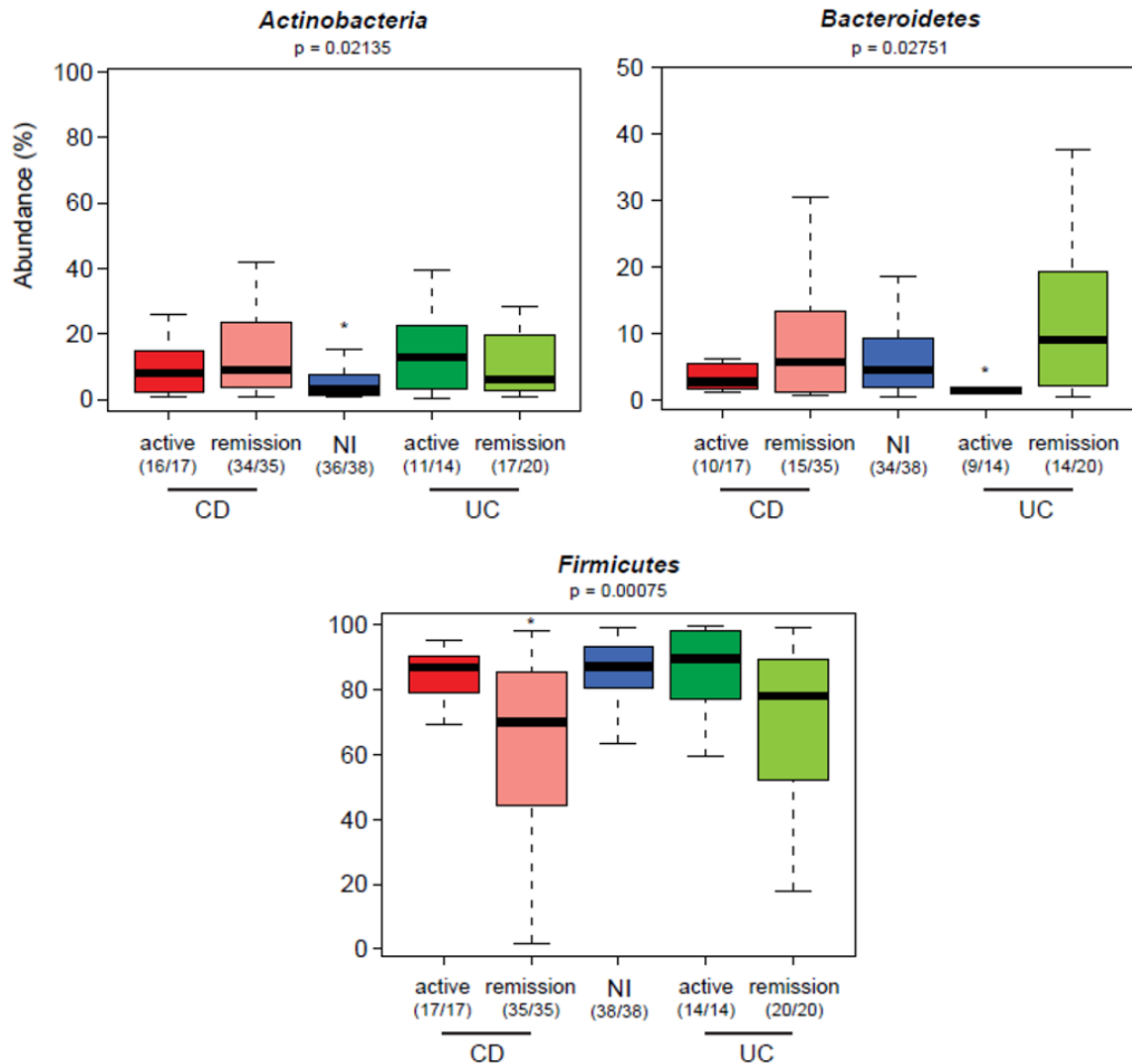


Figure 4.6: Abundance of the most dominant phyla detected in fecal samples. CD: Crohn's disease, NI: non-IBD control anemic subjects, UC: ulcerative colitis. Number of subjects analyzed are given in brackets. The most abundant phylum is Firmicutes, followed by Actinobacteria and Bacteroidetes.

The most dominant phylum found in all subjects was *Firmicutes*. Second dominant phylum found was *Actinobacteria* and followed by the phylum *Bacteroidetes*. In the active phase of inflammation the family of *Bacteroidetes* was totally lost in patients with UC. The abundance of the different phyla is least scattered in non-inflamed subjects.

A drop of the relative abundance of *Clostridiales*, belonging to the family of *Firmicutes*, were observed in CD patients. A higher median abundance of the family of *Christensenellaceae* was found in non-inflamed subjects. *Bifidobacteriaceae*, belonging to the phylum *Actinobacteria*, revealed to be more

abundant in patients with IBD. This might be related to the dietary intake of probiotics, taken in form of commercially yoghurt by 10 participants in this group (see figure 4.7).

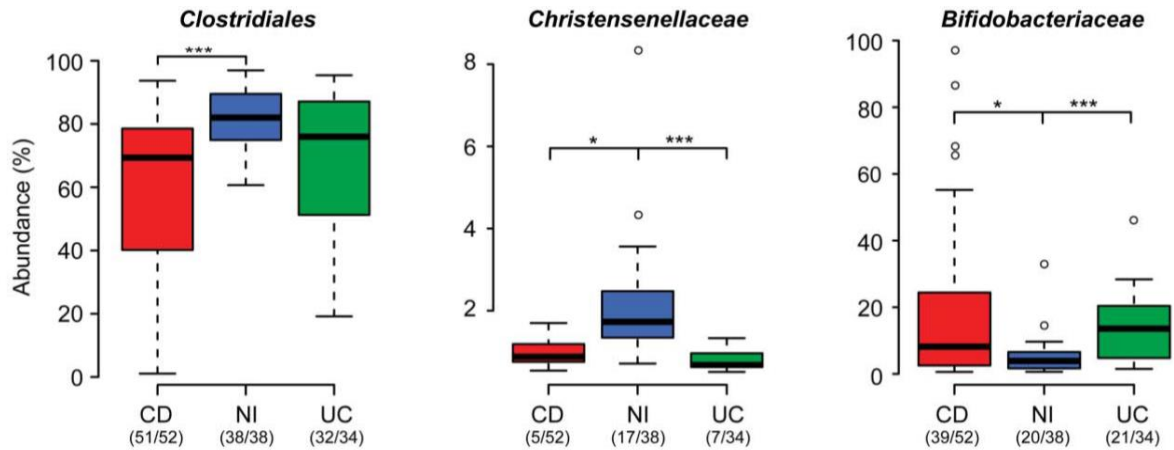


Figure 4.7: Relative abundances of dominant bacterial taxa with significant differences between the CD, UC and control group. The number of samples in which the given bacteria were found are shown in the brackets. CD: Crohn's disease; NI: non-IBD control anemic subjects; UC: ulcerative colitis.

4.1.5 Bacterial communities are prone to instability after iron intervention in anemic IBD patients compared to NI patients

The IBD-specific clustering in the bacterial communities was not overruled by the effect of the iron treatment. We only observed minor effects of the oral and IV iron intervention on the bacterial diversity without any treatment-specific clustering.

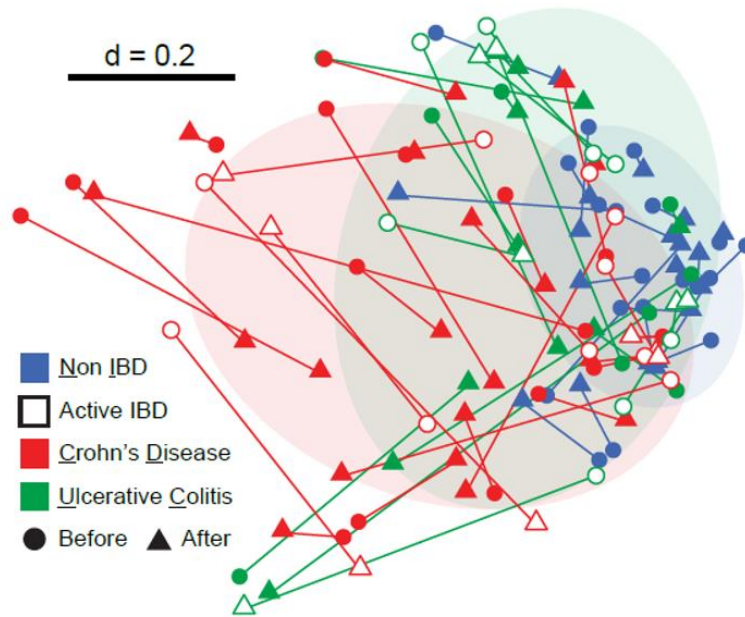


Figure 4.8: NMDS plot showing changes in bacterial diversity between the baseline timepoint and after three months of iron replacement therapy, represented by connected lines. NMDS: non-metric multidimensional scaling. CD: Crohn's disease, NI: non-IBD control anemic subjects, UC: ulcerative colitis.

Moreover, the changes were individual-specific. Distances between the samples before and after the treatment ranged from very short to very high. This might suggest a different sensitivity of the fecal bacterial community from different subjects (see figure 4.9).

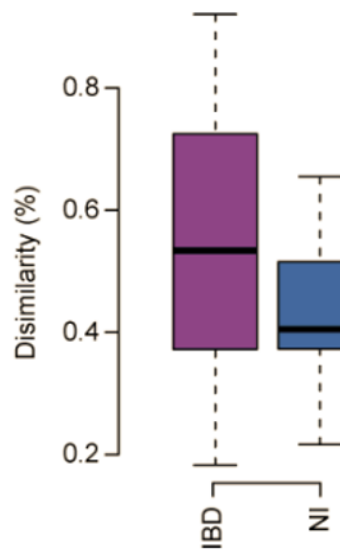


Figure 4.9 Boxplot depict the distribution of generalized UniFrac distances per patient category, indicating that samples before and after IRT are more similar in NI control subjects than in patients with IBD. IBD: Inflammatory bowel diseases, NI: non-IBD control anemic subjects.

Comparing the phylogenetic distances in paired samples we showed that IBD patients (UC and CD as well) were more distantly related as the control paired samples. This might indicate that the fecal bacterial communities of IBD patients are more sensitive to iron-induced alterations than the fecal bacterial communities of the anemic control subjects (see figure 4.10).

CD patients had the lowest number of paired samples (defined as two samples from one individual being most closely related to each other than to any other sample), the control group had the highest number of paired samples.

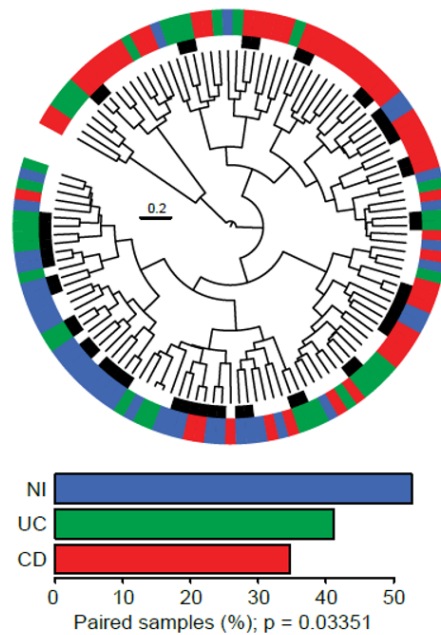


Figure 4.10: Wards clustering dendrogram calculated from phylogenetic distances of all subjects. Paired samples given from one individual located next to each other before and after the iron intervention are marked with black bars at the inner circle. Disease color-code: red for CD, green for UC, blue for NI. The bar plot below shows the percentages of paired samples per group. CD: Crohn's disease, NI: non-IBD control anemic subjects, UC: ulcerative colitis.

We classified patients according to changes in disease status in improved, unchanged and worsen based on the clinical scores and CRP levels.

On the basis of clinical scores and CRP levels, independently of IBD type (CD or UC), a decrease in sequence proportions of a member of the family *Ruminococcaceae* was observed in subjects with improvement of disease (see figure 4.11).

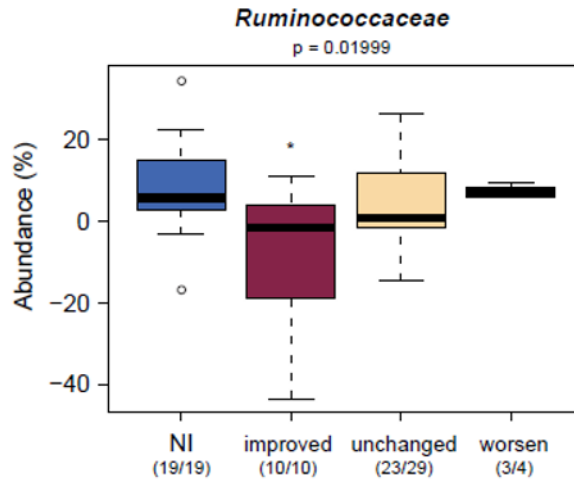


Figure 4.11: A decrease of sequence proportions of the family Ruminococcaceae was observed in subjects with improvement of disease. NI: non-IBD control subjects.

4.1.6 The gut ecosystem is affected by oral iron treatment

Comparing the samples at baseline and after the iron intervention taking into account the route of administration independently of the disease phenotype, the iron content in feces was significantly increased after PO administration ($p = 0.014$) but not after IV treatment ($p = 0.363$). In contrast, the total fecal sulfur concentrations were not significantly changed (see figure 4.12).

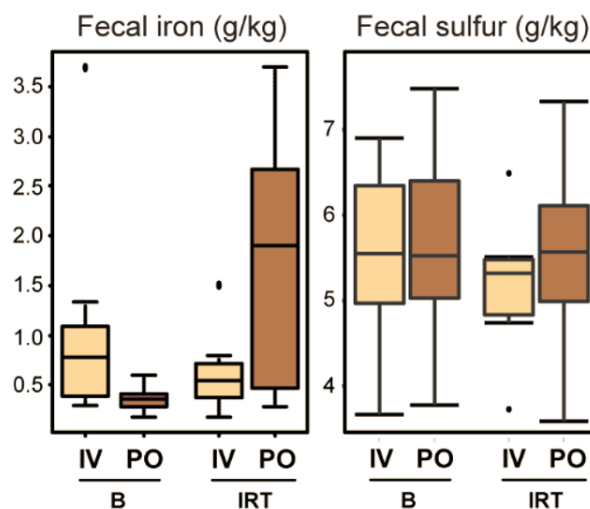


Figure 4.12: Iron and total sulfur content in feces. B: baseline; IRT: after three months of iron treatment therapy; IV: intravenous; PO: per oral.

Independently of disease activity phenotype, we searched for differences between PO and IV treatment when considering delta-values calculated as difference in sequence abundances (after - before). We found five single OTUs that showed differential effects, four of which had lower abundance after oral iron treatment. These four OTUs were identified as *Collinsella aerofaciens* (OTU-6), *Faecalibacterium prausnitzii* (OTU-13), *Ruminococcus bromii* (OTU-23) and *Dorea* sp. *bifidobacterium* (OTU-52). In contrast, one OTU belonging to the genus *Bifidobacterium* (OTU-620) was found in higher relative abundance in feces from subjects treated with iron orally, although four patients in this group consumed prebiotics and probiotics versus six in the IV group (see figure 4.13).

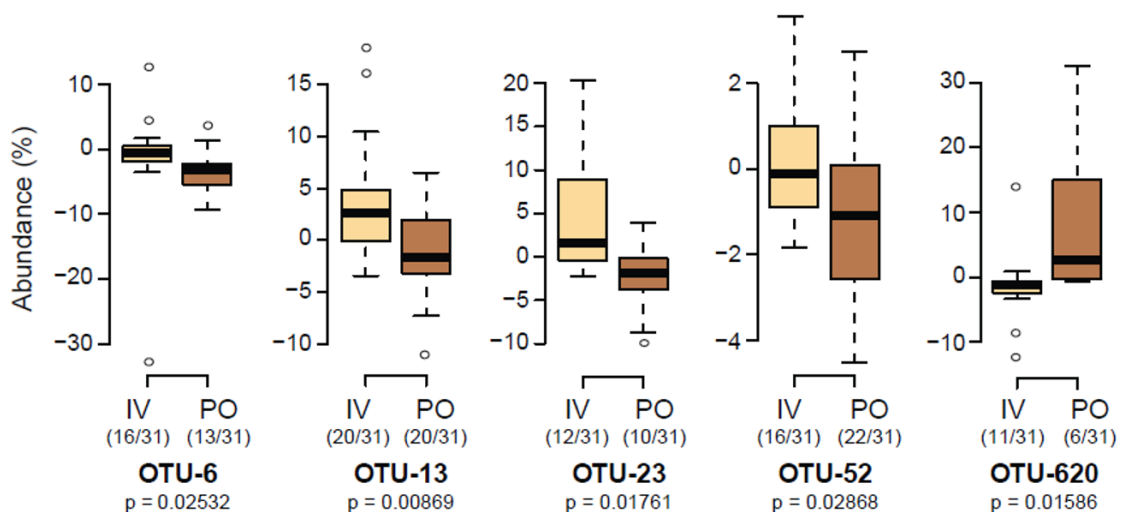


Figure 4.13: Relative abundance of phylotypes that react differently to intravenous (IV) or oral (PO) iron therapy. IRT groups were compared using Mann-Whitney test. Prior to testing, individual counts < 0.5% were zeroed and only prevalent and dominant molecular species (i.e., detected in at least 30% of the participants and with a median sequence abundance > 1% in at least one group) were considered. IRT: iron replacement therapy, OTU: operational taxonomic unit.

4.2 Fth^{Δ/Δ} Mouse model did not show any spontaneous effects but is susceptible for DSS-induced colitis

4.2.1 Ferritin H deletion in intestinal epithelial cells

Fth^{Δ/Δ} mice were characterized for body weight development, tissue weight and iron status. The mice were kept as described in materials and methods for 12 or 20 weeks, respectively. The mice were fed a chow standard diet *ad lib.* and weighted weekly.

4.2.2 Body weight development did not show any abnormalities

The body weight development did not show any abnormalities. There were no statistical differences between both genotypes neither between the male groups nor in the female groups at any point of time. Male Fth^{Δ/Δ} mice were smaller in terms of weight compared to the male control group when killed at the age of 12 weeks with $p > 0.04$. This was not seen in the body weight development of mice living until the age of 20 weeks (see figure 4.14).

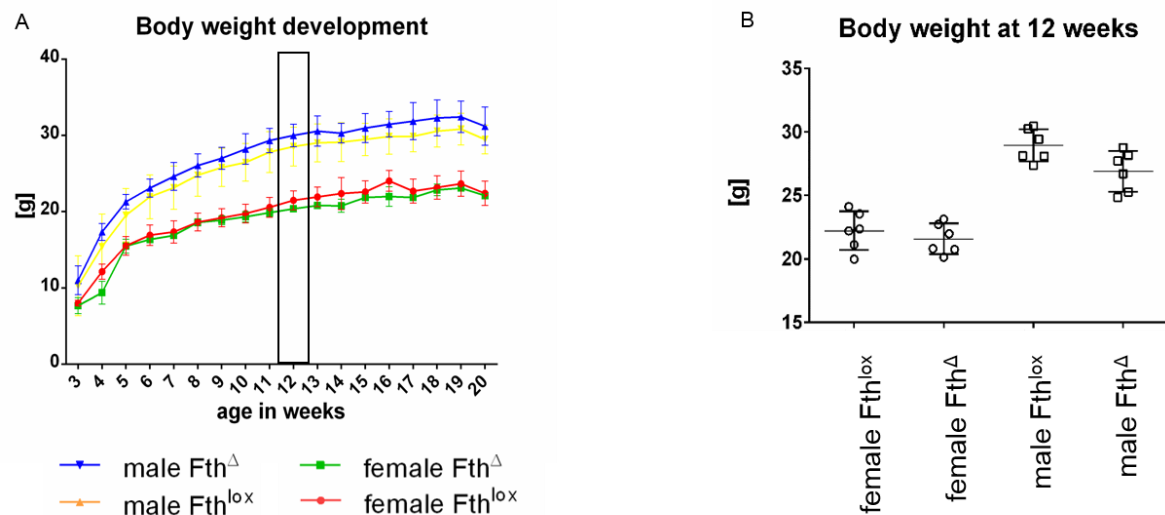


Figure 4.14: Body weight development of Fth^{Δ/Δ} mice and Fth^{lox/lox} mice. Body weight development (A) and body weight at 12 weeks (B) of Fth^{Δ/Δ} mice and control mice (Fth^{lox/lox} mice) over 20 weeks, $n = 6$. Male Fth^{Δ/Δ} mice were statistically thinner than male control mice ($p > 0.04$). There are no statistical differences between the female Fth^{Δ/Δ} mice and the female Fth^{lox/lox} mice nor between the male Fth^{Δ/Δ} mice and the male Fth^{lox/lox} mice (except week 16 for the female mice) in the body weight development of mice until the age of 20 weeks. The black frame in A indicates the timepoint of 12 weeks shown in B.

4.2.3 Regular organ weight parameters in both genotypes

The tissue weights of caeca, spleens, kidneys and stomachs were measured after immediately sacrificing the mice and compared at 12 and 20 weeks of age. At both time points, there was no statistical difference between the different genotypes neither in the male nor in the female groups (see figure 4.15).

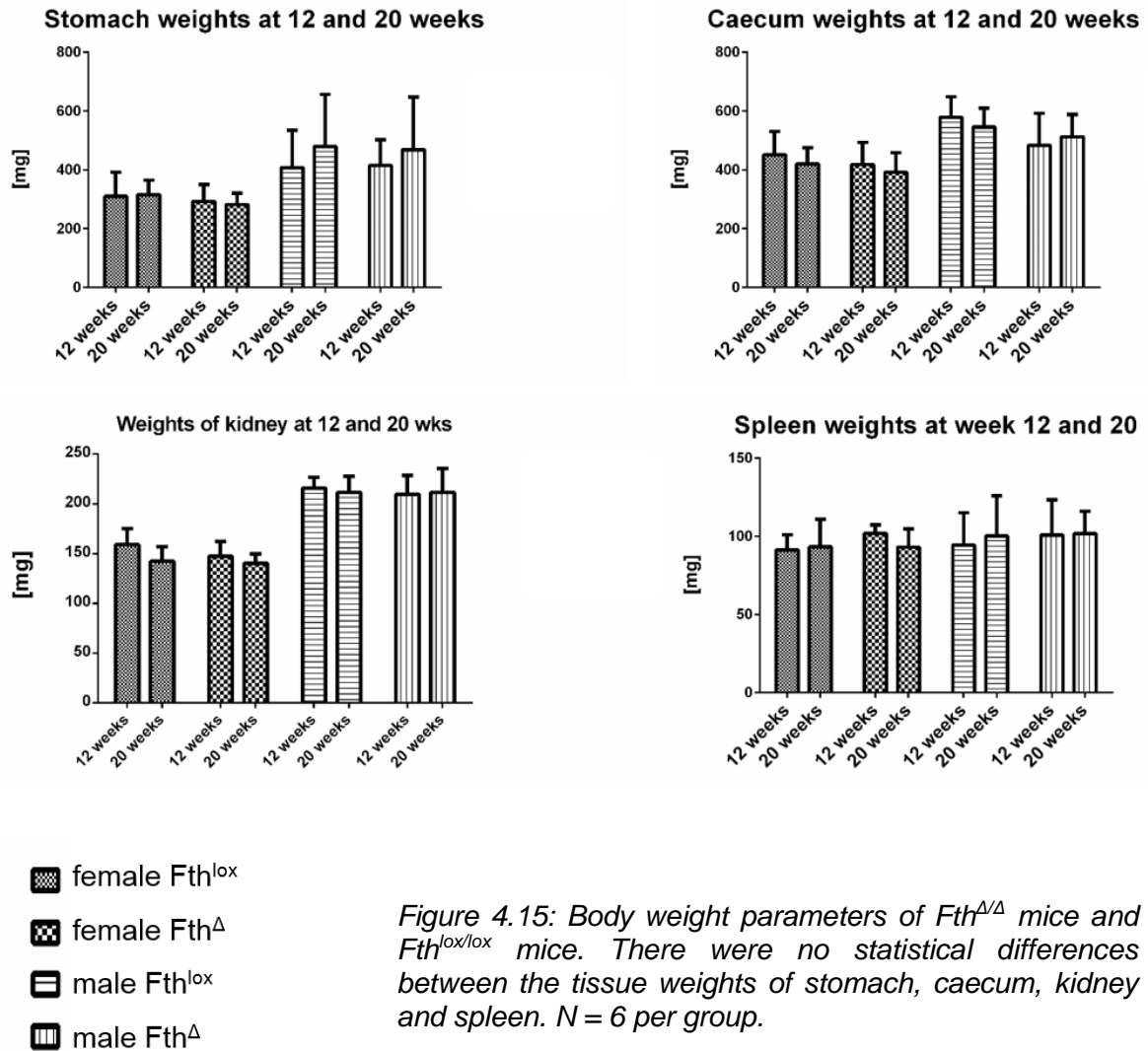
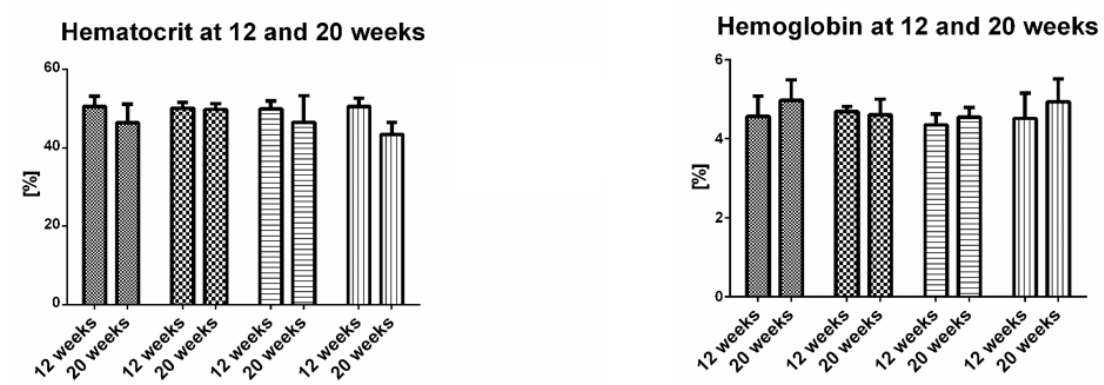


Figure 4.15: Body weight parameters of $Fth^{\Delta/\Delta}$ mice and $Fth^{lox/lox}$ mice. There were no statistical differences between the tissue weights of stomach, caecum, kidney and spleen. $N = 6$ per group.

4.2.3 Iron status tend to be higher in $Fth^{\Delta/\Delta}$ mice

The hematocrit level and the hemoglobin level were measured immediately after sacrificing mice using blood from the *vena cava caudalis* (see figure 4.16).



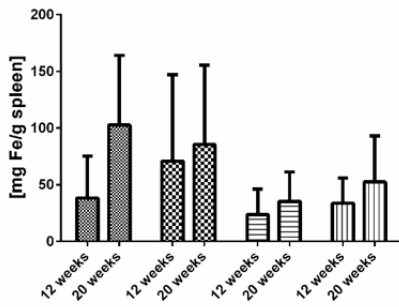
-  female Fth^{lox}
-  female $Fth^{\Delta\Delta}$
-  male Fth^{lox}
-  male $Fth^{\Delta\Delta}$

Figure 4.16: Hematocrit and Hemoglobin of $Fth^{\Delta\Delta}$ mice and $Fth^{lox/lox}$ mice. There are no statistical differences neither for the hematocrit levels nor for the hemoglobin levels between male $Fth^{\Delta\Delta}$ mice and male $Fth^{lox/lox}$ mice at point of time (age of mice) 12 or 20 weeks and no statistical differences between female $Fth^{\Delta\Delta}$ mice vs. $Fth^{lox/lox}$ mice at point of time 12 and 20 weeks.

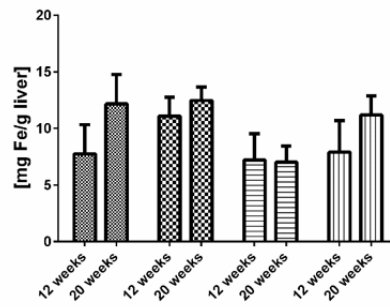
Comparing the Hb and Hkt levels of 12 weeks old mice with 20 weeks old mice in each of the four groups no statistical differences were found except for the Hkt level ($p = 0.002$) and Hb level ($p = 0.03$) in male $Fth^{lox/lox}$ mice.

Non-heme iron was measured in liver tissue and spleen tissue. There is a trend for higher non-heme iron level in $Fth^{\Delta\Delta}$ mice compared to $Fth^{lox/lox}$ mice at 12 weeks of age in both gender groups with significance for the liver tissue of the female mice (see figure 4.17).

Non-heme Fe at 12 and 20 weeks - spleen



Non-heme Fe at 12 and 20 weeks - liver



-  female Fth^{lox}
-  female Fth^{Δ}
-  male Fth^{lox}
-  male Fth^{Δ}

Figure 4.17: Hematocrit and Hemoglobin of $Fth^{\Delta/\Delta}$ mice and $Fth^{lox/lox}$ mice. There are no statistical differences neither for the hematocrit levels nor for the hemoglobin levels between male $Fth^{\Delta/\Delta}$ mice and male $Fth^{lox/lox}$ mice at point of time (age of mice) 12 or 20 weeks and no statistical differences between female $Fth^{\Delta/\Delta}$ mice vs. $Fth^{lox/lox}$ mice at point of time 12 and 20 weeks.

4.2.4 Histological tissue staining revealed no abnormalities in gut tissue structure

Histological sections of different gut sections were examined to compare the morphological and cellular structures (see figure 4.18). H & E stained segments from the small and the large intestine did not show leukocyte infiltration, villus atrophy, crypt hyperplasia or other signs of inflammation. No histological changes could be detected in $Fth^{\Delta/\Delta}$ mice.

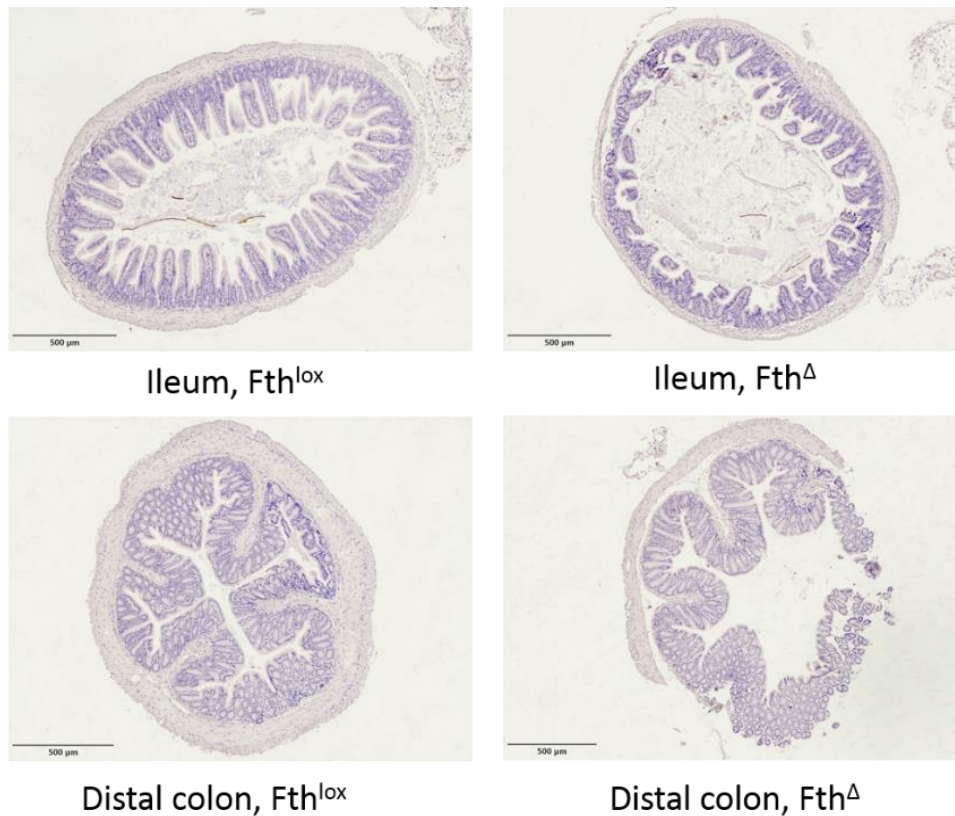


Figure 4.18: H & E staining of intestinal segments of $Fth^{\Delta/\Delta}$ mice and $Fth^{lox/lox}$ mice. H & E: hematoxylin and eosin staining.

4.2.5 High susceptibility of $Fth^{\Delta/\Delta}$ mice to DSS-induced colitis

The mice were challenged with 1 % DSS given via the drinking water. In a first experimental setting the mice were challenged for a time period of 14 days. After the challenge with 1 % DSS the mice received drinking water without DSS (recovery phase). During the whole experiment mice were weighted and examined daily. See figure 4.19 for the experimental design. Abortion criteria were defined as a weight loss of more than 20 %.

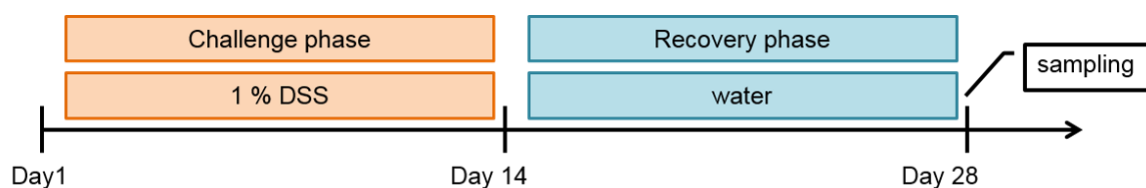


Figure 4.19: Experimental design of the recovery experiment.

1 % DSS was sufficient to induce acute colitis in $Fth^{\Delta/\Delta}$ mice. Male mice were more affected by 1 % DSS than female mice in both genotypes. Female $Fth^{lox/lox}$ mice were less affected by 1 % DSS and recovered from day 14 on back to their origin weight. Female $Fth^{\Delta/\Delta}$ mice started to recover after changing back to drinking water without DSS.

After a short period of weight gain during the first three days in all four groups all mice except the female $Fth^{lox/lox}$ mice lost weight. The most severe weight loss was observed in male $Fth^{\Delta/\Delta}$ mice, followed by male $Fth^{lox/lox}$ mice. After 14 days of 1 % DSS female $Fth^{\Delta/\Delta}$ mice could recover to their initial weight.

All mice in the group of male $Fth^{\Delta/\Delta}$ mice reached abortion criteria between day 7 and day 11 (see figure 4.20).

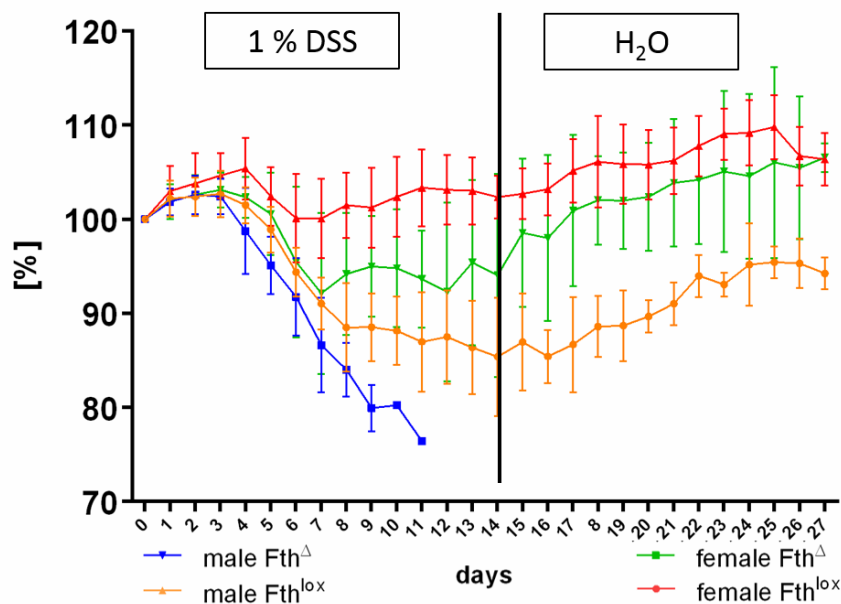


Figure 4.20: Body weight development of $Fth^{\Delta/\Delta}$ mice and $Fth^{lox/lox}$ mice in the 1 % DSS recovery experiment. Day 0: Changeover from normal water to 1 % DSS. Day 14: change back to normal water, $n = 6$ per group. $P = 0.003$ at day 9 for male $Fth^{\Delta/\Delta}$ mice vs. male $Fth^{lox/lox}$ mice. $P < 0.05$ at days 10 to 12 for female $Fth^{\Delta/\Delta}$ mice vs. female $Fth^{lox/lox}$ mice.

The disease activity index was determined daily during the whole experiment (see figure 4.21). In accordance to the body weight development male $Fth^{\Delta/\Delta}$ mice had the highest scoring followed by male $Fth^{lox/lox}$ mice. All six male $Fth^{\Delta/\Delta}$ mice had to be killed during the 1 % DSS phase because of their bad shape, valued as a weight loss of more than 20 %.

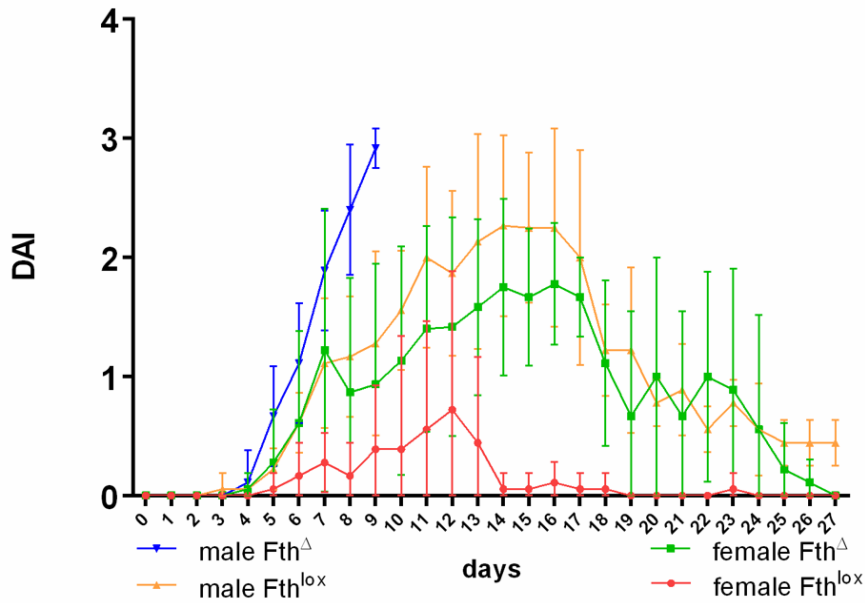


Figure 4.21: Disease activity index of $Fth^{\Delta/\Delta}$ mice and $Fth^{lox/lox}$ mice in the 1 % DSS recovery experiment. Changeover from normal water to 1 % DSS. Day 14: change back to normal water without DSS, $n = 6$ per group. $P = 0.05$ at day 8 and 9 for male $Fth^{\Delta/\Delta}$ mice vs. male $Fth^{lox/lox}$ mice. $P = 0.05$ at day 13 and $p < 0.001$ at day 11 to 18 for female $Fth^{\Delta/\Delta}$ mice vs. female $Fth^{lox/lox}$ mice.

Figure 4.22 shows the results from the recover experiment calculated as a Kaplan-Meier survival curve. Mice had to be killed as soon as they reached a weight loss of more than 20 % compared to their weight at day zero. The mortality rate is in concordance with the body weight development. Whereas none of the male $Fth^{\Delta/\Delta}$

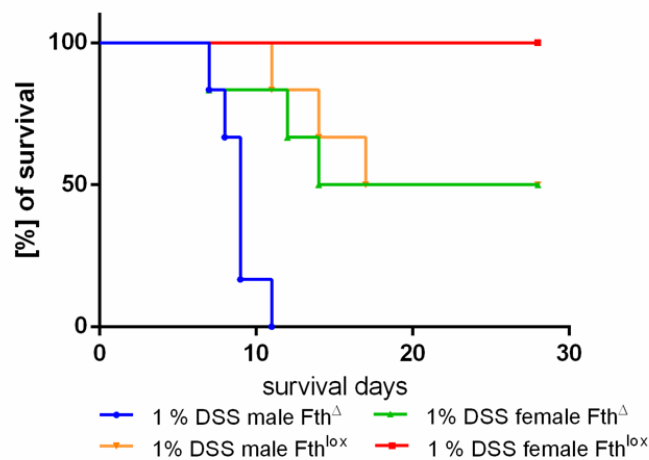


Figure 4.22: Kaplan-Meier survival curve of $Fth^{\Delta/\Delta}$ mice and $Fth^{lox/lox}$ mice in the 1 % DSS recovery experiment. $N = 6$ per group.

mice survived the experiment all female $Fth^{lox/lox}$ mice survived the whole experiment. The survival rate of the female $Fth^{\Delta\Delta}$ mice was 50 % and the survival rate of male $Fth^{lox/lox}$ mice was 50 %.

The DSS-intake was roughly calculated from the daily water intake of each mouse to avoid a bias due to different amounts of DSS intake. The cumulative intake of DSS in 7 days did not differ statistically between the four groups. The lowest intake was found in male $Fth^{\Delta\Delta}$ (data not shown).

As a marker of systemically inflammation SAA in plasma was measured. In accordance to the body weight development and the DAI male mice showed higher level of SAA. $Fth^{\Delta\Delta}$ mice showed higher level than $Fth^{lox/lox}$ mice without reaching significance, see figure 4.23. The high level of SAA in male $Fth^{\Delta\Delta}$ mice indicate systemically inflammation in both $Fth^{\Delta\Delta}$ and $Fth^{lox/lox}$.

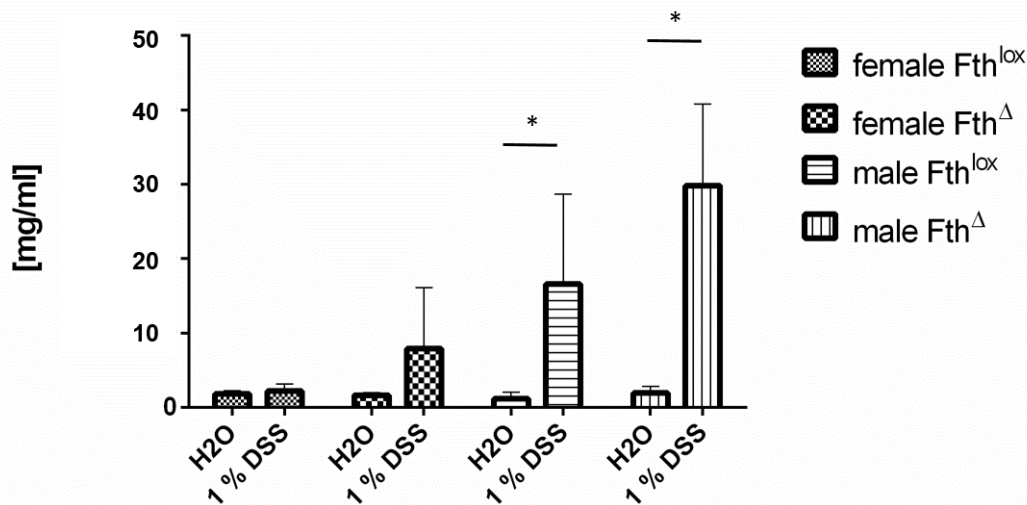


Figure 4.23: SAA in systemic plasma of $Fth^{\Delta\Delta}$ mice and $Fth^{lox/lox}$ mice in the 1 % DSS recovery experiment. $P < 0.002$ for male $Fth^{\Delta\Delta}$ mice and male $Fth^{lox/lox}$ mice on 1 % DSS compared to the control groups on water $n = 6$ per group. DSS: dextran sodium sulfate, SAA: serum amyloid A protein.

Besides the SAA level the iron parameters hematocrit, hemoglobin and non-heme iron in liver and spleen tissue were determined when mice were killed during or after the recovery experiment. Mice receiving 1 % DSS had lower Hkt level and lower Hb level compared to control mice with significance in the group of male

$Fth^{\Delta/\Delta}$. Intestinal bleeding due to 1 % DSS might explain the loss of Hkt and Hb level.

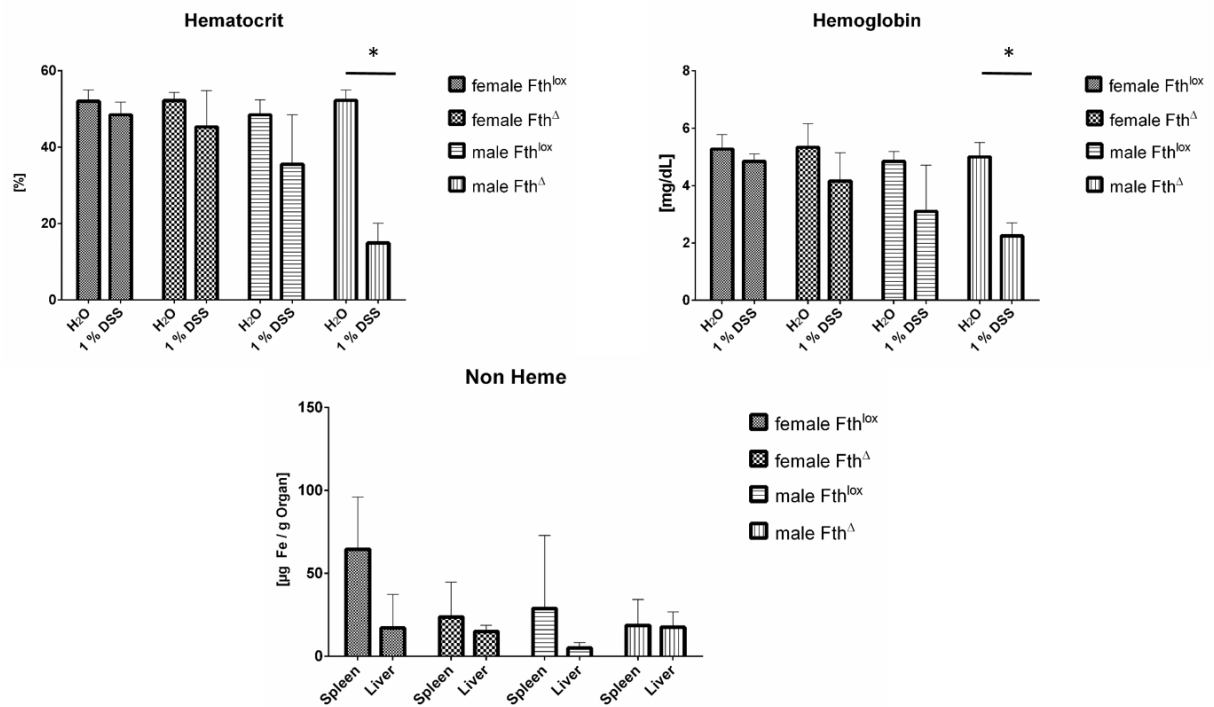


Figure 4.24: Hkt, Hb and non-heme iron of $Fth^{\Delta/\Delta}$ mice and $Fth^{lox/lox}$ mice in 1 % DSS recovery experiment. Both, Hkt and Hb values are significant reduced in male $Fth^{\Delta/\Delta}$ mice ($p < 0.001$) and male $Fth^{lox/lox}$ mice ($p < 0.03$) on 1 % DSS compared to the water control groups. The same trend is visible within the female groups without significance, $n = 6$ per group. DSS: Dextran sodium sulfate, Hb: hemoglobin level, Hkt: hematocrit level.

Swiss roles from the colon tissue were produced from every mouse and H & E stained. Tissue sections from mice which received 1 % DSS were marked by structural loss and thickening of the gut wall (see figure 4.25). The significant decreased hematocrit level and hemoglobin level in male $Fth^{\Delta/\Delta}$ mice can be explained by massive bleeding of these animals.

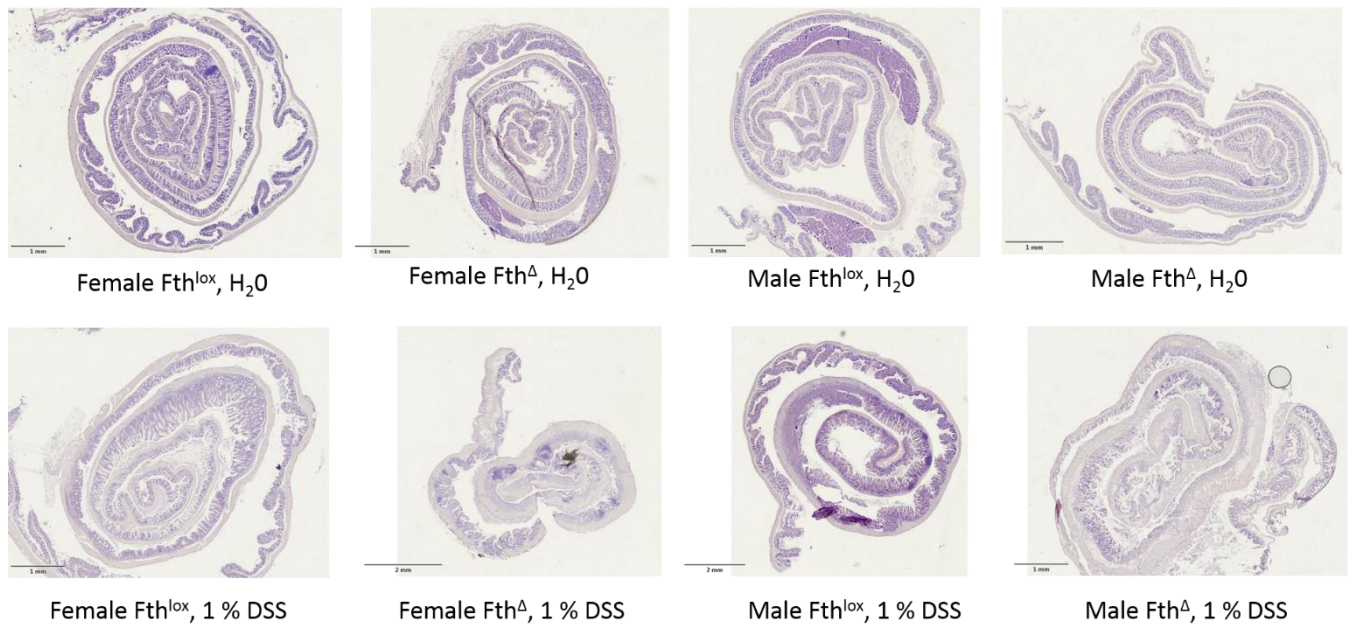


Figure 4.25: Swiss roles of the large intestine after H % E staining from male mice receiving 1 % DSS (recovery experiment).

To validate these initial findings we used only female mice in an independent confirmation experiment.

As male mice were more sensitive to 1 % DSS than female mice we decided to continue with female mice. In a second experiment female mice were challenged with 1 % DSS given via the drinking water for 12 day. All mice were killed after 12 day on 1 % DSS.

The point of time of 12 days was chosen in dependence of the maximal differences in changes of DAI and weight development in the first experiment (recovery experiment).

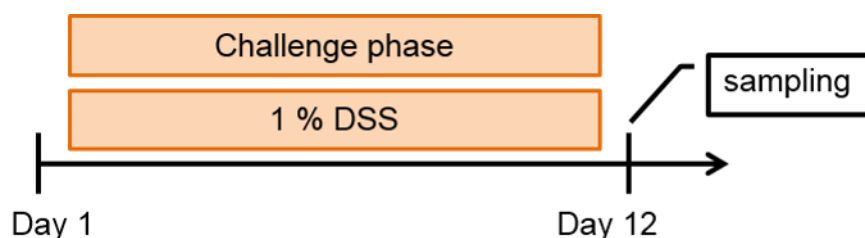


Figure 4.26: Experimental design 1 % DSS in female mice for 12 days Female $Fth^{\Delta/\Delta}$ mice and female $Fth^{lox/lox}$ mice were challenged with 1 % DSS and killed after 12 days, $n = 6$ per group.

The mice were weighted every day. The female $Fth^{\Delta/\Delta}$ mice weight loss was significant from day 7 ($p < 0.05$) compared to the female $Fth^{lox/lox}$ mice which did not lose weight (see figure 4.27).

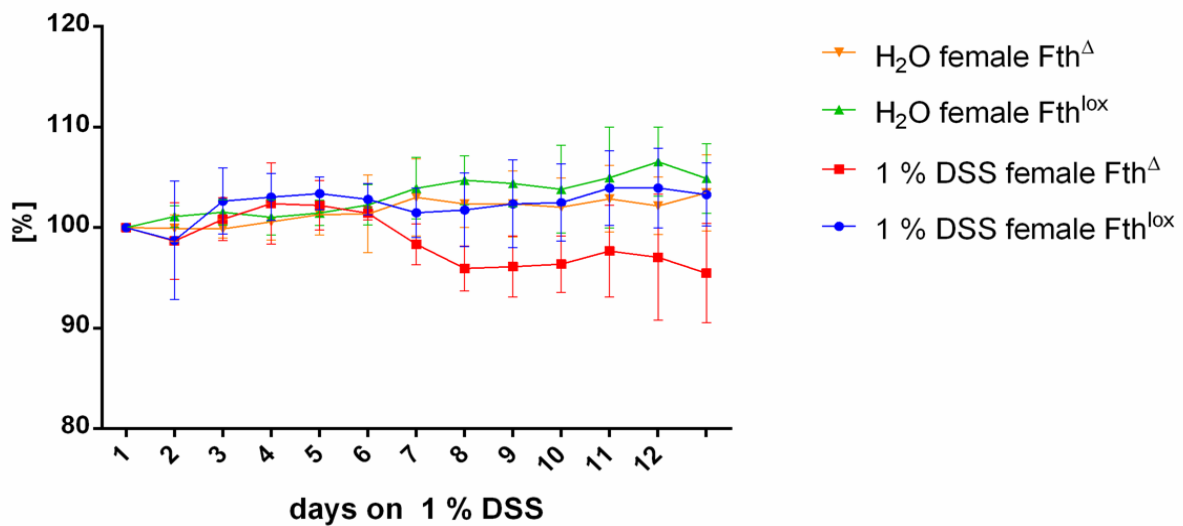


Figure 4.27: Body weight development 1 % DSS in female mice for 12 days. Day 1: Changeover from normal water to 1 % DSS. $p < 0.05$ from day 7 between female $Fth^{\Delta/\Delta}$ mice vs. female $Fth^{lox/lox}$ mice on 1 % DSS, $n = 6$ per group.

The DAI assessment revealed the following pattern: The female $Fth^{lox/lox}$ mice were hardly affected by the DSS administration whereas the female $Fth^{\Delta/\Delta}$ mice were suffered from weight loss, rectal bleeding and stool inconsistency (see figure 4.28).

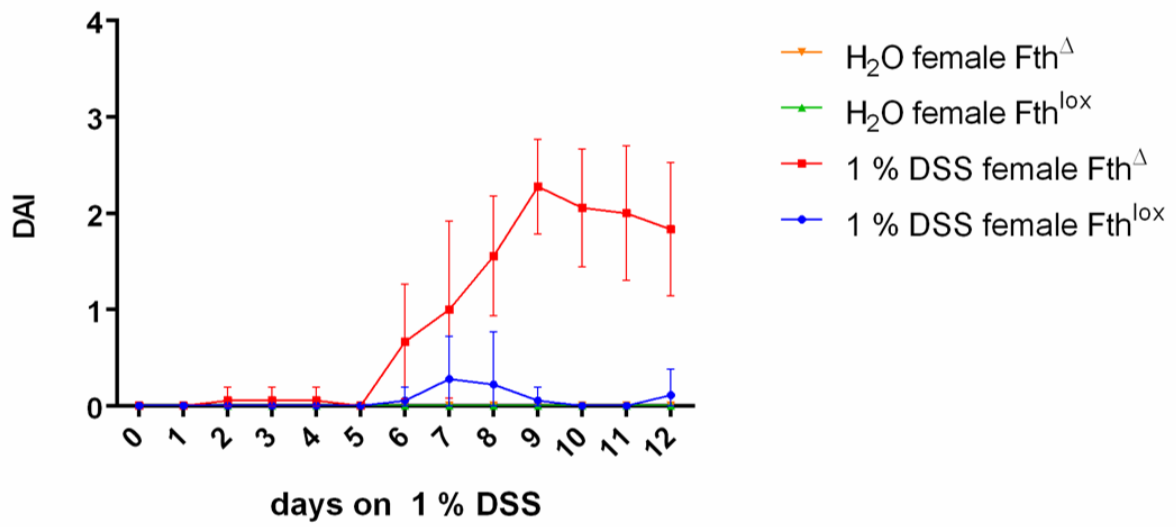


Figure 4.28: Disease activity index - 1 % DSS in female mice for 12 days. Day 0: Changeover from normal water to 1 % DSS. $p = 0.05$ at day 6 and $p < 0.001$ at days 8 - 12 between female $Fth^{\Delta/\Delta}$ mice vs. female $Fth^{lox/lox}$ mice on 1 % DSS, $n = 6$ per group.

5. DISCUSSION

5.1 Oral versus intravenous iron replacement therapy alters gut microbiota in patients with IBD

Iron deficiency is the most prevalent nutritional disorder. One third of IBD patients suffer from recurrent anemia. The high prevalence of iron deficiency anemia in IBD requires therapeutic intervention based on oral iron replacement therapy or intravenous iron replacement therapy (Yilmaz *et al.* 2018). Chronic bleeding in the gastrointestinal tract and unbalanced iron absorption due to increased systemic hepcidin level in the presence of ongoing inflammation are the main reasons behind iron deficiency in IBD patients. This might have an impact on the quality of life of IBD patients due to chronic fatigue and other side effects. Oral iron replacement therapy has long been considered as the standard intervention to treat iron deficiency based on its safety profile, low costs and convenient administration. However, the high frequency of gastrointestinal side effects and the potency to exacerbate intestinal inflammation support clinical implementation of intravenous iron replacement therapy (Tolkien *et al.* 2015; Kulnigg *et al.* 2006). Gastrointestinal side effects of oral iron replacement therapy include nausea, vomiting, diarrhea and/or constipation.

We previously showed that the absence of luminal ferrous iron was associated with major changes in the gut microbiota and the prevention of chronic inflammation in an experimental model for CD-like ileitis. Luminal iron depletion led to a significant reduction of ER stress. Iron repletion by weekly injection maintained the protective effect of iron sulfate free diet in mice (Werner *et al.* 2009; Werner *et al.* 2011). Taken together we speculated that an oral iron replacement therapy may lead to an exacerbation of intestinal inflammation. In contrast, intravenous iron therapy might offer an effective alternative management of iron deficiency since it does not cause gastrointestinal side effects. To follow up on these findings, the aim of the present study was to investigate the impact of oral and intravenous iron treatment on the intestinal milieu via the assessment of fecal bacterial diversity and composition in subjects with iron deficiency suffering from CD or UC.

In accordance with previous reports, distinct bacterial phylogenetic makeups and lower phylotype richness were observed in feces from patients with IBD compared with non-inflamed control iron-deficient subjects (Gevers *et al.* 2014; Lepage *et al.*

2011; Willing *et al.* 2010). We observed a significant drop in taxa richness in IBD patients compared to non-IBD participants. This was most pronounced in patients with CD. Similar to this, Pascal and colleagues described a lower microbial diversity and a more unstable community in CD patients compared to UC patients. They further suggest a combination of eight groups of microorganisms which might be applied as “microbiomarkers” to discriminate between CD and non-CD. These eight groups include *Faecalibacterium*, an unknown *Peptostreptococaceae*, *Anaerostipes*, *Methanobrevibacter*, and unknown *Christensenellaceae*, *Collinsella*, *Fusobacterium* and *Escherichia*. The first six groups are described to be lower in relative abundance in CD patients and the last two groups are described to be higher. This observation was made independently of geographical regions (Pascal *et al.* 2017). Although CD and UC share many epidemiological, clinical and therapeutical features, a microbial signature as described by Pascal would enable a better discrimination between the two subtypes of IBD via non-invasive examination.

Most interesting regarding the impact of iron replacement therapy, fecal bacterial communities in patients with CD were characterized by highest inter-individual differences and were most sensitive to changes after 3 months of treatment. Despite limitations of fecal material for bacterial community analysis, (Momozawa *et al.* 2011) the drop observed in the relative abundance of *Clostridiales spp.* is consistent with the most comprehensive analysis in treatment-naïve paediatric patients with CD (Gevers *et al.* 2014). In the latter study, changes in stool samples were actually representative for differences in biopsy material at the terminal ileum and rectum. This implies an important disease-related effect on members of the order *Clostridiales* independent of medication and sampling procedures. Specifically, reduction of *Clostridium cluster* IV and XIV members has been proposed to contribute to dysbiosis in patients with CD (Andoh *et al.* 2009; Joosens *et al.* 2011) and selected mixtures of corresponding *Clostridia* strains were shown to induce T-regulatory cells with disease-suppressive phenotypes in IBD-related mouse models (Atarashi *et al.* 2013). These results support a potential protective role of certain *Clostridiales spp.* in IBD pathogenesis. In our study, members of the newly described bacterial family *Christensenellaceae* were specific for NI conditions (Morotomi *et al.* 2012). However, other family members within the order *Clostridiales* such as *Ruminococcaceae* as well as the *Veillonellaceae* within the

order *Selenomonadales* are rather increased in patients with IBD (Gevers *et al.* 2014; Willing *et al.* 2010; Png *et al.* 2010) making general disease-related conclusions at these taxonomic levels rather difficult.

The transition from a quiescent state to disease exacerbation in patients with IBD was shown to be associated with alterations of fecal bacterial communities (Wills *et al.* 2014) which supports the hypothesis that inflammatory processes in the intestines of both patients with UC and patients with CD affect the microbial milieu. In our study, IRT-induced shifts in bacterial diversity and composition in feces from patients with IBD were not associated with changes in disease activity, suggesting that patient-specific shifts in fecal microbiota are not necessarily linked to changes in disease severity over short periods of intervention. Regarding the route of iron administration, intravenous therapy confirmed a slightly more effective management of iron deficiency anemia compared with oral treatment with respect to serum ferritin levels. In addition and consistent with the presence of increased iron in feces, the luminal milieu in feces from PO-treated individuals was distinct according to the occurrence of specific bacterial phylotypes. Changes included a significant decrease in the relative abundance of *C. aerofaciens*, *F. prausnitzii*, *R. bromii* and *Dorea sp.*, and an increase in one OTU within the genus *Bifidobacterium*. In contrast to the increase in total fecal iron after oral administration of iron sulfate tablets, the total sulfur concentration did not increase. Oral administration studies of radioactive sulfate indicate a relatively high efficiency of intestinal sulfate absorption, reaching up to 80 % (Bauer 1976). Even doses of up to 8 g anhydrous sodium sulfate per day resulted in 50 – 60 % absorption efficiency (Cocchetto *et al.* 1980). Although the colon might contribute to total sulfate absorption (Florin *et al.* 1991), colonic accumulation of this terminal electron acceptor as growth-limiting substrate of sulfate-reducing bacteria would lead to an increased abundance in human feces, including *Desulfovibrio*, *Desulfomonas* or *Desulfobacter*. However, sequence analysis in our study revealed low relative abundance and no changes in bacterial taxa associated with sulfate metabolism.

Opposite to the IBD-related changes that we observed, iron fortification in Kenyan infants showed an increase in clostridia and a decrease in *Bifidobacteria* (Krebs *et al.* 2013). Interestingly, *Bifidobacterium* strains isolated from stools of iron-deficient infants efficiently sequestered iron (Vazquez-Gutierrez *et al.* 2015), suggesting an inverse relationship between abundance and functionality. Moreover, we cannot

exclude the possibility that the intake of functional foods, including probiotic dairy products, in the present study may have specifically affected results on relative sequence abundances of *Bifidobacteria*. Considering currently available studies, one of the most consistent differences between IBD and NI subjects is the reduced abundance of *F. prausnitzii*, a member of the *Clostridium* cluster IV (Machiels *et al.* 2013, Sokol *et al.* 2009). We demonstrated that the relative sequence abundance of *F. prausnitzii* in stool samples was lower after PO therapy, suggesting that this bacterium is affected not only by disease-intrinsic factors, but also by environmental factors.

The protective effect of an iron sulfate free diet in combination with an intravenous iron replacement therapy which was observed in TNF^{Δ/ARE}mice (Werner *et al.* 2009; Werner *et al.* 2011) could not be affirmed in our human study. This reflects the complexity of the disease pathology with several different players influencing the disease progression as well as the limited controllability of all influencing factors in a human study with free-living people. Further, this might be an example for the restricted transferability of results from mouse model experiments to humans.

In conclusion, IRT in patients with iron deficiency or anemia induced significant shifts in bacterial community structure in feces. Patients with CD seemed to be more prone to IRT-induced shifts and, according to the load of free iron detected in the luminal environment, oral iron therapy affected the presence of specific molecular bacterial species. Still, the fine-tuned balance between iron metabolism and gastrointestinal microbial population remains unclear.

A further step towards the understanding of the role of microbial composition could be to extend the research from functional studies focusing on single bacterial species or strains towards studies looking at the functionality of complete gut microbiome profiles. In this context, Vila and colleagues describe an increased abundance of virulence factors in the gut microbiota of IBD patients. They also found that changes in the composition of the microbiota in IBD patients have an impact on the antibiotic resistance load (Vila *et al.* 2018). Hence, the relevant mechanisms associated with these observations remain unclear.

A higher serum ferritin level was observed in the IV group after the iron replacement compared to the PO group and this might be explained by the fact that the IV route bypasses the requirements of gastric and duodenal digestion and small bowel iron absorption. The higher quality of life score in the IV group of IBD patients (not

significant), as determined by the Shorten form Inflammatory bowel disease questionnaire and Euro-quality 5 dimension analogue scale, might be in context with the improved iron stores enabling a more efficient adenosine triphosphate (ATP) production and enhanced ATP availability. One potential confounder accounting for the higher quality of life score in the IV group of IBD patients might be the concurrent use of biological therapy. Anti-TNF therapy for example has been shown to reduce fatigue and depression scores. There were more patients receiving concurrent biological therapy in the IV group compared to the PO group in IBD patients although this difference did not reach statistical significance. Further research could challenge the question how much iron is needed to keep an intact iron homeostasis without negatively affecting the microbial community neither the quality of life in IBD patients.

We can exclude confounding effects of freezing/thawing cycles or storage at -20°C over a long period of time as stool samples were frozen within 30 min and kept at -80°C until further processing for sequencing.

As the recruitment happened over 18 months, some specimens were kept frozen longer than others. However, this was the case for samples across all groups that were compared, precluding group-specific artefacts observations due to the sampling and/or storage procedure.

The study was not double blinded because of the unavailability of placebo iron sucrose and placebo ferrous sulfate pills. The costs involved in using coloured iron infusion giving sets would be high and do not ensure blinding as iron sucrose was mixed in the Clinical Investigation Unit and double checked by another registered nurse. The costs involved in the making of placebo iron pills which is available to discolor stools is beyond the budgetary allocation for the study. Another limitation of the study is the small sample size. The originally calculated targeted 100 IBD subjects (50 in the IV group and 50 in the PO group) and 100 non inflamed subjects (50 in the IV group and 50 in the PO group) were not met due to several challenges regarding the subject recruitment procedure. There were more male subjects in the IV group compared to the PO group (62% vs. 33%) but it is unlikely to be of clinical relevance.

Independently from the iron needs of IBD patients there is an epidemiological trend towards an increasing IBD rates in Asian countries with several countries in East Asia experiencing a more than double increase in IBD prevalence over the past decade, while Europe has had a plateauing or even decreasing trend of IBD incidence. Even though, historically UC is more common than CD in Asia, a reverse trend is beginning to appear in more developed countries such as Japan, Korea and Hong Kong. The changes in incidence might be coupled to considerable socioeconomic changes give rise to the opportunity to study etiological aspects of IBD. There seem to be several variations between the phenotypes of Western and Asian IBD populations. This is possible a result of the differences in genetic composition and environmental influences (Ng *et al.* 2016).

5.2 Ferritin H deletion in intestinal epithelial cells alters susceptibility to DSS-induced colitis in mice

Mouse models enable researchers to understand the underlying mechanisms of the onset of diseases as well as the inflammatory characteristics better. One common model for studying IBD is the DSS-induced colitis model. DSS produces human ulcerative colitis-like pathologies. The chemical exerts injury to the intestinal epithelium, exposing lamina propria and submucosal compartments to luminal antigens and enteric bacteria, which triggers inflammation (Low *et al.* 2013). The DSS-induced colitis in mice is a popular mouse model due to its reproducibility and controllability. One negative aspect of the DSS-model is that unlike human IBD T and B cells are not required for disease onset (Chassing *et al.* 2014), making this model useful to study the role of the innate immune system. It is further commonly used to assess how genetic factors influence the severity of inflammation. Beside these facts, we chose the DSS-model for our experiments to avoid further backcrossing of our genetic mouse model.

Vanoaica and colleagues described that $Fth^{\Delta/\Delta}$ mice show an impaired iron metabolism characterized by an increasing serum iron and total iron load. This was accompanied by an increased hepcidin mRNA expression and decreased expression of DCytB mRNA and DMT1 mRNA. Despite the feedback mechanism

of hepcidin intestinal ferroportin expression was highly increased and iron absorption was increase more than 2-fold indicating that hepcidin is not able to restrict duodenal iron absorption alone but intact ferritin is required to restrict intestinal iron absorption (Vanoaica *et al.* 2010).

In our experiments mice did not show abnormal Hb and Hkt levels compared to the control mice. Different findings might contribute to different age of mice (35 weeks Vanoaica vs. 20 weeks here), probably different chows, different animal housing and/or different experimental settings regarding the measurement of iron metabolism.

Body weight development and other external characteristics as well as several organ weights did not differ from control mice indicating normal development and functions. No morphological changes were detected in different gut tissues and this is consistent with the findings of Vanoaica and colleagues.

In animal models, a high-iron diet enhances intestinal inflammation, and iron induces ROS production and therefore DNA damage. Iron triggers ER stress in intestinal epithelial cells and ER stress sensitizes the epithelium towards cytotoxic T cell induced apoptosis. Under oral iron deprivation, chronic ileitis in TNF^{ΔARE/WT} mice is prevented and systemic iron repletion maintained the protective effect of luminal iron deprivation. In this setting, ferritin expression is reduced in iron-depleted mice or elevated in highly inflamed mice (Werner *et al.* 2011). We speculated that ferritin in intestinal epithelial cells might play a protective role in context of orally received iron and intestinal inflammatory processes. To follow this hypothesis, we challenged Fth^{ΔΔ} mice with DSS. Fth^{ΔΔ} mice were highly susceptible to DSS-induced colitis with a more pronounced effect in male animals. Our findings indicate a protective role of ferritin in intestinal epithelial cells. This might be due to iron-binding functions.

Fth^{ΔΔ} mice showed a high susceptibility to DSS-induced colitis which was even more pronounced in male Fth^{ΔΔ} mice than in female Fth^{ΔΔ} mice.

Ferritin contributes to a tightly regulated iron homeostasis but is also involved in inflammatory reactions to infections and oxidative stress (Gozzolino *et al.* 2014). Although the exact mechanisms remain unclear, ferritin might contribute to the high susceptibility of Fth^{ΔΔ} mice to DSS-induced colitis.

DSS is often used to induce ulcerative colitis-like inflammation in mice. Advantages of this mode compared to other models of inflammation is a simple handling, a high degree of reproducibility, a fast development of inflammation within a few days and high degree of uniformity (Laroui 2012). Several approaches have been made to clarify the mechanisms behind DSS-induced colitis. But still until today it is not certainly known how DSS induces inflammatory processes in the gut. Laroui and coworker suggest that DSS enters colonocytes via vesicular transport after binding to medium-chain fatty acids (MCFA) and causes inflammatory processes inside colonocytes (Laroui 2012).

One of the remaining questions addresses the regional differences between the inflammation and iron absorption. The inflammation in our mouse model was located in colon but iron uptake mainly happens in the duodenum (Ganz 2013). Still, it is possible that in addition to the inflammatory signs in the colon the small intestine might be affected from inflammation, too. Although according to literature that would be unusual for C57BL/J6 mice (Mähler *et al.* 1996).

Male mice were more sensitive to DSS-induced colitis than female mice in both phenotypes. The different susceptibility between genders and also between several mouse strains and different gut sections is already known from literature (Mähler *et al.* 1996). C57BL/J6 mice show a strong susceptibility to DSS-induced colitis in the colon but are resistant to DSS-induced colitis in the cecum (Mähler *et al.* 1996). Whether these differences can be explained by a stronger inflammatory reaction or a better wound healing wasn't further addressed but could be explored by mucosal healing assays.

Interpreting the phenotype of a deletion model underlies several limitations. The presence of a selection gene (here: cre) may influence the phenotype of the mutation. Second, artefacts could arise due to the fact of a lacking gene product (here: ferritin H) for the whole lifetime of an animal (Feil *et al.* 1996).

One limitation of the cre-system is that the cre recombinase does not certainly result in a recombination in all target cells (Chambers *et al.* 1994). Ferritin expression in intestinal cells was not investigated in our experiments as one limitation of this study.

One explanation for the high susceptibility of chemically induced colitis in Fth^{Δ/Δ} mice would be an elevated oxidative stress level in the intestinal epithelium cells

due to the deletion of ferritin H as it is described for cardiomyocytes after silencing ferritin H (Omiya *et al.* 2008).

CONCLUSION

IRT in patients with iron deficiency or anemia induced significant shifts in bacterial community structure in feces. Patients with CD seemed to be more prone to IRT-induced shifts and, according to the load of free iron detected in the luminal environment, oral iron therapy affected the presence of specific molecular bacterial species.

Mice with a deletion of ferritin in the intestinal epithelium seem to be highly susceptible to DSS-induced colitis pointing out a role of ferritin in iron homeostasis under inflammatory conditions. As a result of inflammation hepcidin expression increases and in consequence iron is restrained in enterocytes. This process is might be ineffective in $Fth^{\Delta\Delta}$ mice.

APPENDIX

Supplemental data

OTU counts and abundances of taxonomic groups (see methods p.28f) are available here:

<https://gut.bmj.com/content/suppl/2016/05/23/gutjnl-2015-309940.DC1>

List of figures

Introduction

Figure 1.1: Figure 2.1: Interacting players for disease initiation, progression and persistence.

Figure 1.2: Microbial habitats on the human body and dominant phyla of bacteria in the gastrointestinal tract.

Figure 1.3: Iron absorption distribution and recycling in the human body (adapted from Pantopoulus et al. 2012).

Aim

Figure 2.1: Schematic diagram of the interdependent topics of this thesis.

Methods

Figure 3.1: Study design. CD: Crohn's disease, IV: intravenous iron therapy, PO: oral iron therapy, UC: ulcerative colitis.

Figure 3.2: Genetic background of the mouse model $Fth^{\Delta/\Delta}$ (Darshan et al. 2009).

Figure 3.3: DSS challenge with recovery phase.

Figure 3.4: DSS challenge with optimized sampling time point.

Results

Figure 4.1: Iron replacement therapy restores iron storage independently of the route of administration. Left: Iron saturation in % after two months of iron replacement therapy and after three months iron replacement therapy. Right: Serum ferritin level in $\mu\text{g/L}$ after two months of iron replacement therapy and after three months iron replacement therapy. IBD: inflammatory bowel disease, IV: intravenous, NI: non-inflamed, PO: per oral.

Figure 4.2: % of changes in quality of life was scored according to Shorten IBD questionnaire (SIBDQ) and Euro Quality 5 Dimension Visual Analogue Scale (EQ5D). CD: Crohn's disease, IV: intravenous, NI: non-IBD control anemic subjects, PO: per oral, UC: ulcerative colitis.

Figure 4.3: IBD activity was assessed with modified Harvey Bradshaw index (MHBI) for CD and partial Mayo score (pMayo) for UC. Values are % changes. CD: Crohn's disease, CRP: C-reactive protein, IV: intravenous, PO: per oral, UC: ulcerative colitis.

Figure 4.4: NMDS plot based on generalized UniFrac distances, including all patients before and after the iron replacement therapy. Patients with CD are most heterogeneous and in distance to UC and control subjects. CD: Crohn's disease, NMDS: Non-parametric multidimensional scaling, UC: ulcerative colitis.

Figure 4.5: Shannon effective diversity box plot shows decreased number of species in both IBD groups, CD and UC. CD: Crohn's disease, NI: non-IBD control anemic subjects; UC: ulcerative colitis.

Figure 4.6: Abundance of the most dominant phyla detected in fecal samples. CD: Crohn's disease, NI: non-IBD control anemic subjects, UC: ulcerative colitis. Number of subjects analyzed are given in brackets. The most abundant phylum is Firmicutes, followed by Actinobacteria and Bacteroidetes.

Figure 4.7: Relative abundances of dominant bacterial taxa with significant differences between the CD, UC and control group. The number of samples in which the given bacteria were found are shown in the brackets. CD: Crohn's disease; NI: non-IBD control anemic subjects; UC: ulcerative colitis.

Figure 4.8: NMDS plot showing changes in bacterial diversity between the baseline timepoint and after three months of iron replacement therapy, represented by connected lines. NMDS: non-metric multidimensional scaling. CD: Crohn's disease, NI: non-IBD control anemic subjects, UC: ulcerative colitis.

Figure 4.9 Boxplot depict the distribution of generalized UniFrac distances per patient category, indicating that samples before and after IRT are more similar in NI control subjects than in patients with IBD. IBD: Inflammatory bowel diseases, NI: non-IBD control anemic subjects.

Figure 4.10: Wards clustering dendrogram calculated from phylogenetic distances of all subjects. Paired samples given from one individual located next to each other before and after the iron intervention are marked with black bars at the inner circle. Disease color-code: red for CD, green for UC, blue for NI. The bar plot below shows the percentages of paired samples per group. CD: Crohn's disease, NI: non-IBD control anemic subjects, UC: ulcerative colitis.

Figure 4.11: A decrease of sequence proportions of the family Ruminococcaceae was observed in subjects with improvement of disease. NI: non-IBD control subjects.

Figure 4.12: Iron and total sulfur content in feces. B: baseline; IRT: after three months of iron treatment therapy; IV: intravenous; PO: per oral.

Figure 4.13: Relative abundance of phylotypes that react differently to intravenous (IV) or oral (PO) iron therapy. IRT groups were compared using Mann-Whitney test. Prior to testing, individual counts < 0.5% were zeroed and only prevalent and dominant molecular species (i.e., detected in at least 30% of the participants and with a median sequence abundance > 1% in at least one group) were considered. IRT: iron replacement therapy, OTU: operational taxonomic unit.

Figure 4.14: Body weight development of $Fth^{\Delta/\Delta}$ mice and $Fth^{lox/lox}$ mice. Body weight development (A) and body weight at 12 weeks (B) of $Fth^{\Delta/\Delta}$ mice and control mice ($Fth^{lox/lox}$ mice) over 20 weeks, $n = 6$. Male $Fth^{\Delta/\Delta}$ mice were statistically thinner than male control mice ($p > 0.04$). There are no statistical differences between the female $Fth^{\Delta/\Delta}$ mice and the female $Fth^{lox/lox}$ mice nor between the male $Fth^{\Delta/\Delta}$ mice and the male $Fth^{lox/lox}$ mice (except week 16 for the female mice) in the body weight development of mice until the age of 20 weeks. The black frame in A indicates the timepoint of 12 weeks shown in B.

Figure 4.15: Body weight parameters of Fth^{Δ/Δ} mice and Fth^{lox/lox} mice. There were no statistical differences between the tissue weights of stomach, caecum, kidney and spleen. N = 6 per group.

Figure 4.16: Hematocrit and Hemoglobin of Fth^{Δ/Δ} mice and Fth^{lox/lox} mice. There are no statistical differences neither for the hematocrit levels nor for the hemoglobin levels between male Fth^{Δ/Δ} mice and male Fth^{lox/lox} mice at point of time (age of mice) 12 or 20 weeks and no statistical differences between female Fth^{Δ/Δ} mice vs. Fth^{lox/lox} mice at point of time 12 and 20 weeks.

Figure 4.17: Hematocrit and Hemoglobin of Fth^{Δ/Δ} mice and Fth^{lox/lox} mice. There are no statistical differences neither for the hematocrit levels nor for the hemoglobin levels between male Fth^{Δ/Δ} mice and male Fth^{lox/lox} mice at point of time (age of mice) 12 or 20 weeks and no statistical differences between female Fth^{Δ/Δ} mice vs. Fth^{lox/lox} mice at point of time 12 and 20 weeks.

Figure 4.18: H & E staining of intestinal segments of Fth^{Δ/Δ} mice and Fth^{lox/lox} mice. H & E: hematoxylin and eosin staining.

Figure 4.19: Experimental design of the recovery experiment.

Figure 4.20: Body weight development of Fth^{Δ/Δ} mice and Fth^{lox/lox} mice in the 1 % DSS recovery experiment. Day 0: Changeover from normal water to 1 % DSS. Day 14: change back to normal water, n = 6 per group. P = 0.003 at day 9 for male Fth^{Δ/Δ} mice vs. male Fth^{lox/lox} mice. P < 0.05 at days 10 to 12 for female Fth^{Δ/Δ} mice vs. female Fth^{lox/lox} mice.

Figure 4.21: Disease activity index of Fth^{Δ/Δ} mice and Fth^{lox/lox} mice in the 1 % DSS recovery experiment. Changeover from normal water to 1 % DSS. Day 14: change back to normal water without DSS, n = 6 per group. P = 0.05 at day 8 and 9 for male Fth^{Δ/Δ} mice vs. male Fth^{lox/lox} mice. P = 0.05 at day 13 and p < 0.001 at day 11 to 18 for female Fth^{Δ/Δ} mice vs. female Fth^{lox/lox} mice.

Figure 4.22: Kaplan-Meier survival curve of Fth^{Δ/Δ} mice and Fth^{lox/lox} mice in the 1 % DSS recovery experiment. N = 6 per group.

Figure 4.23: SAA in systemic plasma of Fth^{Δ/Δ} mice and Fth^{lox/lox} mice in the 1 % DSS recovery experiment. P < 0.002 for male Fth^{Δ/Δ} mice and male Fth^{lox/lox} mice on 1 % DSS compared to the control groups on water n = 6 per group. DSS: dextran sodium sulfate, SAA: serum amyloid A protein.

Figure 4.24: Hkt, Hb and non-heme iron of Fth^{Δ/Δ} mice and Fth^{lox/lox} mice in 1 % DSS recovery experiment. Both, Hkt and Hb values are significant reduced in male Fth^{Δ/Δ} mice (p < 0.001) and male Fth^{lox/lox} mice (p < 0.03) on 1 % DSS compared to the water control groups. The same trend is visible within the female groups without significance, n = 6 per group. DSS: Dextran sodium sulfate, Hb: hemoglobin level, Hkt: hematocrit level.

Figure 4.25: Swiss roles of the large intestine after H % E staining from male mice receiving 1 % DSS (recovery experiment).

Figure 4.26: Experimental design 1 % DSS in female mice for 12 days Female $Fth^{\Delta/\Delta}$ mice and female $Fth^{lox/lox}$ mice were challenged with 1 % DSS and killed after 12 days, n = 6 per group.

Figure 4.27: Body weight development 1 % DSS in female mice for 12 days. Day 1: Changeover from normal water to 1 % DSS. $p < 0.05$ from day 7 between female $Fth^{\Delta/\Delta}$ mice vs. female $Fth^{lox/lox}$ mice on 1 % DSS, n = 6 per group.

Figure 4.28: Disease activity index - 1 % DSS in female mice for 12 days. Day 0: Changeover from normal water to 1 % DSS. $p = 0.05$ at day 6 and $p < 0.001$ at days 8 - 12 between female $Fth^{\Delta/\Delta}$ mice vs. female $Fth^{lox/lox}$ mice on 1 % DSS, n = 6 per group.

List of tables

Introduction

Table 2.1: Annual incidence rates and prevalence values for ulcerative colitis (UC) and Crohn's disease (CD).

Methods

Table 3.1: Inclusion and exclusion criteria for subjects participating in the clinical iron trial. CRP: C-reactive protein, IBD: inflammatory bowel disease, IRT: iron replacement therapy, IV: intravenous.

Table 3.2. Tail buffer. Tail buffer was mixed in ddH₂O. pH was set to 8.3 using 6 M HCl.

Table 3.3. Primer sequences for genotyping. Bp: base pair, PCR: polymerase chain reaction, WT: wildtype.

Table 3.4. PCR mix for genotyping.

Table 3.5. PCR program for genotyping with Crimson tag polymerase.

Table 3.6: Evaluation of mice. Composition of disease activity index.

Table 3.7: Staining program for H & E staining.

Table 3.8: Dehydration program.

List of abbreviations

%	Percentage
°C	Degree centigrade
µl	Microliter
µm	Micrometer
A	Adenine
A	Ampere
aa	Amino acid
<i>Ad lib.</i>	<i>Ad libitum</i>
ARE	Antioxidant responsive element
ATG16L1	Autophagy-related 16-like 1
ATP	Adenosine triphosphate
BMP6	Bone morphogenetic protein 6
bp	Base pairs
BSA	Bovine serum albumine
CD	Cluster of differentiation
CD	Crohn's disease
cDNA	Copy DANN
CED	Chronische Darmerkrankung
cm	Centimeter
CO ₂	Carbon dioxide
CRP	C-reactive protein
Ctrl	Control
CU	Colitis Ulcerosa
d	Day(s)
Da	Dalton
DAI	Disease activity index
DC	Dendritic cell
DCYTB	Duodenal cytochrome b
ddH ₂ O	Bidistilled water
DGE	Deutsche Gesellschaft für Ernährung
DMT-1	Divalent metal transporter 1
DNA	Deoxyribonucleic acid
dNTP	Desoxynucleotide
DSS	Dextran sodium sulfate
DTT	Dithiothreitol
ECL	Enhanced chemiluminescence light
EDTA	Ethylenediaminetetraacetic acid
EFSA	European food safety authority
ELISA	Enzyme linked immunosorbent assay
EPFL	Ecole Polytechnique Fédérale de Lausanne
EQ5D	EuroQol 5-Dimension questionnaire
EtOH	Ethanol
FACs	Fluorescence activity cell sorting
FBS	Fetal bovine serum
Fc	Fragment, crystallizable
FCS	Fetal calf serum
Fe	Iron

Fe(II)	Ferrous iron
Fe(III)	Ferric iron
Fp-1	Ferroportin
Fth	Ferritin-H
Fth ^{lox/lox} mice	Mouse model carrying loxP sites
Fth ^{Δ/Δ} mice	Mouse model carrying ferritin H deletion in intestinal cells
G	Gravity
G	Guanine
GF	Germ-free
GI	Gastrointestinal
GIT	Gastrointestinal tract
GWAS	Genome-wide association studies
H	Hour(s)
H & E	Hematoxin and eosin
H ₂ O	Water
H ₂ O ₂	Hydrogen peroxide
Hb	Hemoglobin
HBSS	Hank's balanced salt solution
hCG	Human chorionic gonadotrophin medium
HCl	Hydrochloric acid
HCP-1	Heme carrier protein 1
HEPH	Hephaestin
HFE	Human hemochromatosis protein („High Fe“)
Hkt	Hematokrit
HO-1 / HO- 2	Heme oxigenase 1 / 2
HTF	Human tubal fluid
i.e.	Id est
i.p.	Intraperitoneal
i.v./IV	Intravenous
IBD	Inflammatory bowel disease
ibid.	Ibidem (in the same place)
ID	Iron deficiency
IDA	Iron deficiency anaemia
IEC	Intestinal epithelial cell
IEL	Intraepithelial lymphocytes
IFN-γ	Interferon gamma
Ig	Immune globuline
IL	Interleukin
IRE	Iron responsive element
IRGM	Immunity-related GTPase family M
IRGM	Immune-related guanosin-triphosphatase
IRP	Iron regulatory protein
IRT	Iron replacement therapy
IRT	Iron replacement therapy
IVF	<i>In-vitro</i> fertilization
Jak2	Janus kinase 2
kDa	Kilo Dalton

LPL	Lamina propria lymphocytes
LPS	lipopolysaccharid
Ly6C	Lymphocyte antigene 6 complex
M	Molar
mA	miliAmpere
MC	Morbus Crohn
MCFA	Medium-chain fatty acid
MDP	Muramyl dipeptide
MeOH	Methanol
Mg	Milligramm
MHBI	Modified Harvey Bradshaw Index
MHC	Major histocompatibility complex
Min	Minute(s)
ml	Milliliter
MLFA	Medium chain length fatty acid
MLN	Mesenteric lymph nodes
mM	Millimolar
mm ³	Cubic millimeter
M-MLV	Moloney Murine leukemia virus
mRNA	Messenger ribonucleic acid
MW	Molecular weight
NBIA2	neurodegeneration with brain iron accumulation type 2
NEAA	Non-essential amino acid cell culture supplement
NFκB	Nuclear factor 'kappa-light chain enhancer' of activated B-cells
ng	Nanogramm
NGS	Next-generation sequencing technologies
NI	Non-inflamed
nm	Nanometer
NMDS	Non-parametric multidimensional scaling
NOD2	Nucleotide-binding oligomerization domain containing 2
OD	Optical density
OTU	Operational taxonomic unit
PBS	Phosphate buffered saline
PCBP1	Poly (rC)-binding protein 1
PCR	Polymerase chain reaction
pH	Potetia hydrogenii
PI	Propidium iodide
PMA	Phorbol 12-myristate 13-acetate
pMayo	Partial Mayo score
PMSG	Pregnant Mare's Serum Gonadotropin medium
PO	Per oral
PRR	Pattern recognition receptor
PVDF	Polyvinylidene difluoride
RNA	Ribonucleic acid
ROS	Reactive oxygen species
RPIM 1640	Roswell park memorial institute medium
Rpm	Revolutions per minute
RT	Room temperature
s.c.	Subcutaneous

SAA	Serum amyloid A
SCFA	Short chain fatty acid
SD	Standard deviation
SDS	Sodium dodecyl sulfate
Sec	Second(s)
SFB	Segmented filamentous bacteria
SIBDQ	Shorten inflammatory bowel disease questionnaire
SNP	Single nucleotide polymorphism
SPF	Specific pathogen-free
TBST	Tris buffered saline
TCA	Trichloroacetic acid
Tf	Transferrin
TfR	Transferrin receptor
TLR	Toll-like receptor
TNBS	Trinitrobenzene sulfonic acid
TNF	Tumor necrosis factor
TUM	Technical University of Munich
U	Unit(s)
UC	Ulcerative colitis
UPL	Universal Probe library
UV	Ultraviolet
V	Volt
v/v	Volume / volume
vs.	Versus
w/v	Mass per volume
WHO	World Health Organization
Wt	Wild type

References

- Alkhateeb, A.** (2010) "Nuclear ferritin: a new role for ferritin in cell biology" *Biochimica and Biophysica Acta* Vol.1800, 793-797.
- Andoh, A.** (2009) "Faecal microbiota profile of Crohn's disease determined by terminal restriction fragment length polymorphism analysis" *Aliment. Pharmacol Ther.* 29, 75-82.
- Andrews, S.C.** (2003) "Bacterial iron homeostasis" *FEMS Microbiology reviews* Vol. 27, 215-237.
- Arosio, P.** (2008) "Ferritins: a family of molecules for iron storage, antioxidation and more" *Biochimica and Biophysica Acta* 1790, 589-599.
- Atarashi, K.** (2013) "Treg induction by rationally selected mixture of Clostridia strains from the human gut microbiota" *Nature* 500, 232-236.
- Avni, T** (2013) "Treatment of anemia in inflammatory bowel disease – systematic review and meta-analysis" *PLOS one*, Vol. 8 (12).
- Balamurugan, R.** (2010) "Low levels of fecal lactobacilli in women with iron-deficiency anemia in south India" *British Journal of Nutrition* Vol. 104, 931-934.
- Bauer, J.** (1976) "Oral administration of radioactive sulfate to measure extracellular fluid space in man" *Journal of applied Physiology* 40 (4), 648-650.
- Beaumont, Ca.** (1995) "Mutation in the iron responsive element of the L ferritin mRNA in a family with dominant hyperferritinaemia and cataract" *Nature genetics* Vol. 11, 444-446.
- Beck, K.L.** (2014) "Dietary determinants of and possible solutions to iron deficiency for young women living in industrialized countries: a review" *Nutrients* 6, 3747-3776.
- Buttó, L.** (2016) "Dysbiosis in intestinal inflammation: cause or consequence" *Int J Med Microbiol.*
- Caporase, G.** (2011) "Global patterns of 16S rRNA diversity at a depth of millions of sequences per sample" *PNAS* 108, 4516-4522.
- Caporase, G.** (2012) "Ultra-high throughput microbial community analysis on the Illumina HiSeq and MiSeq platform" *ISME* 6, 1621-1624.
- Chambers, C.A.** (1994) "TKO'ed: lox, stock and barrel" *BioEssays* Vol. 16 (12) 865-868.

- Chen, J.** (2012) "Associating microbiome composition with environmental covariates using generalizd UniFrac distances" *Bioinformatics* Vol 28. (16) 2106-2113.
- Chifman, J.** (2014) "A systems biology approach to iron metabolism" *Adv Exp Med Biol* 844, 201-225.
- Chun, J.** (2007) "ExTaxon: a weg-based tool for the identification of prokaryotes based on 16S ribosomal RNA gene sequencing" *Int J of Systematic and Evol Microbiol* 57, 2259-2261.
- Cocchetto, D.** (1980) "Absorption of orally administered sodium sulfate in humans" *Journal of Pharmaceutical science* 70 (3) 331-333.
- Colman, R.J.** (2014) "Fecal microbiota transplantation as therapy for inflammatory bowel disease: a systematic review and meta-analysis" *J. Crohn's Colitis*, 8 (12), 1569-1581.
- Colombel, J. F.** (1996) "Clinical characteristics of Crohn's disease in 72 families" *Gastroenterology* 111, 604-607.
- Crohn, B. B.** (1932) "Regional ileitis: a pathologic and clinical entity" *J Am Med Assoc* 99 (16), 1323 – 1329.
- Curtis, A.** (2001) "Mutation in the gene encoding ferritin light polypeptide causes dominant adult-onset basal ganglia disease" *Nature genetics* Vol.28, 350-354.
- Dainty, J.** (2014) "Estimation of dietary iron bioavailability from food iron intake and iron status" *PLOS one* Vol 9 (10).
- Darshan, D.** (2009) "Conditional deletion of ferritin H induces loss of iron storage and liver damage" *Hepatology* Vol. 50, 852-860.
- De Fazio, L** (2014) "Longitudinal analysis of inflammation and microbiota dynamics in a model of mild chronic dextran sulfate sodium-induced colitis in mice" *World Journal of Gastraenterology* Vol. 20 (8), 2051-2061.
- DGE** (2017) "Referenzwerte für die Nährstoffzufuhr".
- Di Sanzo, M.** (2016) "FTH1P3, a novel H-ferritin pseudogene transcriptionally active, is ubiquitously expressed and regulated during cell differentiation" *PLOS one* Vol. 11(3).
- Dostal, A.** (2012) "Iron depletion and repletion with ferrous sulfate or electrolytic iron modifies the composition and metabolic activity of the gut microbiota in rats" *Journal of Nutrition* Vol. 142, 271-277.

- Dostal, A.** (2013) "Low iron availability in continuous in vitro colonic fermentations induces strong dysbiosis of the child gut microbial consortium and a decrease in main metabolites" *FEMS Microbiology Ecology* Vol. 33, 161-175.
- Ebrahimi, K.** (2015) "Self-assembly is prerequisite for catalysis of Fe(II) oxidation by catalytically active subunits of ferritin" *The Journal of biological Chemistry* Vol. 290 (44), 26801-26810.
- Eckburg, P. B.** (2005) "Diversity of the human intestinal microbial flora" *Science* 308, 1635-1638.
- Edgar, R.** (2010) "Search and clustering orders of magnitude faster than BLAST" *Bioinformatics* Vol. 26 (19), 2460-2461.
- Edgar, R.** (2011) "UCHIME improves sensitivity and speed of chimera detection" *Bioinformatics* Vol. 27 (16), 2194-2200.
- Edgar, R.** (2013) "UPRASE: highly accurate OUT sequences from microbial amplicon reads" *Nature Methods*.
- EFSA** (2015) "Scientific opinion for dietary reference values for iron" *EFSA Journal* 2015, Vol. 13 (10).
- El Marjou, F.** (2004) "Tissue-specific and inducible cre-mediated recombination in the gut epithelium" *Genesis* Vol. 39, 186-193.
- Feise, R.** (2002) "Do multiple outcom measures require p-value adjustment?" *BMC Medical Research Methodology* 2 (8).
- Ferreira, C.** (2000) "Early embryonic lethality of H ferritin gene deletion in mice" *The Journal of biological chemistry* Vol. 275 (5), 3021-3024.
- Florin, T.** (1991) "Metabolism of dietary sulphate: absorption and excretion in humans" *Gut* 32, 766-773.
- Franchimont, D.** (2004) "Deficient host-bacteria interactions in inflammatory bowel disease? The Toll-like receptor (TLR)-4 Asp299gly polymorphism is associated with Crohn's disease and ulcerative colitis" *Gut* 53, 987-992.
- Frank D. N.** (2007) "Molecular-phylogenetic characterization of microbial community imbalance in human inflammatory bowel diseases. *PNAS* 104, 13780-13785.
- Fritz, T.** (2011) "Crohn's disease: NOD2, autophagy and ER stress converge" *Gut* 60, 1580-1588.
- Ganz, T.** (2013) "Systematic iron homeostasis" *Physiol Rev.* 93, 1721-1741

- Geuking M. B.** (2014) "The interplay between the gut microbiota and the human immune system" *Gut microbes* 5 (3), 411-418.
- Gao, G.** (2014) "Mitochondrial ferritin in the regulation of brain iron homeostasis and neurodegenerative diseases" *Frontiers in Pharmacology* Vol. 5 (19), 1-7.
- Gevers, D.** (2014) "The treatment-naïve microbiome in new onset Crohn's disease" *Cell Host Microbe* 15 (3) 382-392.
- Girelli, D.** (2017) "Modern iron replacement therapy: clinical and pathophysiological insights" *International Journal of Hematology* 107, 16-30.
- Gong, D.** (2016) "Involvement of reduced microbial diversity in inflammatory bowel disease" *Gastroenterology Research and Practice* Vol. 2016.
- Gozzelino, R.** (2014) "Coupling heme and iron metabolism via ferritin H chain" *Antioxidants & Redox signaling* Vol. 20 (11), 1754 – 1769.
- Gruber, L.** (2013) "High fat diet accelerates pathogenesis of murine Crohn's disease like ileitis independently of obesity" *PloS one* 8.
- Guo, X.** (2014) "Metagenomic profiles and antibiotic resistance genes in gut microbiota of mice exposed to arsenic and iron" *Chemosphere* Vol. 112, 1-8.
- Hasegawa, S.** (2012) "H-ferritin overexpression promotes radiation-induced leukemia/lymphoma in mice" *Carcinogenesis* Vol. 33 (11), 2269-2275.
- Hayashi, H.** (2006) "Genetic background of primary iron overload syndromes in Japan" *Internal Medicine* Vol.45.1876, 1107-1111.
- Hedin, C.** (2016) "Siblings of patients with Crohn's disease exhibit a biologically relevant dysbiosis in mucosal microbial metacommunities" *Gut* 65 (6), 944-953.
- Heeney, D. D.** (2017) "Intestinal Lactobacilli in health and disease, a driver or just along for the ride" *Curr Opin Biotechnol*, 31 (49), 140–147.
- Hollister, E. B.** (2014) "Compositional and functional features of the gastrointestinal microbiome and their effects on human health" *Gastroenterology* 146 (6) 1449-1458.
- Hörmannspurger, G.** (2016) "Intestinal Microbiome" *Aktuelle Ernährungsmedizin* 41, 207-217.
- Hugot, J. P.** (2001) "Association of NOD2 leucine-rich repeat variants with susceptibility to Crohn's disease" *Nature* 411, 599-603.
- Hunt, J.** (2000) "Adaption of iron absorption in men consuming diets with high or low iron bioavailability" *American Journal of Clinical Nutrition* Vol. 71, 94-102.

- Huttenhower, C.** (2013) "Structure, function and diversity of the healthy human microbiome" *Nature* 486, 207-214.
- Imbert, M.** (1998) "On the iron requirement of Lactobacilli grown in chemically defined medium" *Current Microbiology* Vol. 37, 64-66.
- Jansson, J.** (2006) "Metabolomics reveals metabolic biomarkers of Crohn's disease" *Plos One* Vol. 4 (7), 1-10.
- Jappeli, R.** "Cooperativity of mutational effects within a six amino acid residues substitution that induces a major conformational change in human H ferritin" *Biochemical and Biophysical Research Communications* Vol. 250, 342-346.
- Joosens, M.** (2011) "Dysbiosis of the fecal microbiota in patients with Crohn's disease and their unaffected relatives" *Gut* 60, 631-637.
- Jost, L.** (2007) "Partitioning diversity into independent alpha and beta components" *Ecology* 88, 2427-39
- Jostins, L.** (2012) "Host-microbe interactions have shaped the genetic architecture of inflammatory bowel disease" *Nature* 491, 119-124.
- Kaplan, G. G.** (2015) "The global burden of IBD from 2015 to 2025" *Nat. Rev. Gastroenterol Hepatol* 12, 720-727.
- Kato, J.** (2001) "A mutation, in the iron-responsive element of H ferritin mRNA, causing autosomal dominant iron overload" *American Journal of Human Genetics* Vol. 69, 191-197
- Kell, D.** (2014) "Serum ferritin is an important inflammatory disease marker, as it is mainly a leakage product from damaged cells" *Metallomics* Vol. 6, 748-773.
- Kelsen, J.** (2008) "Inflammatory bowel disease: the difference between children and adults" *Infl Bowel Dis* 14 (S2), S9-S11.
- Khor, B.** (2011) "Genetics and pathogenesis of inflammatory bowel disease" *Nature* 474, 307-317.
- Kistler, M.** (2014) "⁵⁹Fe-distribution in conditional ferritin-H-deleted mice" *Experimental Hematology* Vol. 42, 59-69.
- Koegh, M.** (2013) "Neuroferritinopathy" *International review of Neurobiology* Vol.110, 91-123.
- Krebs, N.** (2013) "Effects of different complementary feeding regiments on iron status and enteric microbiota in breastfed infants" *J. Pediatric*. 163 (3) 416- 423.
- Kulnigg, S.** (2006) "Systematic review: managing anemia in Crohn's disease" *Aliment. Pharmacol. Ther.* 24, 1507-1523.

- Kumar, A.** (2015) "The role of conformational dynamics and allestery in the disease development of human ferritin" *Biophysical Journal* Vol. 109, 1273-1281.
- Laroui, H.** (2012) "Dextran sodium sulfate (DSS) induced colitis in mice by forming nano-lipocomplexes with medium chain length fatty acids in the colon" *PLOS one* Vol. 7(3).
- LaVaute T.** (2001) "Targeted deletion of the gene encoding iron regulatory protein-2 causes misregulation of iron metabolism and neurodegenerative disease in mice" *Nature genetics* Vol. 27.
- Lepage, P.** (2011) "Twin study indicates loss of interaction between microbiota and mucosa in patients with Ulcerative Colitis" *Gastroenterology* 141, 227-236.
- Lesage, S.** (2002) "CARD15/NOD2 mutational analysis and genotype-phenotype correlation in 612 patients with inflammatory bowel disease" *Am J Hum Genet.* 70, 845-857.
- Levine J. S.** (2011) "Extraintestinal manifestations of inflammatory bowel disease" *Gastroenterol Hepatol* 7, 235-241.
- Levy, J.** (2000) "The effects of antibiotic use on gastrointestinal function" *Am J Gastroenterol* 95, 8-10.
- Li, J.** (2014) "An integrated catalog of reference genes in the human gut microbiome" *Nature Biotechnol.* 32, 834-841.
- Lin, L.** (2017) "Role of intestinal microbiota and metabolites on gut homeostasis and human disease" *BMC Immunology* Vol. 18 (2).
- Machiels, K.** (2013) "A decrease of the butyrate-producing species *Roseburia hominis* and *Faecalibacterium prausnitzii* defines dysbiosis in patients with ulcerative colitis" *Gut* 68 (8), 1275-83.
- MacKenzie, E.** (2008) "Role and regulation of ferritin H in rotenone-mediated mitochondrial oxidative stress" *Free radic. Boil. Medicine* Vol. 44 (9) 1762-1771.
- Mähler, M.** (1996) "Differential susceptibility of inbred mouse strains to dextran sulfate sodium-induced colitis" *American Physiological Society*
- Mevissen-Verhage, E. A. E.** (1985) "Effect of iron on neonatal gut flora during the first three months of life" *European Journal of clinical Microbiology* Vol. 4 (3), 272-278.
- Minemura, M.** (2015) "Gut microbiota and liver diseases" *World J Gastroenterol* 21 (6), 1691-1702.

- Molodecky, N.** (2012) "Increasing incidence and prevalence for the inflammatory bowel disease with time, based on systematic review" *Gastroenterology* Vol. 142, 46-54.
- Momozawa, Y.** (2011) "Characterization of bacteria in biopsies of colon and stools by high throughput sequencing of the V2 region of bacterial 16S rRNA gene in human" *Plos one* 6 (2) 16952.
- Momozawa, Y.** (2018) "IBD risk loci are enriched in multigenic regulatory modules encompassing putative causative genes" *Nature communication* 9: 2427.
- Morotomi, M.** (2012) "Description of *Christensenella minuta* gen. nov., sp. Nov., isolated from human faeces, which forms a distinct branch in the order Clostridiales, and proposal of *Christensenellaceae* fam. Nov." *Int J Syst Evol Microbiol.* 62, 144-149.
- Ng, W. K.** (2016) "Changing epidemiological trends of inflammatory bowel disease in Asia", *Intestinal research* 2016, 14: 111-119.
- Ohland C.L.** (2010) "Probiotic bacteria and intestinal epithelial barrier function" *American Journal of Physiology* 298, 807-819.
- Omiya, S.** (2008) "Downregulation of ferritin heavy chain increases labile iron pool, oxidative stress and cell death in cardiomyocytes" *Journal of molecular and cellular cardiology* Vol.46, 56-66.
- Ordás, I.** (2012) "Ulcreative colitis" *Lancet*, 380.
- Orholm, M.** (1991) "Familiar occurrence of inflammatory bowel disease" *N Engl J Med* 324, 84-88.
- Pantopoulus, K.** (2012) "Mechanisms of mammalian iron homeostasis" *Biochemistry* 51 (29), 5705-5724.
- Pascal, V.** (2017) "A microbial signature of Crohn's disease" *Gut* 66, 813-822.
- Pinto, D.** (1999) "Regulatory sequences of the mouse villin gene that efficiently drive transgenic expression in immature and differentiated epithelial cells of small and large intestine" *The Journal of biological chemistry* Vol. 274 (10), 6476-6482.
- Png, CW.** (2010) "Mucolytic bacteria with increased prevalence in IBD mucosa augment in vitro utilization of mucin by other bacteria" *AM J Gastroenterol* 105, 1-9.
- Podolsky, D. K.** (2002) "Inflammatory bowel disease" *N Engl J Med*, 347, 417-429.

- Price, M.** (2010) "FastTree 2 – approximately maximum-likelihood trees for large alignments" PLOS one Vol. 5 (3).
- Przybyszewska, J.** (2014) "The role of hepcidin, ferroportin, HCP1 and DMT-1 protein in iron absorption in the human digestive tract" Przeglad Gastroenterologiczny Vol. 9 (4), 208-213.
- Qin, J.** (2010) "A human gut microbial gene catalogue established by metagenomics sequencing" Nature 464 (7285), 59-65.
- Rochette, L.** (2015) "The iron-regulatory hormone hepcidine: a possible therapeutic target?" Pharmacology&Therapeutics
- Rouault, T.** (2001) "Iron in the brain" Nature genetics Vol.28, 299-300.
- Sartor, R.B.** (2008) "Microbial influences in inflammatory bowel diseases" Gastroenterology 134, 577-594.
- Satsangi, J.** (1996) "Two stage genome-wide search in inflammatory bowel disease provides evidence for susceptibility loci on chromosome 3, 7 and 12" Nature genetics 14, 199-202.
- Schaubeck, M.** (2015) "Reciprocal interaction of diet and microbiome in inflammatory bowel disease" Current Opinion Gastroenterology 31 (6), 464 – 470.
- Silva, F.** (2016) "The immunological basis of inflammatory bowel disease" Gastroenterology Research and Practice Vol. 2016, 11ff.
- Smith, P. M.** (2013) "The microbial metabolites, short-chain fatty acids, regulate colonic Treg cell homeostasis" Science 341 (6145), 569-573.
- Sokol, H.** (2009) "Low counts of *Faecalibacterium prausnitzii* in colitis microbiota" Inflammatory Bowel Disease 15 (8), 1183-9.
- Su, H.** (2018) "Inflammatory bowel disease and its treatment in 2018: global and Taiwanese status update" JFMA, 1-10.
- Te Velde, A.** (2006) "Critical appraisal of the current practice in murine TNBS-induced colitis" Inflammatory Bowel Disease Vol. 12 (10), 995-999.
- Tlaskalowa-Hogenova, H.** (2004) "Commensal bacteria (normal microflora), mucosal immunity and chronic inflammatory and autoimmune diseases" Immunology letters 93 (2-3), 97-108.
- Tolkien, Z.** (2015) "Ferrous sulfate supplementation causes significant gastrointestinal side-effects in adults: a systematic review and meta-analysis" Plos one 10 (2), 1-20.

- Topping, D. L.** (2001) "Short-chain fatty acids and human colonic function: roles of resistant starch and nonstarch polysaccharides" *Physiol Rev* 81, 1031-1064.
- Torti, F.** (2002) "Regulation of ferritin genes and protein" *Blood* Vol.99 (10), 3505-3516.
- Tysk, C.** (1988) "Ulcerative colitis and Crohn's disease in an unselected population of monozygotic and dizygotic twins. A study of heritability and the influence of smoking" *Gut* 29, 990-996.
- Vanoaica, L.** (2010) "Intestinal ferritin H is required for an accurate control of iron absorption" *Cell metabolism* Vol. 12, 273-282.
- Vazques-Gutierrez, P.** (2015) "Bifidobacteria strains isolated from stools of iron deficient infants can efficiently sequester iron" *BMC Microbiol.* 15 (3).
- Venema, W.** (2017) "The genetic background of inflammatory bowel disease: from correlation to causality" *Journal of Pathology* Vol. 241, 146-158.
- Vila, A. V.** (2018) "Gut microbiota composition and functional changes in inflammatory bowel disease and irritable bowel syndrome" *Science translation medicine* 10, 1-11.
- Wai, S.N.** (1996) "Construction of a ferritin-deficient mutant of *Campylobacter jejuni*: contribution of ferritin to iron storage and protection against oxidative stress" *Molecular microbiology* Vol. 20 (6), 1127-1134.
- Wang, Q** (2007) "Naïve Bayesian classifier for rapid assignment of rRNA sequences into the new bacterial taxonomy" *Appl and Environ Microbiol*, Vol. 73 (16), 5261-5267.
- Werner, T.** (2009) "Intestinal epithelial cell proteome from wild-type and *tnf^{delta}are/wildtype* mice: effect of iron on the development of chronic ileitis" *Journal of Proteome research* 8, 3252-3264.
- Werner, T.** (2011) "Depletion of luminal iron alters the gut microbiota and prevents Crohn's disease-like ileitis" *Gut* Vol. 60, 325-333.
- WHO** (2001) "Iron deficiency anemia – Assessment, prevention and control – A guide for programme managers"
- Wilks, S.** (1859) "Lectures on pathological anatomy" p. 408.
- Willing, B.P.** (2010) "A pyrosequencing study in twins shows that gastrointestinal microbial profiles vary with inflammatory bowel disease phenotype" *Gastroenterology* 139, 1844-1854.

Wills, E.S. (2014) "Fecal microbial composition of Ulcerative Colitis and Crohn's disease patients in remission and subsequent exacerbation" Plos One 9 (3), e90981

Wirtz, S. (2007) "Chemically induced mouse models of intestinal inflammation" Nature Protocols Vol. 2 (3), 541-546.

Yilmaz, B. (2018) "Gut microbiota and iron: the crucial actors in health and disease" Pharmaceuticals 11, 98.

Zandman-Goddart, G. (2007) „Ferritin in autoimmune diseases“ Autoimmunity Reviews Vol. 6, 457-463.

Zimmermann, M.B. (2010) "The effect of iron fortification on the gut microbiota in African children: a randomized controlled trial in Côte d'Ivoire" The American Journal of Clinical Nutrition Vol. 92, 1406-1415.

Lebenslauf

Persönliche Daten

Vollständiger Name: Annemarie Ilka Ruth Schmidt
Geburtstag: 14. Oktober 1985
Geburtsort: Hildesheim
Familienstand: ledig
Nationalität: deutsch

Derzeitige Tätigkeit

Seit 02/2017

Wissenschaftliche Mitarbeit im Referat Wissenschaft der Deutschen Gesellschaft für Ernährung

- Erarbeitung einer Leitlinie zum Thema Protein und ernährungsmitbedingter Krankheiten

Promotion

11/2011 – 04/2020

Technische Universität München

- “Impact of dietary iron on chronic intestinal inflammation: role of iron storage protein ferritin and replacement therapy“
- Doktorvater: Prof. Dr. Dirk Haller
- Lehrstuhl für Ernährung und Immunologie

Studium

Sommersemester 2011

Beuth Hochschule für Technik, Berlin

Fernstudium Patentrecht für Naturwissenschaftler und Ingenieure (1,0)

Sommersemester 2011

MRC Human Nutrition Research, Cambridge (GB)

- Studium der Ernährungswissenschaft
- Thema der Masterarbeit: “The influence of nanoparticulate iron on the gut microbiota in rats and *in vitro* nanoparticulate iron availability assays“ (1,0)
- Gesamtnote Master of Science: sehr gut (1,2)

Wintersemester 2006 -
Sommersemester 2011

Technische Universität München

- Studium der Ernährungswissenschaft
- Thema der Bachelorarbeit: “Crosstalk signal between intestinal epithelial cells and CD8 $\alpha\alpha$ intraepithelial lymphocytes: protective effect of IL 15 on regulation of gut homeostasis“ (1,0)
- Gesamtnote Bachelor of Science: sehr gut (1,4)

Schulische Ausbildung

- 1996 - 2005 **Gymnasium Andreanum**, Hildesheim
- Leistungskurse: Biologie, Musik
 - Abiturnote: 2,1
- 1992 – 1996 **Grundschule Greifswalder Straße**, Hildesheim

Arbeitserfahrung

- 08/2013 – 08/2014 Abendsekretärin bei Kuhnen und Wacker
Patent- und Rechtsanwaltskanzlei, Freising
- 08/2015 – 12/2016 Weinlaborantin bei Weinlabor Bohn, Zell/Mosel

Praktika und Ausland

- 04 - 05/2010 VW, Wolfsburg
- Patentableitung
- 03/2009 Deutsches Patentgericht, München
- Markensenat
- 08 – 09/2009 Kriminalinstitut, Campinas (BR)
- Forensisches Labor
- 03 - 05/2008 MRI – Bundesforschungsanstalt für Lebensmittel, Münster
- Abteilung Lipidforschung
- 09/2005 - 09/2006 Evangelische Gemeinde, Sydney (AUS)
- Gemeindepraktikum

Ehrenamtliches Engagement

- 01 - 07/2012 Mentorin bei „Step Inside“, Mentorenprogramm der TU München
- 10/2011 - 09/2011 Mentee von Dr. PA Kathrin Fücksle, Hoffmann & Eitle, München
- 10/2008 - 09/2010 Studentische Vertreterin der Studienbeitragskommission
- 10/2007 - 09/2010 1. Vorsitzende der Fachschaft Ernährung
- 10/1996 - 09/2010 Jahrgangssprecherin (Schülerrat und Fachschaft Ernährung)

Zusatzqualifikationen

Sprachen	Deutsch (Muttersprache) Englisch (fließend in Wort und Schrift) Latein (Latinum), Griechisch (Graekum)
EDV	MS Office (word, excel, powerpoint)
Führerschein	A2, B

Stipendien und Preise

Seit 11/2012	PhD-Stipendium der DFG im Rahmen des Graduiertenkollegs 1482
Seit 12/2012	Online-Stipendium von e-fellows
Schuljahr 2002	1. Preis des Schülerwettbewerbs „Fremde Religionen in der Nachbarschaft der EKD Hannover
Schuljahr 1996	Schulinterne Auszeichnung für besonderes Engagement

Interessen

Sport (DLRG Rettungsschwimmen)
Musik (Orgel)

List of publications

Pereira DI,...,**Schmidt A** et al. „Dietary iron depletion at weaning imprints low microbiome diversity and this is not recovered with oral nano Fe (III)”
Microbiology open 2015 February 4(1)
PMID: 25461615

Wagner SJ, **Schmidt A** et al. “Semisynthetic diet ameliorates Crohn’s disease like ileitis in TNFΔARE/WT mice through antigen-independent mechanism of gluten”
Inflammatory Bowel Disease 2013 May 19 (6)
PMID: 23567784

Lee T,...**Schmidt A** et al. „Oral versus intravenous iron replacement therapy distinctly alters the gut microbiota and metabolome in patients with inflammatory bowel diseases” *Gut* 2016 Feb 4
PMID: 26848182